Spatial and temporal dynamics of biogeochemical gradients in a tar oil-contaminated porous aquifer – biodegradation processes revealed by high-resolution measurements

Dissertation

zur Erlangung des Grades eines Doktors der Naturwissenschaften

der Geowissenschaftlichen Fakultät
der Eberhard Karls Universität Tübingen

vorgelegt von
Bettina Anneser
aus Trostberg

2008

Tag der mündlichen Prüfung: 25.07.2008

Dekan: Prof. Dr. Peter Grathwohl

1. Berichterstatter: Prof. Dr. Rainer U. Meckenstock

2. Berichterstatter: Prof. Dr. Peter Grathwohl

Abstract

The transport and distribution of organic contaminants in porous aquifers are subject to groundwater-sediment interactions and underlie a variety of physical-chemical and microbiological reactions, such as biodegradation. The complexity of these processes is aggravated by heterogeneities of the sediment matrix and fluctuating environmental conditions. Comprehensive knowledge of the hydrogeology and biogeochemistry of a given site and of the factors limiting biodegradation is therefore crucial for a reasonable implication of remediation concepts.

Numerical simulations and lab experiments revealed biodegradation processes to take place predominantly at the fringes of organic contaminant plumes, where transverse dispersion provides mixing of electron donors from the plume center with electron acceptors from the adjacent groundwater. In the resulting transition zone, which is restricted to a small area in the centimeter range, pronounced bioactivities are indicated by steep gradients of redox-sensitive parameters. In contrast to well controllable numerical and experimental models, sampling in aquifers is tainted with considerable financial and technical efforts. The monitoring of contaminated sites is therefore mostly restricted to groundwater analyses performed at an insufficient temporal and spatial scale, which conceal detailed information on the localization and relevance of individual redox processes as well as on rates and limitations of biodegradation.

By means of a novel high-resolution multi-level groundwater well, biodegradation processes in a tar oil-contaminated porous aquifer could be investigated for the first time at an appropriate scale with a vertical resolution of down to 2.5 cm. From the comparison of steep fine-scale gradients of electron donors, electron acceptors and metabolites, sulfate and iron reduction could be identified as the dominant biodegradation processes with highest activities at the fringe of the contaminant plume. In individual zones of the contaminated aquifer these two redox processes were observed to take place simultaneously instead of following a defined order according to their thermodynamic efficiency. High cell numbers as well as increased activities of extracellular enzymes and bacterial carbon production at the plume fringe substantially support the concept of mixing-controlled biodegradation. These patterns are further underlined by a significant shift in stable isotope signatures of dissolved toluene ($\delta^{13}C$) and sulfate ($\delta^{34}S$, $\delta^{18}O$) concomitant with decreasing concentrations, thus pointing at the relevance of transverse dispersion. At the same time, however, gradients at our sampling site frequently displayed zones where BTEX and sulfate overlapped, which hints at additional limitations, such as toxicity of pollutants or biokinetic constraints.

The redox processes identified from groundwater samples were additionally evaluated in comparison to freshly collected sediment samples. The results emphasize the role of sediments as "long term archives", which – in contrast to "snapshots" gained from groundwater analysis – provide insight into the history of biogeochemical processes. In addition, conclusions on aquifer heterogeneity and on the complexity of the site were inferred from comparative analysis of groundwater and sediment data.

Unlike often assumed, groundwater systems do not represent static and inanimate environments, but rather are subject to pronounced spatial and temporal dynamics, as could be demonstrated by recording the variability of biogeochemical gradients and related redox processes over a period of almost two years. First insights into the adaptive capacities of microbial communities towards changing environmental conditions and their effects on the degradation potential of the bacteria could be obtained.

The data presented in this thesis provide a fundamental amelioration for the validation and advancement of reactive transport models, which are indispensable in practice for evaluating biodegradation processes and the applicability of natural attenuation concepts.

Zusammenfassung

Der Transport und die Verteilung organischer Schadstoffe in porösen Grundwasserleitern unterliegen einer Vielzahl physikalisch-chemischer und mikrobiologischer Reaktionen sowie Wechselwirkungen zwischen Grundwasser und Sediment. Die Komplexität dieser Prozesse wird zusätzlich verstärkt durch Heterogenitäten der Bodenmatrix und schwankende Umweltbedingungen. Eine umfassende Kenntnis sowohl der Hydrogeologie und Biogeochemie des Standortes als auch der abbaulimitierenden Faktoren ist daher unabdingbare Voraussetzung für eine effiziente Umsetzung von Sanierungskonzepten, die auf natürlichen Selbstreinigungsprozessen (gemeinhin als „Natural Attenuation" bezeichnet) basieren. Numerische Simulationen und Laborexperimente in Mikrokosmen haben gezeigt, dass sich biologische Abbaureaktionen in gesättigten Grundwasserleitern überwiegend an den Rändern organischer Schadstofffahnen abspielen. Dort wird durch transversale Dispersion eine Mischung von Elektrondonoren aus dem Fahnenzentrum und Elektronenakzeptoren aus dem umgebenden Grundwasser gewährleistet. In der entstehenden Übergangszone - auf einen schmalen Saum von wenigen Zentimetern begrenzt - ist die Bioaktivität im Vergleich zu umliegenden Bereichen deutlich erhöht, was durch steile Gradienten redoxrelevanter Parameter ersichtlich wird. Anders als gut kontrollierbare numerische und experimentelle Modelle stellen Grundwasserleiter jedoch offene und schwer zugängliche Systeme dar, deren Beprobung mit erheblichem technischem und finanziellem Aufwand verbunden ist. Das Monitoring von Schadensfällen beschränkt sich somit in den meisten Fällen auf Grundwasseranalysen in grober zeitlicher und räumlicher Auflösung, die keine detaillierten Aussagen über die Lokalisierung und Relevanz individueller Redoxprozesse sowie Limitierungen und Raten des Schadstoffabbaus erlauben.

Mit Hilfe einer speziell konstruierten Multi-Level-Grundwassermessstelle konnten abbaurelevante Prozesse in einem mit Teeröl kontaminierten porösen Grundwasserleiter erstmalig mit einer vertikalen räumlichen Auflösung von bis zu 2,5 cm untersucht werden.

Anhand steiler Gradienten von Elektronendonoren, Elektronenakzeptoren und Abbauprodukten wurde gezeigt, dass die am Schadstoffabbau maßgeblich beteiligten Prozesse (Sulfat- und Eisenreduktion) im gesamten Bereich der Schadstofffahne, am ausgeprägtesten jedoch an deren Rand auftreten. In bestimmten Zonen wurde außerdem beobachtet, dass die Redoxprozesse häufig gleichzeitig ablaufen anstatt einer definierten Abfolge entsprechend ihrer thermodynamischen Effizienz zu folgen.

Hohe Zellzahlen sowie erhöhte Enzymaktivitäten und Produktivitäten im Fahnenrandbereich stützen das Konzept des mischungskontrollierten Schadstoffabbaus im Aquifer. Ebenso bestätigt ein signifikanter Anstieg der Isotopensignaturen von in Grundwasser gelöstem Toluol ($\delta^{13}C$) und Sulfat ($\delta^{34}S$, $\delta^{18}O$) bei gleichzeitig abnehmenden Konzentrationen in diesen Übergangszonen die Rolle der transversalen Dispersion als maßgeblichen abbaulimitierenden Faktor. Gleichzeitig weisen jedoch Überlappungsbereiche von Schadstoffen und Elektronenakzeptoren auf zusätzliche Limitierungen hin, welche von der Toxizität der Schadstoffe bis hin zu kinetisch bedingten Restriktionen sehr vielfältiger Natur sein können.

Des Weiteren konnten die im Grundwasser identifizierten Redoxprozesse mit räumlich hochaufgelösten Sedimentdaten abgeglichen werden. Dabei wurde die Bedeutung der Bodenmatrix als „Langzeit-Archiv" aufgezeigt, das - anders als aus dem Grundwasser gewonnene „Momentaufnahmen" - Einblicke in die Historie des Schadstoffabbaus am Standort gewährt. Der Vergleich kleinräumiger Vertikalprofile von Grundwasser- und Sedimentdaten erlaubt zugleich Rückschlüsse auf die Heterogenität des Aquifers und die Komplexität der darin stattfindenden Abbauprozesse.

Die über einen Zeitraum von knapp zwei Jahren verzeichnete Variabilität der Redoxprozesse demonstriert, dass Grundwassersysteme nicht, wie oftmals vermutet, statische

und weitgehend unbelebte Lebensräume darstellen, sondern einer hohen räumlichen und zeitlichen Dynamik unterworfen sind. Mit Hilfe mikrobiologischer und geochemischer Gradienten konnten erste Erkenntnisse über die Anpassungsfähigkeit der mikrobiellen Gemeinschaft an veränderte Umweltbedingungen sowie deren Auswirkungen auf das Abbaupotenzial der Mikroorganismen erlangt werden.

Die in dieser Arbeit gewonnenen Daten stellen eine wichtige Erweiterung für die Validierung und Weiterentwicklung reaktiver Transportmodelle dar, die in der Praxis unentbehrlich für die Evaluierung des Schadstoffabbaus und die Umsetzbarkeit von Natural Attenuation-Konzepten sind.

Table of contents

INDEX

Table of contents

1. Introduction

1.1. Microbes – key players of groundwater quality management

Currently, the world's population grows by 1.2 % per year (bpb, 2004), while global water use increases at more than twice this rate. By 2025, about 2/3 of the world's population may experience water stress conditions (UN Water, 2006). Facing the threat of increasing water scarcity and the striking awareness of the finiteness of drinking water resources, the interest in preserving this essential good finally hit publicity and entered the consciousness of water managers and policy makers. A multitude of cross-national regula-tions and interdisciplinary research programmes such as the European Water Framework Directive (WFD; European Commission, 2008) or the project on Global Change and the Hydrological Cycle (GLOWA; BMBF, 2008) have been launched to bring together science and politics. Thus, notice was finally attracted also to groundwater ecosystems, which so far were often considered as inhospitable, predominantly isolated and static environments. Thanks to intensive fundamental research, this antiquated perception could be replaced by the awareness of a quite lively and diverse association of microorganisms and meiofauna thriving and cavorting in complete darkness several meters below the subsurface (Gibert et al., 1994; Bachofen et al., 1998; Alley et al.,

Table 1.1 Relevance of groundwater for public drinking water supplies (from Thornton et al., 2002).

Contribution of groundwater in providing public drinking water supplies (% by volume)			
Australia	14	Malta	100
Austria	97	Netherlands	100
Belgium	64	Norway	5
Canada	14	Poland	50
Cyprus	100	Portugal	49
Czechoslovakia	61	Romania	50
Denmark	98	Spain	30
Finland	52	Sweden	39
France	70	Switzerland	70
Germany	75	Turkey	50
Greece	32	Russia	70
Hungary	78	UK	35
Ireland	15	US	45
Luxembourg	71	Yugoslavia	75

2002). More than this, bacteria have been recognized as the ones in charge of groundwater quality control, being to a large extent involved in essential biogeochemical cycling processes (Madsen and Ghiorse, 1993; Haack and Bekins, 2000; Chapelle, 2001; Fredrickson and Fletcher, 2001). Their capability also to degrade a range of contaminants (e.g. tar oil compounds or pesticides) under a variety of environmental conditions is nowadays widely implemented for cost efficient, non-invasive treatment of contaminated sites. The combined physical, chemical and biological processes that "act without human intervention to reduce mass, toxicity, mobility, volume and concentration of contaminants in soil or groundwater" (OSWER Directive, 1999) are generally referred to as natural attenuation (NA; Christensen et al., 2001). Unlike physical-chemical processes such as dilution, sorption or volatilization, biodegradation not only slows down the propagation of a contaminant plume, but ideally results in complete removal of the pollutants (Wiedemeier et al., 1999; Christensen et al., 2001). In European countries, the efficiency and reliability of this catch-phrased "qualified idleness" has been subject to enduring tenacious debates amongst sanitation liables and environmental agencies, who to date have not agreed upon uniform regulations and guidelines for the application of NA as a contaminated land management option. The OSWER directive of the US environmental protection agency (US-EPA) suggests three lines of evidence to be followed in order to evaluate the occurrence and progress of intrinsic biodegradation: (1) demonstration of decreasing contaminant concentrations in association with a stable or retreating plume, (2) hydrological and geochemical data that indirectly prove natural attenuation processes (e.g. decreasing concentrations of electron acceptors and nutrients

relative to background values), and (3) direct evidence of active biodegradation either *in situ* or in microcosms inoculated with site material (OSWER Directive, 1999).

Under aerobic conditions, virtually all organic compounds can be degraded by a variety of metabolic pathways (Chapelle, 2001). In anaerobic environments, however, organic compounds, above all the higher molecular aromatic hydrocarbons, are highly recalcitrant and often show a high persistence in nature (Philp et al., 2005). Nevertheless, under favourable conditions many of these sometimes tenacious pollutants - especially the monoaromatic hydrocarbons, which rank amongst the main pollutants of concern in contaminated aquifers - are attacked and degraded by microorganisms (Heider et al., 1999; Coates and Anderson, 2000; Spormann and Widdel, 2000; Widdel and Rabus, 2001; Boll et al., 2002; Gibson and Harwood, 2002; Chakraborty and Coates, 2004; Meckenstock et al., 2004a). The poor accessibility of the subsurface, however, and the fact that only about 1 % of the inherent bacterial population can be cultured in the lab (Amann et al., 1995; Torsvik et al., 1998; Kirk et al., 2004; O'Donnell et al., 2007), so far rendered physiological requirements and limitations of anaerobic contaminant degraders rather speculative. Improved classical microbiological techniques and the boosting development of molecular approaches meanwhile allow cultivation-independent investigations of bacteria, providing information on the diversity, abundance and activity of subsurface populations (Amann et al., 1997; Amann and Kuhl, 1998; Lovley, 2003). Furthermore, highly sensitive analytical techniques nowadays permit a detailed description on the distribution of contaminants and redox-specific parameters and thus facilitate an evaluation of the complex interactions of biotic and abiotic processes taking place in contaminated soils and groundwater.

1.2. Transport and fate of organic contaminants

Decades-lasting careless handling of tar oil compounds as well as industrial and military deposits, accidental spills, and other origins (Fig. 1.1) have lead to the contamination of innumerable sites worldwide, of which at least 271,000 are registered alone in Germany (UBA, 2006). Owing to the high solubility of monoaromatic compounds and the toxicity of
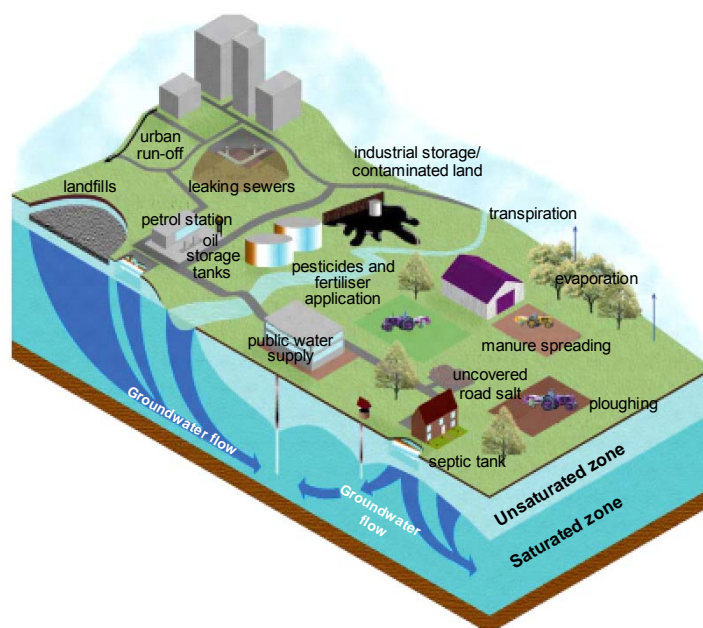

Figure 1.1 Sources of sediment and groundwater pollution by organic and chemical contaminants.

both mono- and polycyclic aromatic hydrocarbons (PAH), this class of pollutants is of specific concern regarding groundwater quality issues (Thornton et al., 2002). Once released into the aquifer, the more soluble portion of the organic pollutants dissolves from the non-aqueous phase liquids (NAPLs) and is transported with groundwater flow. By the time, the resulting contaminant plume reaches stationarity or, ideally, retreats and shrinks in size (Wiedemeier et al., 1999).

As a consequence of the low solubility of oxygen and its rapid depletion by biotic and abiotic oxidation reactions, aerobic biodegradation is self-limited in subsurface environments and anaerobic processes typically prevail (e.g. Coates and Anderson, 2000; Andreoni and Gianfreda, 2007). From a thermodynamic point of view, the energetically most favourable electron acceptors are depleted according to their Gibb's free energy in the order $O_2 > NO_3^- > Mn(IV)$ oxides $> Fe(III)$ oxides $> SO_4^{2-} > CO_2$ (Tab. 1.2; Christensen et al., 2000; Lovley, 2001).

Table 1.2 Redox half reactions according to their standard electron activity p_ε at pH 7 and terminal electron accepting processes given for the degradation of toluene (modified from Stumm & Morgan, 1996).

Redox half reaction of microbial processes	Stoichiometry of toluene (C_7H_8) degradation reactions
p_ε: -10 -5 0 +5 +10 +15	
O_2 red.	$C_7H_8 + 9\,O_2 \Rightarrow 7\,CO_2 + 4\,H_2O$
Denitrification	$5\,C_7H_8 + 36\,NO_3^- + H^+ \Rightarrow 35\,HCO_3^- + 3\,H_2O + 18N_2$
Mn (IV) red.	$C_7H_8 + 18\,MnO_2 + 29\,H^+ \Rightarrow 7\,HCO_3^- + 18\,Mn^{2+} + 15\,H_2O$
Fe (III) red.	$C_7H_8 + 36\,FeOOH + 65\,H^+ \Rightarrow 7\,HCO_3^- + 36\,Fe^{2+} + 51\,H_2O$
SO_4^{2-} red.	$2\,C_7H_8 + 9\,SO_4^{2-} + 6\,H_2O \Rightarrow 14\,HCO_3^- + 5\,H_2S + 4\,HS^-$
Methanogen.	$2\,C_7H_8 + 10\,H_2O \Rightarrow 5\,CO_2 + 9\,CH_4$

(Decreasing energy yield)
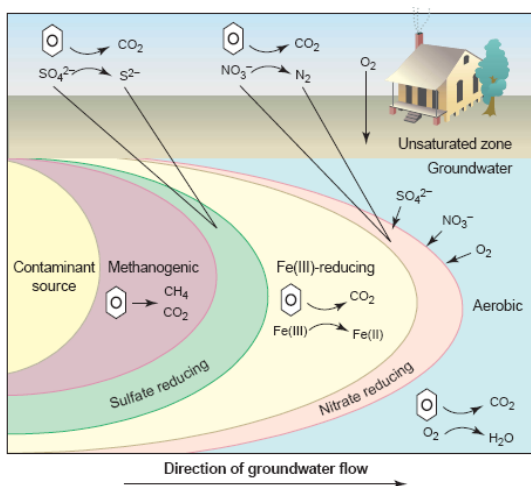
Figure 1.2 Stratification of redox zones in a petroleum contaminated aquifer after sequential depletion of electron acceptors according to their respective energy yield (from Lovley 2001).

The resulting sequential pattern of terminal electron accepting processes (TEAPs) is frequently described as a characteristic succession of individual redox processes, with most reduced (methanogenic) conditions close to the contamination source and increasing redox potential with increasing distance from the source (Fig. 1.2; Lovley and Chapelle, 1995; Lovley, 2001; Chapelle et al., 2002). The partial equilibrium approach proposed by Postma and Jakobsen (1996), however, considers the reactivity and amount of organic matter, *i.e.* its complete degradation to H_2 and CO_2, as the rate-determining factor. Chemical equilibrium is approached by reaction of the fermentation products with inorganic electron acceptors. In oxygen-limited aquifers, an almost instantaneous reaction between electron acceptor and electron donor is expected

to occur across transition zones, such as the fringes of organic contaminant plumes (Borden and Bedient, 1986; Rifai and Bedient, 1990; Prommer and Barry, 2005). An overlap of reactants, however, which was observed in natural as well as in artificial hydrocarbon plumes, contradicts the hypothesis of spontaneous biodegradation (Anneser et al., 2007; Bauer et al., 2008).

Regardless of thermodynamic constraints, lab and field studies revealed the co-occurrence of different TEAPs, which were displayed by steep biogeochemical gradients arising predominantly at physical-chemical and hydrogeological interfaces. Experimental and modeled data exhibited hydro-dynamic transverse dispersion, *i.e.* mechanical dispersion and (molecular) diffusion, to be a driving factor of biodegradation (Cirpka et al., 1999; Mayer et al., 2001; Cirpka et al., 2006; Bauer et al., 2008). The mixing area in homogeneous porous media is restricted to a narrow zone in the mm- to cm-range by low transverse dispersivities (Ham et al., 2004; Cirpka, 2005; Cirpka and Valocchi, 2007; Maier et al., 2007; Bauer et al., 2008). In heterogeneous sediments, high-conductivity lenses have been shown to cause a focussing of the groundwater flow and subsequent spreading of the plume, which lead to increased mixing and, consequently, enhanced biodegradation (Werth et al., 2006; Bauer et al., submitted). Likewise, numerical models have shown hydraulic changes, e.g. water table fluctuations, to increase transverse dispersion and mixing of reactants and thus to promote biodegradation activities (Prommer et al., 2002; McGuire et al., 2005).

By now, studies evaluating limitations and controlling factors of NA are primarily based on lab experiments and numerical simulations. The lack of scale-adapted groundwater sampling techniques so far considerably hampered the transferability of experimental and modeled results to *in situ* conditions. Conventional monitoring wells with sampling intervals of 0.5 to 1 m are biased by insufficient spatial resolution, missing the steep abiotic and biotic gradients and bearing the risk of hydraulic shortcuts. Consequently, mixing of waters of different composition from different depths is likely to occur during groundwater sampling (Puls and Barcelona, 1996; Einarson and Cherry, 2002). The distribution of relevant analytical parameters and the delineation of distinct redox zones therefore remains rather speculative, thus raising the demand for scale-adapted sampling techniques in order to gain a comprehensive understanding of biodegradation processes (Wilson et al., 2004).

1.3. Methods to assess *in situ* biodegradation processes

Even the best sampling technique, however, is useless if subsequent handling and analytical procedures for water and sediment samples are not deliberately selected as well. On the way from the anoxic aquifer to the oxygen-saturated surface the water chemistry may be altered by oxidation, volatilization, and/or precipitation reactions, thereby influencing microbial communities. Life in aquifers is to a large degree confined to the sediment, which harbours 90 – 99 % of the bacteria (Griebler, 2001; O'Donnell et al., 2007). Consequently, a comprehensive survey of groundwater ecosystems and NA processes demands for the identification of both sediment and groundwater characteristics by application of individually tailored analytical protocols.

Standard procedures in the field of groundwater research comprise the evaluation of geohydraulic settings (e.g. sediment composition, porosity, hydraulic conductivity) and analysis of the sediment and groundwater chemistry. The latter includes pH, p_ε and specific conductivity measurements as well as the analysis of electron donors (e.g. organic contaminants), electron acceptors (O_2, NO_3^-, SO_4^{2-} etc.) or reaction products (e.g. Fe^{2+}, Mn^{2+}, H_2S, CH_4, CO_2) (Borden et al., 1995; Höhener et al., 1998; Bolliger et al., 1999; Wiedemeier et al., 1999; Christensen et al., 2000; Hunkeler et al., 2002), complemented by the determination of major anions and cations for ion balance calculations. Changes in the physical-chemical composition of groundwater are often indicative of microbial activities.

The diversity and abundance of bacteria in aquifers is often defined by their versatility in terms of the types of redox reactions mediated and may be assessed via classical microbiological techniques or by use of molecular tools (e.g. Amann and Kuhl, 1998; Bekins et al., 1999; Lovley, 2003; Kirk et al., 2004; Oremland et al., 2005; Tyson and Banfield, 2005; Andreoni and Gianfreda, 2007). Microscopic counts of fluorescently labeled cells are commonly applied to assess the spatial distribution and abundance of total bacteria in the aquifer (Ludvigsen et al., 1999; Griebler et al., 2002). Individual physiological groups may be targeted by most probable number (MPN) assays and fluorescence *in situ* hybridization (FISH). Functional marker genes, which code for characteristic key enzymes and, hence, certain metabolic pathways, allow for a cultivation-independent determination of the abundance and relevance of specific contaminant degraders within their natural habitats (Rotthauwe et al., 1997; Braker et al., 2000; Wagner et al., 2006). This way, the toluene degrader-specific bssA gene, which encodes the key enzyme of anaerobic toluene and xylene degradation, benzylsuccinate synthase (Leuthner and Heider, 2000; Boll et al., 2002), was used for identification, localization, and quantification of the respective degraders at the site investigated in this study (Winderl et al., 2007; Winderl et al., 2008).

Even though the aforementioned approaches reveal the presence of microbes and the potential for natural attenuation at a given site, they don't tell us whether the degrader community is actually metabolically active. Proving bioactivity *in situ* is substantially hampered by the poor accessibility of the subsurface and by the generally low cellular abundance and metabolic rates prevailing in these environments (Franzmann et al., 1996). Evaluation of *in situ* biodegradation rates is commonly performed in microcosms inoculated with site material (e.g. Harrison et al., 2001). However, since a realistic simulation of the complexity of groundwater environments is actually not possible, we have to be aware that lab-assessed biodegradation rates do not properly reflect *in situ* conditions. The best way to overcome this obstacle would be to "take the lab to the microbes and not the microbes to the lab" (Bachofen et al., 1998). One of the most common approaches to obtain direct qualitative evidence of biodegradation is screening for metabolic intermediates or co-metabolic by-products, which are released from the microbes into the extracellular medium and optimally can be assigned to one parent compound and a specific degradation pathway (e.g. Beller, 2000; Meckenstock et al., 2004a; Griebler et al., 2004; Chakraborty and Coates, 2005; Safinowski et al., 2006; Botton and Parsons, 2007). *In situ* bioactivities can be tracked by incubating freshly sampled sediment or groundwater with fluorescently or radioactively labeled substrates. Upon enzymatic cleavage of the labeled complex, a fluorescent signal is released, which can be detected spectrometrically (Freeman et al., 1995; Lehman and O'Connell, 2002). Using radioactive labels, the amount of radioactive compounds incorporated into individual cell compartments during growth can be traced in a scintillation counter (Kirchman et al., 1985). In both cases, a direct correlation to microbial enzyme activities or cellular productivities can be obtained from the intensity of the signals.

The low biodegradation rates typically found in groundwater systems considerably aggravate the documentation of microbial activities *in situ* (Chapelle and Lovley, 1990; Phelps et al., 1994; Richnow et al., 2003b). A promising approach to identify degradation pathways and to qualitatively and quantitatively trace even faint hints of biodegradation is measuring the stable isotope signature of electron donors and/or electron acceptors via compound-specific stable isotope analysis (CSIA) (Clark and Fritz, 1997; Dempster et al., 1997; Kendall and Caldwell, 1998; Mancini et al., 2003; Zwank et al., 2003; Meckenstock et al., 2004b; Elsner et al., 2005; Young and Phelps, 2005). The principle of this method is based on the fact that each element exhibits a typical, constant ratio of heavy and light isotopes, which can be distinguished, for instance, by gas chromatograph-combustion-isotope ratio mass spectrometry (GC-C-IRMS) (Meier-Augenstein, 1999; Jochmann et al., 2006). Owing to lower dissociation energies, bonds between lighter isotopes of an element are more readily

broken during physical, chemical or biological reactions than bonds between heavier isotopes. During biodegradation, this selective behaviour, which is referred to as isotope fractionation, leads to an enrichment of heavier isotopes in the remaining substrate pool and to a respective depletion in the reaction product compared to the initial isotope ratio (Bolliger et al., 1999; Richnow et al., 2003a; Meckenstock et al., 2004b; Griebler et al., 2004). Thus, biodegradation of aromatic hydrocarbons, for instance, is indicated by an enrichment of the heavier ^{13}C isotope in the (partially degraded) sample relative to the ^{13}C/^{12}C ratio determined in the contaminant source, where biodegradation is considered to be more or less absent (Schmidt et al., 2004). Likewise, terminal electron accepting processes can be verified by shifts in the stable isotope composition of the respective electron acceptors. Since the isotopic effect of abiotic processes, such as sorption, dilution or volatilization, is considered to be negligible, changes in the isotope ratios of a specific organic compound can unequivocally be ascribed to microbial degradation activities (Meckenstock, 1999). Apart from applying stable isotopes for the evaluation of biodegradation processes, CSIA is often used to assess hydrological flowpaths or to determine water ages by means of the natural stable isotope ratios of D/H and ^{18}O/^{16}O in groundwater, respectively (Clark and Fritz, 1997). In terms of environmental forensics, CSIA can even be applied to trace back the origin of pollutants or natural groundwater components (Meier-Augenstein, 1999).

1.4. Intentions and objectives of the study

Basis of this work was the construction of a specific high-resolution multi-level groundwater well, which was installed in a tar oil-contaminated sandy aquifer at a former gasworks site in Düsseldorf-Flingern, Germany. Following the plume fringe concept, which states main biodegradation activities are taking place at the transition between contaminated and uncontaminated groundwater (Cirpka et al., 1999; Prommer et al., 2006; Bauer, 2007), the well was used to test whether the hypothesis of fringe-controlled biodegradation as observed in lab experiments also applies to *in situ* conditions.

Groundwater samples obtained at an exceptionally high spatial resolution of 2.5 to 33 cm were analyzed for a variety of geochemical and microbiological parameters with the major intention to achieve a detailed vertical profile of biogeochemical species. These, subsequently, can be evaluated and correlated in order to identify and characterize key biodegradation reactions in the BTEX plume undergoing natural attenuation and to find an answer on the following questions: (i) where and under which conditions does biodegradation occur, (ii) what are the driving forces and which are the factors limiting biodegradation, and (iii) what is the impact of spatial and temporal variabilities on the distribution and efficiency of biodegradation processes?

In conclusion, this PhD thesis aims at an enlargement of the overall understanding of biodegradation processes in organically contaminated porous aquifers and thus forms the framework for an improvement of NA prediction tools and sanitation concepts.

1.5. References

Alley, W.M., Healy, R.W., LaBaugh, J.W., and Reilly, T.E. (2002) Flow and storage in groundwater systems. *Science* 296: 1985-1990.

Amann, R., and Kuhl, M. (1998) *In situ* methods for assessment of microorganisms and their activities. *Curr Opin Microbiol* 1: 352-358.

Amann, R., Glöckner, F.-O., and Neef, A. (1997) Modern methods in subsurface microbiology: in situ identification of microorganisms with nucleic acid probes. *FEMS Microbiol Rev* 20: 191-200.

Amann, R.I., Ludwig, W., and Schleifer, K.H. (1995) Phylogenetic identification and *in situ* detection of individual microbial cells without cultivation. *Microbiol Rev* 59: 143-169.

Andreoni, V., and Gianfreda, L. (2007) Bioremediation and monitoring of aromatic-polluted habitats. *Appl Microbiol Biotechnol* 76: 287-308.

Anneser, B., Richters, L., and Griebler, C. (2007) Identification and localization of redox processes in an aromatic hydrocarbon plume via high-resolution sampling of biotic and abiotic gradients. In *WAter POllution in natural POrous media at different scales. Assessment of fate, impact and indicators. WAPO^2*. Candela, L., Vadillo, I., Aagard, P., Bedbur, E., Trevisan, M., Vanclooster, M. et al. (eds). Barcelona (Spain), April 11-13 2007, Instituto Geológico y Minero de Espana, pp. 339-345.

Bachofen, R., Ferloni, P., and Flynn, I. (1998) Microorganisms in the subsurface. *Microbiol Res* 153: 1-22.

Bauer, R.D. (2007) Control and limitations of microbial degradation in aromatic hydrocarbon plumes – experiments in 2-D model aquifers. In *Geowissenschaftliche Fakultät*. . Tübingen: Eberhard-Karls-Universität, p. 161.

Bauer, R.D., Maloszewski, P., Zhang, Y., Meckenstock, R.U., and Griebler, C. (2008) Mixing-controlled biodegradation in a toluene plume - results from two-dimensional laboratory experiments. *J Contam Hydrol* 96: 150-168.

Bauer, R.D., Rolle, M., Eberhardt, C., Grathwohl, P., Bauer, S., Kolditz, O. et al. (2008) Enhanced biodegradation by hydraulic heterogeneities in petroleum hydrocarbon plumes. submitted to *J Contam Hydrol*.

Bekins, B.A., Godsy, E.M., and Warren, E. (1999) Distribution of microbial physiologic types in an aquifer contaminated by crude oil. *Microb Ecol* 37: 263-275.

Beller, H.R. (2000) Metabolic indicators for detecting *in situ* anaerobic alkylbenzene degradation. *Biodegradation* 11: 125-139.

BMBF (2008). Global change and the hydrological cycle. http://www.glowa.org/index.php

Boll, M., Fuchs, G., and Heider, J. (2002) Anaerobic oxidation of aromatic compounds and hydrocarbons. *Curr Opin Chem Biol* 6: 604-611.

Bolliger, C., Höhener, P., Hunkeler, D., Häberli, K., and Zeyer, J. (1999) Intrinsic bioremediation of a petroleum hydrocarbon-contaminated aquifer and assessment of mineralization based on stable carbon isotopes. *Biodegradation* 10: 201-217.

Borden, R.C., and Bedient, P.B. (1986) Transport of dissolved hydrocarbons influenced by reaeration and oxygen limited biodegradation: 1. Theoretical development. *Water Res Research* 22: 1973-1982.

Borden, R.C., Gomez, C.A., and Becker, M.T. (1995) Geochemical indicators of intrinsic bioremediation. *Ground Water* 33: 180-189.

Botton, S., and Parsons, J.R. (2007) Degradation of BTX by dissimilatory iron-reducing cultures. *Biodegradation* 18: 371-381.

bpb (2004) Bevölkerungsentwicklung. *Bundeszentrale für politische Bildung, Informationen zur politischen Bildung* 282.

Braker, G., Zhou, J., Wu, L., Devol, A.H., and Tiedje, J.M. (2000) Nitrite reductase genes (nirK and nirS) as functional markers to investigate diversity of denitrifying bacteria in pacific northwest marine sediment communities. *Appl Environ Microbiol* 66: 2096-2104.

Chakraborty, R., and Coates, J.D. (2004) Anaerobic degradation of monoaromatic hydrocarbons. *Appl Microbiol Biotechnol* 64: 437-446.

Chakraborty, R., and Coates, J.D. (2005) Hydroxylation and carboxylation--two crucial steps of anaerobic benzene degradation by *Dechloromonas* strain *RCB*. *Appl Environ Microbiol* 71: 5427-5432.

Chapelle, F.H. (2001) *Groundwater Microbiology and Geochemistry*. John Wiley & Sons, New York.

Chapelle, F.H., and Lovley, D.R. (1990) Rates of microbial metabolism in deep coastal plain aquifers. *Appl Environ Microbiol* 56: 1865-1874.

Chapelle, F.H., Bradley, P.M., Lovley, D.R., O'Neill, K., and Landmeyer, J.E. (2002) Rapid evolution of redox processes in a petroleum hydrocarbon-contaminated aquifer. *Ground Water* 40: 353-360.

Christensen, T.H., Bjerg, P.L., Banwart, S.A., Jakobsen, R., Heron, G., and Albrechtsen, H.-J. (2000) Characterization of redox conditions in groundwater contaminant plumes. *J Contam Hydrol* 45: 165-241.

Christensen, T.H., Kjeldsen, P., Bjerg, P.L., Jensen, D.L., Christensen, J.B., Baun, A. et al. (2001) Biogeochemistry of landfill leachate plumes. *Appl Geochem* 16: 659-718.

Cirpka, O.A. (2005) Effects of sorption on transverse mixing in transient flows. *J Contam Hydrol* 78: 207-229.

Cirpka, O.A., and Valocchi, A. (2007) Two-dimensional concentration distribution for mixing controlled bioreactive transport in steady state. *Adv Water Res* 30: 1668-1679.

Cirpka, O.A., Frind, E.O., and Helmig, R. (1999) Numerical simulation of biodegradation controlled by transverse mixing. *J Contam Hydrol* 40: 159-182.

Cirpka, O.A., Olsson, A., Ju, Q., Rahman, M.A., and Grathwohl, P. (2006) Determination of transverse dispersion coefficients from reactive plume lengths. *Ground Water* 44: 212-221.

Clark, I.D., and Fritz, P. (1997) *Environmental isotopes in hydrogeology.* CRC Press LLC, Boca Raton, USA.

Coates, J.D., and Anderson, R.T. (2000) Emerging techniques for anaerobic bioremediation of contaminated environments. *Trends in Biotechnology* 18: 408-412.

Dempster, H.S., Sherwood Lollar, B., and Feenstra, S. (1997) Tracing organic contaminants in groundwater: a new method using compound-specific isotopic analysis. *Environ Sci Technol* 31: 3193-3197.

Einarson, M.D., and Cherry, J.A. (2002) A new multilevel groundwater monitoring system using multichannel tubing. *Ground Water Monit. Rem.* 4: 52-65.

Elsner, M., Zwank, L., Hunkeler, D., and Schwarzenbach, R.P. (2005) A new concept linking observable stable isotope fractionation to transformation pathways of organic pollutants. *Environ Sci Technol* 39: 6896-6916.

European Commission (2008). The EU Water Framework Directive - integrated river basin management for Europe.
http://ec.europa.eu/environment/water/water-framework/index_en.html

Franzmann, P.D., Patterson, B.M., Power, T.R., Nichols, P.D., and Davis, G.B. (1996) Microbial biomass in a shallow, urban aquifer contaminated with aromatic hydrocarbons: analysis by phospholipid fatty acid content and composition. *J Appl Bacteriol* 80: 617-625.

Fredrickson, J.F., and Fletcher, M.M. (2001) *Subsurface Microbiology and Biogeochemistry.*: John Wiley & Sons, Inc., New York.

Freeman, C., Liska, G., Ostle, N.J., Jones, S.E., and Lock, M.A. (1995) The use of fluorogenic substrates for measuring enzyme activity in peatlands. *Plant Soil* 175: 147-152.

Gibert, J., Danielopol, D.L., and Stanford, J.A. (1994) *Groundwater Ecology*. Academic Press Ltd., London, UK.

Gibson, J., and Harwood, C. S. (2002) Metabolic diversity in aromatic compound utilization by anaerobic microbes. *Annu Rev Microbiol* 56: 345-369.

Griebler, C. (2001) Microbial ecology of the subsurface. In *Groundwater ecology. A tool for management of water resources.* Griebler, C., Danielopol, D.L., Gibert, J., Nachtnebel, H.P., and Notenboom, J. (eds): European Commission, Brussels, Belgium.

Griebler, C., Mindl, B., Slezak, D., and Geiger-Kaiser, M. (2002) Distribution patterns of attached and suspended bacteria in pristine and contaminated shallow aquifers studied with an *in situ* sediment exposure microcosm. *Aquat Microb Ecol* 28: 117-129.

Griebler, C., Safinowski, M., Vieth, A., Richnow, H.H., and Meckenstock, R.U. (2004) Combined application of stable carbon isotope analysis and specific metabolites determination for assessing *in situ* degradation of aromatic hydrocarbons in a tar oil-contaminated aquifer. *Environ Sci Technol* 38: 617-631.

Haack, S.K., and Bekins, B.A. (2000) Microbial populations in contaminant plumes. *Hydrogeol J* 8: 63-76.

Ham, P.A.S., Schotting, R.J., Prommer, H., and Davis, G.B. (2004) Effects of hydrodynamic dispersion on plume lengths for instantaneous bimolecular reactions. *Adv Water Res* 27: 803-813.

Harrison, I., Williams, G.M., Higgo, J.J., Leader, R.U., Kim, A.W., and Noy, D.J. (2001) Microcosm studies of microbial degradation in a coal tar distillate plume. *J Contam Hydrol* 53: 319-340.

Heider, J., Spormann, A.M., Beller, H.R., and Widdel, F. (1999) Anaerobic bacterial metabolism of hydrocarbons. *FEMS Microbiol Rev* 22: 459-473.

Höhener, P., Hunkeler, D., Hess, A., Bregnard, T., and Zeyer, J. (1998) Methodology for the evaluation of engineered *in situ* bioremediation: lessons from a case study. *Journal of Microbiological Methods* 32: 179-192.

Hunkeler, D., Höhener, P., and Zeyer, J. (2002) Engineered and subsequent intrinsic *in situ* bioremediation of a diesel fuel contaminated aquifer. *J Contam Hydrol* 59: 231-245.

Jochmann, M.A., Blessing, M., Haderlein, S.B., and Schmidt, T.C. (2006) A new approach to determine method detection limits for compound-specific isotope analysis of volatile organic compounds. *Rapid Commun Mass Spectrom* 20: 3639-3648.

Kendall, C., and Caldwell, E.A. (1998) Fundamentals of Isotope Geochemistry. In *Isotope Tracers in Catchment Hydrology*. Kendall, C., and McDonnell, J.J. (eds). Elsevier Science B.V., Amsterdam NL, pp. 51-86.

Kirchman, D., K'Nees, E., and Hodson, R. (1985) Leucine incorporation and its potential as a measure of protein synthesis by bacteria in natural aquatic systems. *Appl Environ Microbiol* 49: 599-607.

Kirk, J.L., Beaudette, L.A., Hart, M., Moutoglis, P., Klironomos, J.N., Lee, H., and Trevors, J.T. (2004) Methods of studying soil microbial diversity. *J Microbiol Methods* 58: 169-188.

Lehman, R.M., and O'Connell, S.P. (2002) Comparison of extracellular enzyme activities and community composition of attached and free-living bacteria in porous medium columns. *Appl Environ Microbiol* 68: 1569-1575.

Leuthner, B., and Heider, J. (2000) Anaerobic toluene catabolism of *Thauera aromatica*: the bbs operon codes for enzymes of beta oxidation of the intermediate benzylsuccinate. *J Bacteriol* 182: 272-277.

Lovley, D.R. (2001) Anaerobes to the rescue. *Science* 293: 1444-1446.

Lovley, D.R. (2003) Cleaning up with genomics: applying molecular biology to bioremediation. *Nat Rev Microbiol* 1: 35-44.

Lovley, D.R., and Chapelle, F.H. (1995) Deep subsurface microbial processes. *Rev Geophys* 33: 365-381.

Ludvigsen, L., Albrechtsen, H., Ringelberg, D.B., Ekelund, F., and Christensen, T.H. (1999) Distribution and composition of microbial populations in a landfill leachate contaminated aquifer (Grindsted, Denmark). *Microb Ecol* 37: 197-207.

Madsen, E.L., and Ghiorse, W.C. (1993) Groundwater microbiology: subsurface ecosystem processes. In *Aquatic microbiology – an ecological approach.*: Blackwell Scientific Publications, pp. 167-213.

Maier, U., Rügner, H., and Grathwohl, P. (2007) Gradients controlling natural attenuation of ammonium. *Appl Geochem* 22: 2606-2617.

Mancini, S.A., Ulrich, A.C., Lacrampe-Couloume, G., Sleep, B., Edwards, E.A., and Lollar, B.S. (2003) Carbon and hydrogen isotopic fractionation during anaerobic biodegradation of benzene. *Appl Environ Microbiol* 69: 191-198.

Mayer, K.U., Benner, S.G., Frind, E.O., Thornton, S.F., and Lerner, D.N. (2001) Reactive transport modeling of processes controlling the distribution and natural attenuation of phenolic compounds in a deep sandstone aquifer. *J Contam Hydrol* 53: 341-368.

McGuire, J.T., Long, D.T., and Hyndman, D.W. (2005) Analysis of recharge-induced geochemical change in a contaminated aquifer. *Ground Water* 43: 518-530.

Meckenstock, R., Safinowski, M., and Griebler, C. (2004a) Anaerobic degradation of polycyclic aromatic hydrocarbons. *FEMS Microbiol Ecol* 49: 27-36.

Meckenstock, R.U. (1999) Fermentative toluene degradation in anaerobic defined syntrophic cocultures. *FEMS Microbiol Lett* 177: 67-73.

Meckenstock, R.U., Morasch, B., Griebler, C., and Richnow, H.H. (2004b) Stable isotope fractionation analysis as a tool to monitor biodegradation in contaminated acquifers. *J Contam Hydrol* 75: 215-255.

Meier-Augenstein, W. (1999) Applied gas chromatography coupled to isotope ratio mass spectrometry. *J Chromatogr A* 842: 351-371.

O'Donnell, A.G., Young, I.M., Rushton, S.P., Shirley, M.D., and Crawford, J.W. (2007) Visualization, modelling and prediction in soil microbiology. *Nat Rev Microbiol* 5: 689-699.

Oremland, R.S., Capone, D.G., Stolz, J.F., and Fuhrman, J. (2005) Whither or wither geomicrobiology in the era of 'community metagenomics'. *Nat Rev Microbiol* 3: 572-578.

OSWER Directive Initiation Request (1999).
http://www.epa.gov/swerust1/directiv/d9200417.pdf

Phelps, T.J., Pfiffner, S.M., Sargent, K.A., and White, D. (1994) Factors influencing the abundance and metabolic capacities of microorganisms in eastern coastal plain sediments. *Microb Ecol* 28: 351-364.

Philp, J., Bamforth, S.M., Singleton, I., and Atlas, R.M. (2005) Environmental pollution and restoration: a role for bioremediation. In *Bioremediation*. Atlas, R.M., and Philp, J. (eds). ASM Press, Washington, DC.

Postma, D., and Jakobsen, R. (1996) Redox zonation: equilibrium constraints on the Fe (III)/SO$_4^{2-}$reduction interface. *Geochim Cosmochim Acta* 60: 3169-3175.

Prommer, H., and Barry, D.A. (2005) Modeling bioremediation of contaminated groundwater. In *Bioremediation*. Atlas, R.M., and Philp, J. (eds). ASM Press Washington, DC.

Prommer, H., Barry, D.A., and Davis, G.B. (2002) Modelling of physical and reactive processes during biodegradation of a hydrocarbon plume under transient groundwater flow conditions. *J Contam Hydrol* 59: 113-131.

Prommer, H., Tuxen, N., and Bjerg, P.L. (2006) Fringe-controlled natural attenuation of phenoxy acids in a landfill plume: integration of field-scale processes by reactive transport modeling. *Environ Sci Technol* 40: 4732-4738.

Puls, R.W., and Barcelona, M.J. (1996) Low-flow (minimal drawdown) groundwater sampling procedures. In *EPA Groundwater Issue, April 1996*. US-EPA (ed), p. 12.

Richnow, H.H., Annweiler, E., Michaelis, W., and Meckenstock, R.U. (2003a) Microbial *in situ* degradation of aromatic hydrocarbons in a contaminated aquifer monitored by carbon isotope fractionation. *J Contam Hydrol* 65: 101-120.

Richnow, H.H., Meckenstock, R.U., Reitzel, L.A., Baun, A., Ledin, A., and Christensen, T.H. (2003b) *In situ* biodegradation determined by carbon isotope fractionation of aromatic hydrocarbons in an anaerobic landfill leachate plume (Vejen, Denmark). *J Contam Hydrol* 64: 59-72.

Rifai, H.S., and Bedient, P.B. (1990) Comparison of biodegradation kinetics with an instantaneous reaction model for groundwater. *Water Resour Res* 26: 637-645.

Rotthauwe, J.H., Witzel, K.P., and Liesack, W. (1997) The ammonia monooxygenase structural gene amoA as a functional marker: molecular fine-scale analysis of natural ammonia-oxidizing populations. *Appl Environ Microbiol* 63: 4704-4712.

Safinowski, M., Griebler, C., and Meckenstock, R.U. (2006) Anaerobic cometabolic transformation of polycyclic and heterocyclic aromatic hydrocarbons: evidence from laboratory and field studies. *Environ Sci Technol* 40: 4165-4173.

Schmidt, T.C., Zwank, L., Elsner, M., Berg, M., Meckenstock, R.U., and Haderlein, S.B. (2004) Compound-specific stable isotope analysis of organic contaminants in natural environments: a critical review of the state of the art, prospects, and future challenges. *Anal Bioanal Chem* 378: 283-300.

Spormann, A.M., and Widdel, F. (2000) Metabolism of alkylbenzenes, alkanes, and other hydrocarbons in anaerobic bacteria. *Biodegradation* 11: 85-105.

Stumm, W., and Morgan, J.J. (1996) *Aquatic Chemistry*: John Wiley & Sons Inc, New York.

Thornton, S.F., Lerner, D.N., and Davison, R.M. (2002) Groundwater monitoring. In *Encyclopedia of Environments*. El-Shaarawi, A.H., and Piegorsch, W.W. (eds). John Wiley & Sons, Ltd., Chichester, UK, pp. 960-974.

Torsvik, V., Daae, F.L., Sandaa, R.A., and Ovreas, L. (1998) Novel techniques for analysing microbial diversity in natural and perturbed environments. *J Biotechnol* 64: 53-62.

Tyson, G.W., and Banfield, J.F. (2005) Cultivating the uncultivated: a community genomics perspective. *Trends Microbiol* 13: 411-415.

UBA (2006) Bundesweite Übersicht zur Altlastenstatistik. www.umweltbundesamt.de/boden-und-altlasten/altlast/web1/deutsch/1_3.htm

UN Water (2006). Coping with water scarcity. A strategic issue and priority for system-wide action. www.un.org/waterforlifedecade/

Wagner, M., Nielsen, P.H., Loy, A., Nielsen, J.L., and Daims, H. (2006) Linking microbial community structure with function: fluorescence *in situ* hybridization-microautoradiography and isotope arrays. *Curr Opin Biotechnol* 17: 83-91.

Werth, C.J., Cirpka, O.A., and Grathwohl, P. (2006) Enhanced mixing and reaction through flow focusing in heterogeneous porous media. *Wat Res Research* 42: 1-10.

Widdel, F., and Rabus, R. (2001) Anaerobic biodegradation of saturated and aromatic hydrocarbons. *Curr Opin Biotechnol* 12: 259-276.

Wiedemeier, T.H., Rifai, H.S., Newell, C.J., and Wilson, J.T. (1999) *Natural Attenuation of Fuels and Chlorinated Solvents in the Subsurface*: John Wiley & Sons, New York.

Wilson, R.D., Thornton, S.F., and Mackay, D.M. (2004) Challenges in monitoring the natural attenuation of spatially variable plumes. *Biodegradation* 15: 359-369.

Winderl, C., Schaefer, S., and Lueders, T. (2007) Detection of anaerobic toluene and hydrocarbon degraders in contaminated aquifers using benzylsuccinate synthase (bssA) genes as a functional marker. *Environ Microbiol* 9: 1035-1046.

Winderl, C., Anneser, B., Griebler, C., Meckenstock, R.U., and Lueders, T. (2008) Depth-resolved quantification of anaerobic toluene degraders and aquifer microbial community patterns in distinct redox zones of a tar oil contaminant plume. *Appl Environ Microbiol* 74: 792-801.

Young, L.Y., and Phelps, C.D. (2005) Metabolic biomarkers for monitoring *in situ* anaerobic hydrocarbon degradation. *Environ Health Perspect* 113: 62-67.

Zwank, L., Berg, M., Schmidt, T.C., and Haderlein, S.B. (2003) Compound-specific carbon isotope analysis of volatile organic compounds in the low-microgram per liter range. *Anal Chem* 75: 5575-5583.

2.   Application of high-resolution groundwater sampling in a tar oil-contaminated sandy aquifer. Studies on small-scale abiotic gradients.

2.1. Introduction

Organic hydrocarbons, such as the monoaromatic compounds benzene, toluene, ethylbenzene and xylene (BTEX), as well as polycyclic aromatic hydrocarbons (PAH), which have quantitatively been released during tar oil processing and still enter the environment accidentally, rank among the most important pollutants threatening groundwater quality in industrialized regions. According to their individual characteristics, the more soluble compounds partition from the non-aqueous phase into groundwater and are subsequently transported with groundwater flow (Christensen et al., 2000). In mature and quasi-steady state hydrocarbon plumes, however, the release of compounds from the non-aqueous phase liquids (NAPL) equals the removal of contaminants via microbiological degradation, thus preventing a further expansion of the plume. In such cases, Monitored Natural Attenuation (MNA), which makes use of the intrinsic self-remediation potential of groundwater ecosystems, may represent a cost- and labour-efficient site management strategy (Wiedemeier et al., 1999; Lovley, 2001).

In order to evaluate the hypothesis of mixing-controlled biodegradation, which so far was only proven in numerical models and lab experiments (Cirpka et al., 1999; Prommer et al., 2006), sophisticated sampling methods are required to capture the steep counter gradients arising at transition zones. However, the poor accessibility, the heterogeneity, and the physical-chemical complexity of subsurface environments considerably hamper the collection of detailed information on the spatial distribution of *in situ* biodegradation activities, thus complicating the transferability of these findings to field conditions. Hence, the existence of steep, small-scale biogeochemical gradients as indicators of enhanced bioactivities at transition zones remains rather speculative to date.

Normally, collection of groundwater samples is performed using either fully screened monitoring wells or, for depth-resolved withdrawal of groundwater, by means of conventional multi-level wells (C-MLW), which are usually restricted to a 0.5 to 1 m vertical sampling resolution. A few examples of high-resolution sampling efforts are reported in the literature. Van Breukelen and co-workers, for instance, investigated processes occurring at the fringe of a landfill leachate plume using a "nested" multi-level arrangement. In this approach, a cluster of three multi-level wells with screening intervals of 0.3 m each were inserted at 0.5 m horizontal distance from each other (van Breukelen and Griffioen, 2004). This allowed collection of groundwater samples at a vertical resolution of 0.1 to 0.15 m. A distinctly different approach was applied in a study of Ronen et al. (2005), who aimed at resolving gradients arising within an aquifer contaminated with volatile organic compounds (VOC). In this case, conventional pumping of groundwater was not suitable because of the volatility of the analytes. Degassing during sampling consequently was circumvented by use of stainless steel dialysis cells, which were arranged in a modular manner at 6 cm vertical intervals within a continuous PVC tube. Passive diffusion of compounds from groundwater, even from porewater of the unsaturated zone, allowed detection of gradients of different metabolites (e.g. TCE, PCE and DCE) across the saturated-unsaturated interface. Recently, passive diffusion samplers were applied in a landfill leachate-contaminated aquifer in order to investigate biogeochemical gradients arising across various types of transition zones. Using these "peepers", sediment-water and silt-sand interfaces were described at a unique resolution of only $0.5 - 1$ cm (Báez-Cazull et al., 2007). Analytical biases regarding the small sample volumes obtained by this approach were tackled by use of capillary electrophoresis, a technique that allows detection of important analytes from even microliter sample volumes.

The present study also points out the need for scale-adapted groundwater sampling, describing a first data set obtained from investigations at a sandy tar oil-contaminated aquifer by means of a novel high-resolution multi-level well. Groundwater sampled at vertical intervals of 2.5 to 33 cm across a BTEX plume revealed details that remained undetected applying a conventional monitoring well with a resolution of 0.5 to 1 m. The steep, small-scale biogeochemical gradients arising predominantly at the plume fringe were used to assess prevailing redox processes and to evaluate potential factors limiting biodegradation.

2.2.   Field site description

The study area is a Quaternary sandy aquifer located at a former gasworks site in the Rhine valley in the district Düsseldorf – Flingern, Germany (Fig. 2.1A). Apart from thin gravel inclusions in deeper layers (>12 m below land surface (bls)), the sandy sediments show a relatively homogeneous composition with a mean permeability of $k_f = 1 \times 10^{-3}$ m s^{-1}, which was previously determined via pumping tests and *in situ* flow meter measurements (Eckert, 2001). Low permeability Tertiary fine sand layers confine the aquifer at a depth of about 15 m bls. Groundwater moves from east to west with an average flow velocity of 0.5 - 2 m d^{-1}, following a hydraulic gradient of about 6 ‰ (Fig. 2.1B).
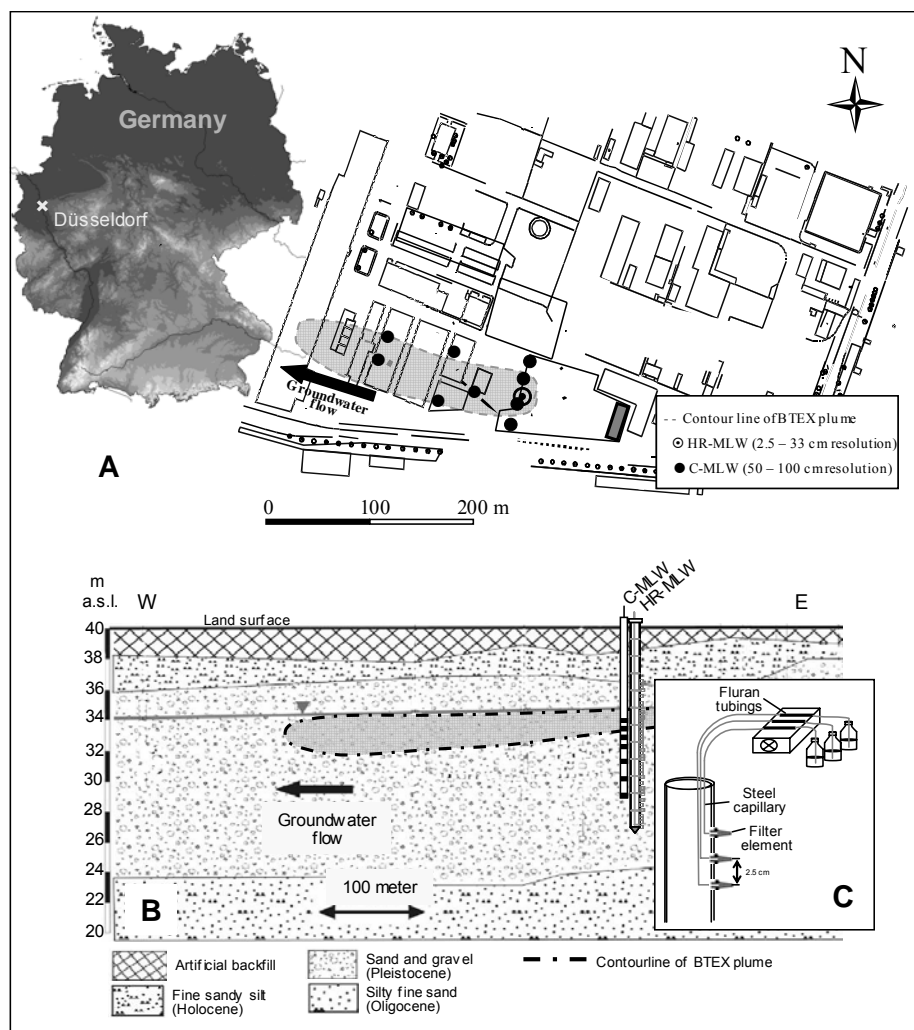
Figure 2.1 A) Schematic view of the sampling area, B) cross section through the studied aquifer, showing the position of the high-resolution multi-level well (HR-MLW) and the conventional multi-level well (C-MLW) in relation to the BTEX plume; C) detailed view of filter screens and sampling equipment assembly.

From 1893 until 1967, benzene, gas, coke, and different tar oil components were produced on an area of about 170,000 m^2. Operation and break-down of the plant in 1968, following partial destruction during the Second World War, caused a significant release of aromatic hydrocarbons into the subsurface, resulting in concentrations of more than 100 mg l^{-1} of benzene, toluene, ethylbenzene and xylenes (BTEX) and ~ 20 mg l^{-1} of total polycyclic aromatic hydrocarbons (PAHs). In order to prevent further spreading of the contaminant plume, which initially exhibited a length of about 600 m and a width of 100 m, 55,000 m^3 of soil were excavated and thermally treated for cleanup. The removed contaminated soil was replaced by clean sand and gravel.

Even though the major part of the tar oil phase could be removed successfully, reducing the plume extension to approx. 200 × 40 m, the target soil sanitation threshold of 2 mg kg^{-1} for BTEX and 5 mg kg^{-1} for PAH was not achieved and considerable amounts of mono- and polycyclic aromatic hydrocarbons are still detectable within groundwater and sediments.

2.3. Materials and methods

2.3.1. Evaluation of sampling procedure and materials

Owing to the high sorption affinity and volatility of aromatic hydrocarbons, the materials and methods for groundwater sampling had to be carefully selected in advance. In preceding pumping tests using multi-channel peristaltic pumps, three different tube materials were tested for their suitability concerning sorption and permeability of aromatic hydrocarbons (see Tab. 2.1).

Table 2.1 Tube types tested with regard to loss of aromatic hydrocarbons by sorption.

	Tygon ST R-3603	Tygon HC F-4040A	Fluran HCA F5500-A
Characteristics[a]	allround tube for different applications	specific for hydrocarbons and mineral oil products	highly resistant against chemicals, oils, fuels, and solvents
Gas permeability[a]	high	medium	low

[a] according to manufacturer specifications (Ismatec, Wertheim, Germany)

A 30 µM toluene stock solution was pumped at a rate of 2 ml min^{-1} through the individual tubes (in duplicates) by means of a peristaltic pump. Non-tube interconnections were bridged with inert and impermeable steel capillaries. After passage through the tubes, samples were collected at set time intervals and toluene concentrations determined via HPLC. For each tube type, the loss of toluene was calculated by difference to the initial toluene concentration.

The tube material showing the least loss over time, *i.e.* Fluran (see Section 2.4.1), was tested in a subsequent experiment, in which the tubes were equilibrated or saturated by passage of a solution for several hours containing different concentrations of toluene (500 µM), benzene (5.5 µM) or ethylbenzene (12 µM) as model compounds. At certain time intervals, the amounts of the individual compounds were determined via GC-MS analysis and the contaminant losses were again calculated from the difference from the initial concentration. The individual concentrations of the selected contaminants were chosen according to the known contaminants in the aquifer, where toluene always constituted the

major contaminant and ethylbenzene and benzene were found at concentrations one to two orders of magnitude lower.

2.3.2. Groundwater sampling

Groundwater from several depths in the upper saturated zone was collected in September 2005 at vertical intervals of 2.5 – 33 cm using a specially designed high-resolution multi-level well (HR-MLW). The well consists of 12 single high-density polyethylene (HDPE) tubes (15 cm inner diameter) equipped with filter units ($\varnothing$ 1 cm) at pre-selected depths. The degree of spatial resolution and the location of the filter ports were chosen in correspondence with the location of the plume center and fringes, which were derived from the gradients of an adjacent monitoring well (see below). Loss of contaminants by sorption or volatilization during sampling was avoided by use of steel capillaries, which were connected to a peristaltic pump via low sorption Fluran tubes. In order to prevent hydraulic shortcuts, 28 selected ports were sampled simultaneously at low pumping rates adjusted close to natural groundwater flow conditions.

For comparison of high-resolution vs. customary groundwater sampling, a conventional multi-level well (C-MLW), which is located 1 m distant to the high-resolution well (Fig. 2.1B), was sampled four weeks later. This C-MLW is equipped with 5 cm filter elements exhibiting a vertical spacing of 0.5 to 1 m. Groundwater samples from this well were withdrawn through teflon tubes at a rate of several litres per minute by use of a multi-channel suction pump.

2.3.3. Sample preparation and analysis

Groundwater from the HR-MLW was collected in 100 ml pre-washed narrow-neck bottles and subsampled immediately after collection for the analysis of various biotic and abiotic parameters.

For analysis of dissolved sulfide, 200 µl of groundwater were fixed in duplicates in 1 ml of a 2% (w/v) zinc acetate solution and processed according to the protocol of Cline (1969). Samples were measured photometrically directly on site. For determination of soluble Fe(II), 100 µl of groundwater were fixed in 900 µl 1M HCl and concentrations measured photometrically following the ferrozine assay of Stookey (1970).

For BTEX analysis, a sample volume of 3 ml was transferred in duplicates into 10 ml GC-headspace vials. Samples from the field site were additionally amended with 300 µl of 1M NaOH (final concentration 0.1M) to terminate biological activity. Vials were sealed with gas tight polytetrafluoroethylene (PTFE) septa. Field samples dedicated to analysis of the priority polycyclic aromatic hydrocarbon (PAH) species as defined by the US Environmental Protection Agency (16 EPA-PAHs) were filled into 15 ml Supelco glass vials (Supelco/Sigma-Aldrich, Munich, Germany), fixed with NaOH (final concentration 0.1M) and closed avoiding headspace using PTFE-coated screw caps. BTEX and PAH samples were stored at 4°C in the dark until further analysis.

Concentrations of BTEX were determined by HPLC (tube tests) or GC-MS analysis (field samples), respectively. Samples dedicated to HPLC measurements and UV/vis detection at 210 nm were fixed 1:10 with 96% ethanol and measured on a HPLC equipped with a Hyperchrome column NC-03-200 (200 × 3.0 mm) that contained a PRONTOSIL 120-3-C18-H 3.0 µm filling as stationary phase (Bischoff Chromatography, Leonberg, Germany). A mixture of 70/30 (v/v) acetonitrile/water was used at a constant flow rate of 0.6 ml min^{-1} as mobile phase. The concentrations of the aromatic hydrocarbons were calculated using external calibration with the pure substances (for further information see Jahn et al., 2005).

Determination of BTEX concentrations using GC-MS (Trace DSQ, Thermo Electron, Dreieich, Germany) was done by headspace analysis, while EPA-PAHs were analyzed by liquid injection after extraction from the groundwater sample with cyclohexane during 60 min of intensive shaking at room temperature. Further details on the analysis of both contaminant groups are given in section 4.3.3.2 and Anneser et al., 2008.

After filtration of the sample through a 0.45 μm pore size filter, major anions and cations were measured by ion chromatography. Dissolved organic carbon (DOC) contents were determined in a TOC analyzer (TOC 500, Shimadzu Co.) after combustion of organic carbon at 650°C.

Sampling and analysis of groundwater from the C-MLW were performed by an analytical lab of the Stadtwerke Düsseldorf AG. By means of a multi-channel suction pump, which was operated at a rate of several liters per minute, groundwater was sampled simultaneously from all investigated filter screens of the C-MLW. Samples for physical-chemcial analysis were collected in appropriate synthetic or glass vessels after achieving stability of physical parameters. For analysis of BTEX, PAH, DOC, and cations, samples were acidified by addition of 30% HCl. Analysis of BTEX and PAH was performed on a GC-MS, and DOC was determined by catalytical combustion. Concentrations of anions were measured by ion chromatography, cations were determined via atomic absorption spectrometry (AAS). For further details on the protocols used for analysis see section 4.3.3.2 and Anneser et al., 2008.

2.4. Results

2.4.1. Pumping tests

Prior to sampling in the field, different tube materials were tested for their suitability regarding sorption and contaminant permeability (indirect volatilization) during pumping. While the Tygon tubings both exhibited over 5 hours a more or less constant loss of toluene of about 25% and 50%, respectively, the loss through the Fluran material continuously declined from as high as 56% in the first minutes to 13% after pumping $\geq$ 1.75 h (Fig. 2.2A).
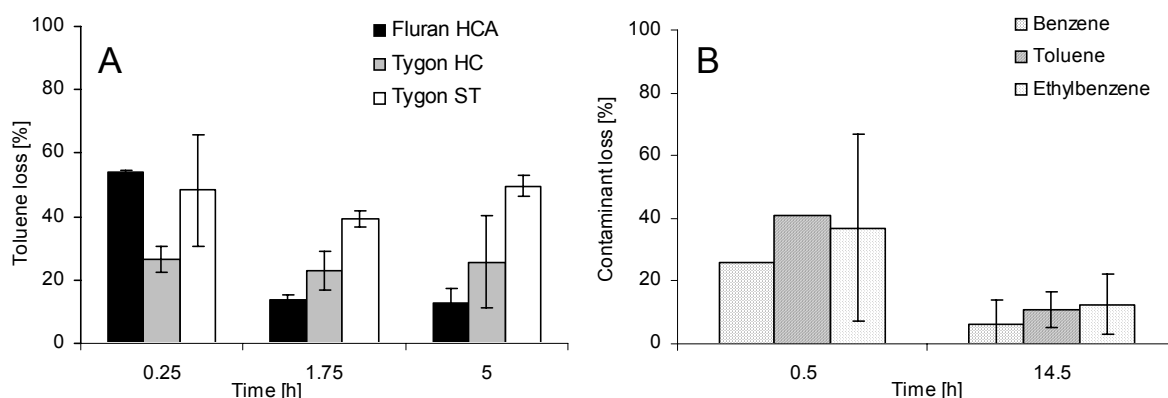
Figure 2.2 A) Mass losses of toluene during 5 hours of fast pumping (2 ml min^{-1}) through different types of peristaltic tubes; B) development of mass losses of model aromatic compounds during 14.5 hours of slow pumping through Fluran HCA tubes. Values represent means of duplicate measurements ($\pm$ SD) or, in a few cases, single measurements.

Consequently, Fluran was chosen for a further pumping test, where the time required for equilibration-saturation was evaluated. As can be seen in Fig. 2.2B, after pumping for about 14.5 hours the contaminant losses were reduced to about 10% on average, which was considered to be acceptable for determination of contaminant concentrations in the field.

2.4.2. Distribution of contaminants and selected physical-chemical parameters in the tar oil-contaminated aquifer

The vertical distribution of BTEX compounds determined with the high-resolution multi-level well (HR-MLW) was restricted to a narrow zone beneath the groundwater table (6.41 m below land surface [bls] at time of sampling) and extended to only about 1.1 m in depth (Fig. 2.3A). Gradients for BTEX as well as for naphthalene exhibited a steep decrease at the lower plume fringe, with a reduction in measured concentrations by more than two orders of magnitude within only 0.21 m. At 7.31 m bls, BTEX concentrations fell below detection limit. In contrast, groundwater samples obtained from the conventional multi-level well (C-MLW) implied a BTEX plume more than 1.5 m wide. Furthermore, contaminant concentrations were significantly underestimated by samples originating from the low-resolution well, as shown in figures 2.3A and 2.4A.

Analyses of the 16 EPA-PAHs exhibited comparably low concentrations of the higher-molecular compounds acenaphthene and fluorene within the BTEX zone (Fig. 2.3B). With depth, concentrations of these compounds increased, but constantly remained below 1.0 mg l^{-1}. With the exception of acenaphthene, which was significantly overestimated within groundwater from the C-MLW, concentrations of naphthalene and total EPA-PAHs were considerably underestimated when compared to the HR-MLW samples.

Maximum DOC concentrations were observed, as expected, in the zone of highest contamination (Fig. 2.3C). Starting with maximum concentrations at the uppermost sampling port, DOC exhibited a continuous decrease down to a depth of 7 m bls, followed by a less pronounced gradient to 8 m bls, where DOC started to level off at about 6 mg l^{-1}. In the case of the C-MLW, DOC values revealed much higher concentrations at the first two sampling depths (Fig. 2.3C). This is probably due to sample preparation, since DOC samples taken from the HR-MLW had been subject to volatilization during comparable long standing times in the autosampler of the TOC analyzer.

Redox potential values indicated anoxic conditions across the saturated zone, with most reduced conditions prevailing in the zone of highest contamination. In contrast, groundwater samples collected from the C-MLW exhibited aerobic conditions at all sampled depths (Fig. 2.3D). A better match of high-resolution and low-resolution data was obtained for the pH (Fig. 2.3E). However, highest pH values determined from the HR-MLW were measured at 6.81 m bls, while the C-MLW exhibited a pH maximum at 8 m bls. Similarly, vertical patterns of specific conductivity were comparable for both the high-resolution and the conventional MLW, with exception of the uppermost C-MLW value (Fig. 2.3F). Within the first 1.6 m below the groundwater table specific conductivity, as determined in HR-MLW samples, increased from about 975 to 1150 µS cm^{-1} and started to level off at about 9 m bls, while the low resolution data showed no further change below 8 m bls.

2.4.3. Electron acceptors available and gradients indicating biodegradation

Of the monoaromatic hydrocarbons, toluene constituted the major contaminant, accounting for up to 75% of total BTEX. Similar to the distribution of BTEX, the toluene contamination zone was restricted to the upper 1.1 m below the water table (Fig. 2.4A).

From the gradients it was possible to delineate the BTEX plume core, which was defined as the zone exhibiting >50% of the maximal BTEX concentration. The groundwater table and the capillary fringe zone formed the border of the upper plume fringe. The definition of the border of the lower plume fringe was more difficult but was based on three premises. First, the lower fringe was in high accordance with observed HS$^-$ and Fe(II) peaks (Fig. 2.4 D+E), so where the Fe(II) and HS$^-$ peaks dropped we assumed the outer limit of the plume. Second, lab experiments indicated threshold concentrations for toluene degradation to range between 10 to 100 µg l^{-1} for sulfate and iron reduction (Schmid, 2004), which corresponds to the toluene concentrations measured at the depth interval of 7 – 8 m bls. Finally, molecular community analyses of the "sulfidogenic" fringe zone revealed a similar microbial community of low diversity, which was mainly constituted by highly specialized microorganisms (Winderl et al., 2008).
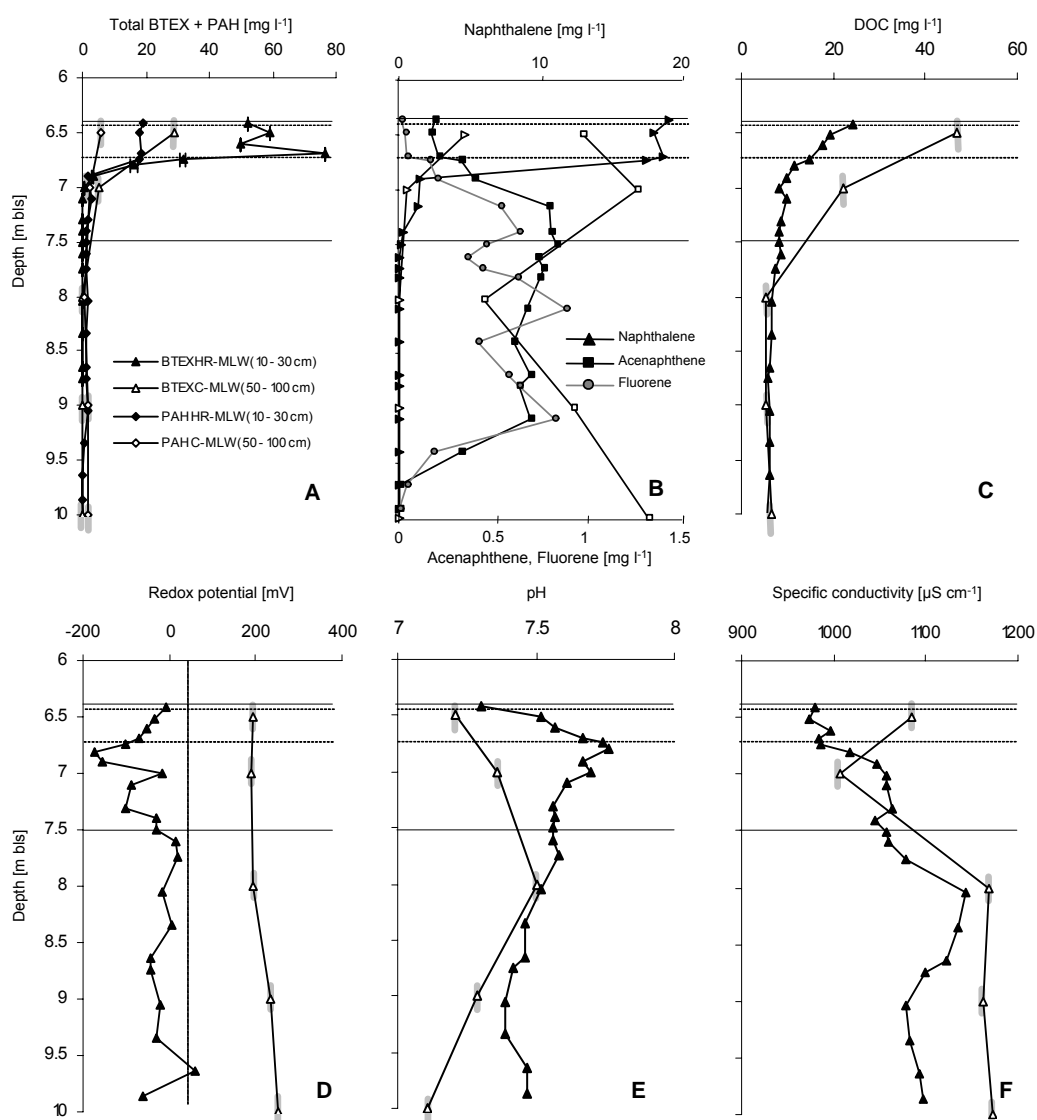
Figure 2.3 Vertical profiles of selected mono- and polycyclic aromatic hydrocarbons and dissolved organic carbon (DOC) as well as individual physico-chemical parameters derived from high-resolution (black symbols) and low-resolution (white symbols) groundwater sampling. Values represent means of duplicate measurements (± SD) or single measurements, respectively (no SD). The solid lines mark the estimated upper and lower border of the plume. The dashed lines depict the plume core defined by > 50% of the maximal BTEX concentration. For further information see text.

Scarcely any nitrate was available within the investigated plume section, exhibiting concentrations close to the detection limit of 0.1 mg l^{-1} throughout the major part of the investigated aquifer (Fig. 2.4B). Only at a depth of 7.3 m bls, at the inner lower plume fringe, a moderate nitrate peak was observed. By contrast, no variations in nitrate concentrations were detected in samples from the C-MLW, where measured values persistently amounted to 0.2 mg l^{-1}. Due to the "insolubility" of ferric iron, no information on its availability could be gained from water samples. However, referring to the analysis of sediment cores taken five months after the first groundwater sampling campaign in February 2006, hardly any ready extractable Fe(III) was available in the saturated zone below the capillary fringe (see section 3.4.2). Sulfate concentrations determined from HR-MLW samples partially indicated complete depletion in the upper part of the plume core. With increasing depth, a steep increase was observed until a maximum (background) concentration of about 240 mg l^{-1} was reached (Fig. 2.4C). Unfortunately, sulfate concentrations from the HR-MLW could be obtained only to a depth of 6.83 m. Concomitant with increasing sulfate concentrations towards the lower plume fringe two distinct sulfide peaks were observed (Fig. 2.4D), which were not displayed by data of the C-MLW. Here, the uppermost sampling point at 6.5 m bls exhibited the highest sulfide values. Analoguous to sulfide, high-resolution ferrous iron data showed steep, small-scale gradients and distinct peaks. Maximum concentrations were found directly below the groundwater table at 6.41 m bls, *i.e.* at the upper plume fringe (Fig. 2.4E). A second peak was detected at the lower plume fringe (6.81 m bls), along with maximum sulfide concentrations, and a third peak appeared at 8 m bls. Unfortunately, no Fe(II) concentrations were available from the C-MLW for comparison.
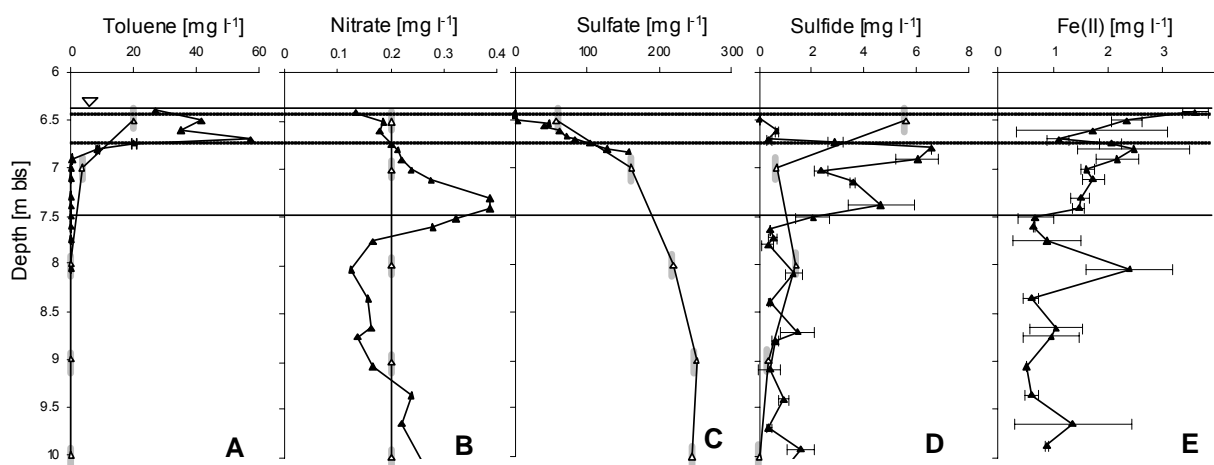
Figure 2.4 Vertical concentration profiles of toluene (model electron donor), nitrate, sulfate (electron acceptors) as well as sulfide and Fe(II) (metabolic end products), as determined in groundwater samples from the high-resolution multi-level well (black symbols). Open symbols depict concentrations resulting from low-resolution sampling at the C-MLW. The solid lines mark the estimated upper and lower border of the plume. The dashed lines depict the plume core defined by > 50% of the maximal toluene concentration.

2.5. Discussion

2.5.1. What gain in information do we get from high-resolution groundwater sampling?

Model simulations and bench-scale experiments, which represent valuable tools for evaluating the transport and fate of organic contaminants in porous media, substantially contributed to the understanding of biodegradation processes by pointing at the importance of

small-scale gradients at transition zones, *i.e.* the plume fringes, as hot spots of bioactivity (Cirpka et al., 1999; Prommer et al., 2006; Tuxen et al., 2006; Bauer et al., 2008; Rees et al., 2007). Improving the predictability of plume development by reactive transport models asks for continuous adaptation of input variables and, consequently, raises the claim for the collection of scale-adapted field data. According to McKinley (2001) "the finest scale of sampling that logistics allow will provide the best information on variations in microbiology and geochemistry". The gradients obtained from our high-resolution multi-level well (HR-MLW) confirm the need for scale-adapted sampling and impressively demonstrate the new gain in information compared to conventionally applied sampling strategies.

Striking differences regarding maximum concentrations and the spatial distribution of individual biogeochemical parameters became obvious from comparing data from the high-resolution MLW with data from the low-resolution MLW. As can be seen in Fig. 2.3 A+B and Fig. 2.4A, distinct gradients in the cm- to dm-scale reflect the architecture of the plume. Sampling of large volumes at high pumping rates has been reported to cause hydraulic shortcuts and mixing of groundwater from different depths, which typically leads to an underestimation of real concentrations (e.g. Puls and Barcelona, 1996). This is apparent when gradients of the HR-MLW and the C-MLW are compared (Fig. 2.4 A+B). The effect of sampling groundwater at larger intervals can also be demonstrated mathematically according to the following equation:

$$c_x = \frac{\sum \Delta z_i \times c_i}{\sum \Delta z_i} \qquad \text{(eq. 2.1),}$$

where c_i is the toluene concentration measured at a given depth i and Δz_i is the total distance associated with the given sampling interval. Fig. 2.5 shows that if groundwater had been collected at vertical intervals of 20 or 50 cm, the calculated maximal toluene concentration c_x at 6.5 m bls accounts for only 80% or 84%, respectively, of the maximum concentration determined from the high-resolution profile at the respective depth and for only 58% or 61%,
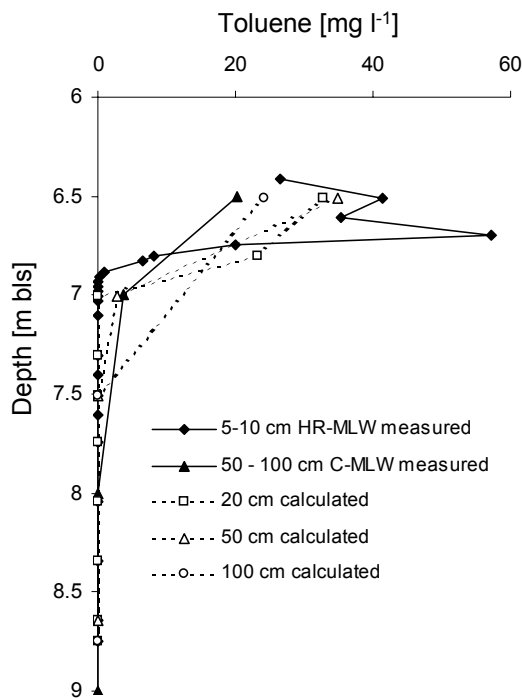
Figure 2.5 Calculated toluene gradients applying a sampling resolution of 20 cm (squares, dashed line), 50 cm (triangles, dashed line) or 100 cm (circles, dashed line), respectively, compared to toluene concentrations measured in groundwater samples from a conventional multi-level well (C-MLW; black triangles) and a high-resolution multi-level well (HR-MLW; black diamonds).

respectively, of the overall highest toluene concentration measured. Sampling at 100 cm intervals theoretically yields only 58% of the toluene concentration at 6.5 m bls, and only 42% of the highest toluene concentration measured. Comparing calculated and measured values shows that toluene concentrations derived from the C-MLW were even lower, exhibiting only 49% of the concentrations derived from high-resolution groundwater sampling.

Consequently, applying short filter screens and simultaneous sampling at pumping rates adapted to natural groundwater flow successfully reduces the risk of blending groundwater samples by hydraulic shortcuts. Even though low-flow pumping increases the risk of a loss of contaminants due to volatilization or sorption during passage in the sampling tubes, significantly higher concentrations were detected with the high-resolution approach compared to the conventional sampling technique. Laboratory experiments performed prior to sampling showed that the application of pre-saturated Fluran tubes minimized the loss of contaminants due to sorption (Fig. 2.2). Volatilization of compounds from the sampling vessels during pumping did not account for a loss of individual compounds of more than 10% (data not shown). Collecting groundwater at sampling rates adjusted to natural flow velocities only allows withdrawal of limited volumes, which may impede subsequent standard analytical measurements that often require hundreds of millilitres. Thus, in some cases only single measurements could be performed instead of duplicates and triplicates. Consequently, the development of high-resolution sampling methods at sites characterized by low compound concentrations at the same time requires elaboration of improved and highly efficient analytical methods (Báez-Cazull et al., 2007).

2.5.2.   What gradients can tell us about biodegradation processes

The detection of steep biogeochemical gradients allows the allocation of bioactive zones, which can be found where chemical disequilibria are present (Kappler et al., 2005). The gradients may help to identify dominant redox processes and indicate limiting factors for biodegradation.

In subsurface environments, where oxygen is limited and anoxic conditions prevail, redox processes are driven by the availability of alternative electron acceptors (e.g. (Christensen et al., 2000; Cozzarelli et al., 2001). As is evident from the high-resolution redox values, biodegradation at the study site almost exclusively takes place under reduced conditions (Fig. 2.3A). The uppermost sampling zone below the capillary fringe may temporarily receive some oxygen by recharge, which is likely to be depleted immediately for abiotic re-oxidation processes and aerobic respiration. The elevated Fe(II) values contradict oxic or even hypoxic conditions at time of sampling (Fig. 2.4E). Owing to the low nitrate concentrations, nitrate reduction is supposed to be only of minor importance for contaminant conversion at the point of investigation. This does not generally exclude nitrate reduction. There is strong evidence from upgradient areas for the oxidation of sulfides with nitrate. This was the result of a local upgradient infiltration experiment, which showed nitrate reduction coupled to oxidation of Fe^{2+} and FeS prior to oxidation of organic pollutants (Eckert and Appelo, 2002). While sulfate is nearly depleted in the plume center, considerable amounts are detected in the lower plume fringe and within deeper zones of the aquifer (Fig. 2.4C). Concomitant with increasing contaminant concentration, the availability of sulfate decreases in the plume center. At the same time, pronounced sulfide peaks were found in the fringe zone, hinting at sulfate reduction as one important redox process. Qualitative evidence for microbial sulfate reduction was obtained from compound-specific stable isotope analysis, i.e. determination of $\delta^{34}S$ and $\delta^{18}O$ of sulfate in groundwater samples collected at a later sampling date, which showed significant enrichment at the plume fringes, but also in the core zone (Anneser et al., 2008).

A previous study already indicated sulfate and iron reduction to be the dominant redox processes associated with contaminant removal at the Flingern site (Wisotzky and Eckert, 1997; Eckert, 2001). The ratio of dissolved sulfide to ferrous iron in water samples exhibited a clear prevalence of sulfide at the lower plume fringe, while the upper plume fringe and the core showed a surplus of Fe(II). Nevertheless, with increasing extent of contamination, the Fe(II) gradient decreased, but still exhibited concentrations >1 mg l^{-1}. The availability and/or accessibility of ferric iron seems strongly limited in the saturated zone, thus restricting biodegradation rates based on iron reduction. However, the low concentrations of dissolved sulfide and Fe(II) in the plume core may also be attributed to precipitation of FeS (Tucillo et al., 1999), which is indicated by deeply black-coloured sediments within this zone (Fig. 3.5).

At the lower plume fringe, elevated concentrations of both ferrous iron and sulfide are observed, showing a sulfide/Fe(II) ratio of 1.1. This may partly be a consequence of small FeS particles sampled together with groundwater. Alternatively, these peaks may hint at simultaneous sulfate and iron reduction, occurring at rates exceeding the kinetics of FeS precipitation. An overlap of redox zones has also been reported in previous plume studies (e.g. McGuire et al., 2002), suggesting that the co-occurrence of different redox processes is mainly attributed to the availability of electron acceptors, which corresponds to the partial equilibrium approach proposed by (Postma and Jakobsen, 1996; see also section 4.5.2). Competitive exclusion of specific terminal electron accepting processes due to thermodynamic constraints, as frequently hypothesized (Lovley and Chapelle, 1995; Franzmann et al., 2002), is therefore not mandatory.

Ratios of Fe(II) to sulfide suggest iron reduction processes to occur across the whole of the saturated zone, especially at the upper plume fringe (6.61 m bls), where infiltrating recharge is likely to trigger the iron cycle from time to time via re-oxidation of reduced iron species, thus enhancing the availability of ferric oxyhydroxides. Even though sulfate reduction activities at the upper plume fringe are not indicated by increased sulfide concentrations, stable isotope data of sulfate unambiguously prove microbially mediated sulfate reduction at both the upper and lower plume fringe as well as in the plume center (Anneser et al., 2008 and section 5.3.3). Re-oxidation of the reduced metabolite and precipitation of iron sulfides, however, are likely to scavenge free sulfide in groundwater, thus preventing its detection in the upper plume fringe and in the core (Ulrich et al., 1998; McGuire et al., 2002; Ulrich et al., 2003; Scholl et al., 2006).

2.5.3.   What limits biodegradation?

Numerous studies report the role of hydrodynamic mixing as a major controlling process of biodegradation within saturated porous aquifers (Mayer et al., 2001; Thullner et al., 2002; Cirpka, 2005). Model simulations, bench-scale experiments and field investigations successfully demonstrated increased bioactivities at the fringes of organic contaminant plumes (Prommer et al., 2006; Tuxen et al., 2006; Bauer et al., 2008; Baéz-Cazull et al., 2007). Ideally, steep counter-gradients of electron donors, electron acceptors and metabolites at the plume fringes point out the role of transverse dispersion. As observed in the Düsseldorf-Flingern aquifer, sulfate was not completely depleted in the plume center. Relatively broad zones of overlapping electron acceptors and electron donors contradict an instantaneous biodegradation as soon as electron donor and acceptor meet and suggest biodegradation to be additionally limited by factors other than dispersion. Those may be imposed by biokinetic constraints and the higher complexity of redox reactions like the reduction of SO_4^{2-} to HS^-, which is characterized by a number of individual reaction steps and intermediates with individual kinetics (Thornton et al., 2001; Safinowski et al., 2006; Bauer et al., 2008). Further factors may include the obviously low carrying capacity of BTEX-contaminated aquifers that also limits the total number of active degrading sites (= cells). Last but not least, toxicity of

individual contaminants or metabolites may significantly influence the distribution of bioactive zones. All of these circumstances may not allow for a fast instantaneous reaction.

Even though the relevance of transverse dispersion as the driving factor for biodegradation in porous media is indisputable, mixing processes affecting the entire aquifer, as they may arise due to changing hydraulic conditions or recharge events, so far have not been addressed at a spatially and temporally appropriate scale. Hydraulic fluctuations have been reported to cause a change in geochemical conditions and, consequently, in the composition of the microbial community (McGuire et al., 2002). Dilution of contaminants and supply of "fresh" electron acceptors and nutrients by groundwater recharge very likely promote conditions favourable to biodegradation (Röling and van Verseveld, 2002; Haack et al., 2004). However, disturbance of the surrounding environment may impose physiological stress to the mainly sediment-associated degrader community and cause deceleration of degradation reactions. Investigation of the site at a temporally and spatially high resolution in consideration of both biotic and abiotic variables as described in chapter 5 provided further insights into the dynamics and ecology of biodegradation.

2.6. Conclusions and outlook

Efficient and reasonable implementation of natural attenuation as a strategy for the management of contaminated aquifers demands a comprehensive understanding of the hydrogeology of the site and the processes involved in biodegradation. Monitoring techniques, which fail to reflect *in situ* conditions, impede the acceptance and implementation of such management concepts. The information provided by conventional long-screen monitoring wells may not quantitatively reflect groundwater quality, since measured concentrations only represent a composite of compounds and concentrations over the screened interval and fail to resolve gradients arising at small scales.

A novel, high-resolution multi-level well that was installed in a tar oil-contaminated sandy aquifer in Düsseldorf-Flingern, Germany, allowed to demonstrate the presence of small-scale physical-chemical gradients, which serve as indicators for the distribution of bioactive zones and help to get an insight into the complexity of anaerobic biodegradation processes. Albeit it was possible to assess dominant redox processes and to point out the importance of transverse dispersion as a major factor controlling biodegradation, broad overlapping zones of dissolved electron donors and electron acceptors hint at additional limiting factors in this anoxic aquifer. Moreover, further investigations will address the impact of temporal and spatial fluctuations on biodegradation rates.

2.7. References

Anneser, B., Einsiedl, F., Meckenstock, R.U., Richters, L., Wisotzky, F., and Griebler, C. (2008) High-resolution monitoring of biogeochemical gradients in a tar oil-contaminated aquifer. *Appl Geochem* 23: 1715-1730.

Báez-Cazull, S.B., McGuire, J.T., Cozzarelli, I.M., Raymond, A., and Welsh, L. (2007) Centimeter-scale characterization of biogeochemical gradients at a wetland-aquifer interface using capillary electrophoresis. *Appl Geochem* 22: 2664-2683.

Bauer, R.D., Maloszewski, P., Zhang, Y., Meckenstock, R.U., and Griebler, C. (2008) Mixing-controlled biodegradation in a toluene plume - Results from two-dimensional laboratory experiments. *J Contam Hydrol* 96: 150-168.

Christensen, T.H., Bjerg, P.L., Banwart, S.A., Jakobsen, R., Heron, G., and Albrechtsen, H.-J. (2000) Characterization of redox conditions in groundwater contaminant plumes. *J Contam Hydrol* 45: 165-241.

Cirpka, O.A. (2005) Effects of sorption on transverse mixing in transient flows. *J Contam Hydrol* 78: 207-229.

Cirpka, O.A., Frind, E.O., and Helmig, R. (1999) Numerical simulation of biodegradation controlled by transverse mixing. *J Contam Hydrol* 40: 159-182.

Cline, J.D. (1969) Spectrophotometric determination of hydrogen sulfide in natural waters. *Limnol Oceanogr* 14: 454-458.

Cozzarelli, I.M., Bekins, B.A., Baedecker, M.J., Aiken, G.R., Eganhouse, R.P., and Tuccillo, M.E. (2001) Progression of natural attenuation processes at a crude-oil spill site: I. Geochemical evolution of the plume. *J Contam Hydrol* 53: 369-385.

Eckert, P. (2001) Untersuchungen zur Wirksamkeit und Stimulation natürlicher Abbauprozesse in einem mit gaswerksspezifischen Schadstoffen kontaminierten Grundwasserleiter. In *Bochumer Geologische und Geotechnische Arbeiten*. PhD thesis, Ruhr-Universität Bochum, Germany, p. 123.

Eckert, P., and Appelo, C.A.J. (2002) Hydrogeochemical modeling of enhanced benzene, toluene, ethylbenzene, xylene (BTEX) remediation with nitrate. *Water Res Res* 38: 1-11.

Franzmann, P.D., Robertson, W.J., Zappia, L.R., and Davis, G.B. (2002) The role of microbial populations in the containment of aromatic hydrocarbons in the subsurface. *Biodegradation* 13: 65-78.

Haack, S.K., Fogarty, L.R., West, T.G., Alm, E.W., McGuire, J.T., Long, D.T. et al. (2004) Spatial and temporal changes in microbial community structure associated with recharge-influenced chemical gradients in a contaminated aquifer. *Environ Microbiol* 6: 438-448.

Jahn, M.K., Haderlein, S.B., and Meckenstock, R.U. (2005) Anaerobic degradation of benzene, toluene, ethylbenzene, and o-xylene in sediment-free iron-reducing enrichment cultures. *Appl Environ Microbiol* 71: 3355-3358.

Kappler, A., Emerson, D., Edwards, K., Amend, J.P., Gralnick, J.A., Grathwohl, P. et al. (2005) Microbial activity in biogeochemical gradients - new aspects of research. *Geobiology* 3: 229-233.

Lovley, D.R. (2001) Anaerobes to the rescue. *Science* 293: 1444-1446.

Lovley, D.R., and Chapelle, F.H. (1995) Deep subsurface microbial processes. *Rev Geophys* 33: 365-381.

Mayer, K.U., Benner, S.G., Frind, E.O., Thornton, S.F., and Lerner, D.N. (2001) Reactive transport modeling of processes controlling the distribution and natural attenuation of phenolic compounds in a deep sandstone aquifer. *J Contam Hydrol* 53: 341-368.

McGuire, J.T., Long, D.T., Klug, M.J., Haack, S.K., and Hyndman, D.W. (2002) Evaluating behavior of oxygen, nitrate, and sulfate during recharge and quantifying reduction rates in a contaminated aquifer. *Environ Sci Technol* 36: 2693-2700.

McKinley, J.P. (2001) The use of geochemistry and the importance of sample scale in investigations of lithologically heterogeneous microbial ecosystems. In *Subsurface Microbiology and Biogeochemistry*. Fredrickson, J.K., and Fletcher, M. (eds). Wiley-Liss, Inc., New York, USA.

Postma, D., and Jakobsen, R. (1996) Redox zonation: equilibrium constraints on the Fe (III)/SO_4^{2-} reduction interface. *Geochim Cosmochim Acta* 60: 3169-3175.

Prommer, H., Tuxen, N., and Bjerg, P.L. (2006) Fringe-controlled natural attenuation of phenoxy acids in a landfill plume: integration of field-scale processes by reactive transport modeling. *Environ Sci Technol* 40: 4732-4738.

Puls, R.W., and Barcelona, M.J. (1996) Low-flow (minimal drawdown) groundwater sampling procedures. In *EPA Groundwater Issue, April 1996*. Agency, U.S.E.P. (ed), p. 12.

Rees, H.C., Oswald, S.E., Banwart, S.A., Pickup, R.W., and Lerner, D.N. (2007) Biodegradation processes in a laboratory-scale groundwater contaminant plume assessed by fluorescence imaging and microbial analysis. *Appl Environ Microbiol* 73: 3865-3876.

Röling, W.F., and van Verseveld, H.W. (2002) Natural attenuation: what does the subsurface have in store? *Biodegradation* 13: 53-64.

Ronen, D., Graber, E.R., and Laor, Y. (2005) Volatile organic compounds in the saturated-unsaturated interface region of a contaminated phreatic aquifer. *Vadose Zone Journal* 4: 337-344.

Safinowski, M., Griebler, C., and Meckenstock, R.U. (2006) Anaerobic cometabolic transformation of polycyclic and heterocyclic aromatic hydrocarbons: evidence from laboratory and field studies. *Environ Sci Technol* 40: 4165-4173.

Schmid, N. (2004) Contaminant threshold concentrations in bacterial mineralization of individual petroleum hydrocarbons. MSc thesis. In *Institute for Geoscience, Center for Applied Geoscience (ZAG)*: Eberhard Karls University Tübingen, Germany.

Scholl, M.A., Cozzarelli, I.M., and Christenson, S.C. (2006) Recharge processes drive sulfate reduction in an alluvial aquifer contaminated with landfill leachate. *J Contam Hydrol* 86: 239-261.

Stookey, L.L. (1970) Ferrozine - a new spectrophotometric reagent for iron. *Anal Chem* 42: 779-781.

Thornton, S.F., Quigley, S., Spence, M.J., Banwart, S.A., Bottrell, S., and Lerner, D.N. (2001) Processes controlling the distribution and natural attenuation of dissolved phenolic compounds in a deep sandstone aquifer. *J Contam Hydrol* 53: 233-267.

Thullner, M., Mauclaire, L., Schroth, M.H., Kinzelbach, W., and Zeyer, J. (2002) Interaction between water flow and spatial distribution of microbial growth in a two-dimensional flow field in saturated porous media. *J Contam Hydrol* 58: 169-189.

Tucillo, M.E., Cozzarelli, I.M., and Herman, J.S. (1999) Iron reduction in the sediments of a hydrocarbon-contaminated aquifer. *Appl Geochem* 14: 655-667.

Tuxen, N., Albrechtsen, H.J., and Bjerg, P.L. (2006) Identification of a reactive degradation zone at a landfill leachate plume fringe using high resolution sampling and incubation techniques. *J Contam Hydrol* 85: 179-194.

Ulrich, G.A., Breit, G.N., Cozzarelli, I.M., and Suflita, J.M. (2003) Sources of sulfate supporting anaerobic metabolism in a contaminated aquifer. *Environ Sci Technol* 37: 1093-1099.

Ulrich, G.A., Martino, D., Burger, K., Routh, J., Grossman, E.L., Ammerman, J.W., and Suflita, J.M. (1998) Sulfur cycling in the terrestrial subsurface: commensal interactions, spatial scales, and microbial heterogeneity. *Microb Ecol* 36: 141-151.

van Breukelen, B.M., and Griffioen, J. (2004) Biogeochemical processes at the fringe of a landfill leachate pollution plume: potential for dissolved organic carbon, Fe(II), Mn(II), NH_4^+, and CH_4 oxidation. *J Contam Hydrol* 73: 181-205.

Wiedemeier, T.H., Rifai, H.S., Newell, C.J., and Wilson, J.T. (1999) *Natural Attenuation of Fuels and Chlorinated Solvents in the Subsurface*: John Wiley & Sons, New York.

Winderl, C., Anneser, B., Griebler, C., Meckenstock, R.U., and Lueders, T. (2008) Depth-resolved quantification of anaerobic toluene degraders and aquifer microbial community patterns in distinct redox zones of a tar oil contaminant plume. *Appl Environ Microbiol* 74: 792-801.

Wisotzky, F., and Eckert, P. (1997) Sulfat-dominierter BTEX-Abbau im Grundwasser eines ehemaligen Gaswerksstandortes. *Grundwasser* 2: 11-20.

3. Small-scale biogeochemical gradients in a tar oil-contaminated aquifer – match and dismatch of groundwater vs. sediment information

3.1. Introduction

Complex mixtures of organic compounds like petroleum hydrocarbons or fuels are known to exhibit a long-term persistence in soils and aquifers, which may be in the range of several weeks to thousands of years (Eberhardt and Grathwohl, 2002). In such cases, even vigorous physical-technical remediation technologies (e.g. air sparging, thermal treatment or pump and treat techniques) or biostimulation may fail to completely remove the contaminant source, thus rendering natural attenuation (NA) an attractive and cost-efficient option for monitoring the transport and fate of pollutants in subsurface environments (Bamforth and Singleton, 2005). Consequently, there's a growing interest to predict the spread and development of contaminant plumes and to understand their degradation behaviour.

The biodegradability of organic compounds such as aromatic hydrocarbons is largely dependent on their chemical structure and bioavailability, whereas sediment-porewater interactions, such as advection, hydrodynamic dispersion, and sorption substantially control their distribution and transport within groundwater systems (Haack and Bekins, 2000; McGuire et al., 2000). Sediment characteristics and groundwater chemistry therefore play a crucial role for the assessment of contaminant distribution and NA activities.

Over the past years, the relevance of scale and resolution for the assessment of NA was recognized, drawing the attention towards investigation of gradients in the centimeter to millimeter range (Ronen et al., 2005; Tuxen et al., 2006; Báez-Cazull et al., 2007; Anneser et al., 2008). Lab experiments and reactive transport models revealed biodegradation activities in homogeneous sediments to be primarily located at the fringe of organic contaminant plumes, where transverse dispersion processes continuously provide mixing of electron donors and electron acceptors and thus create conditions favourable to biodegradation (Mayer et al., 2001; Rahman et al., 2005). Thus, in mixing-controlled organic contaminant plumes, enhanced bioactivities at such interfaces are reflected by steep physical-chemical and biological gradients in the centimeter to millimeter scale (Klenk and Grathwohl, 2002; Prommer et al., 2006; Maier et al., 2007; Bauer et al., 2008). In heterogeneous packings, streamline meandering was reported to enhance vertical spreading of organic contaminant plumes, thus leading to increased transversal dispersivities and, consequently, increased bioactivity (Jose and Cirpka, 2004; Cirpka, 2005; Rahman et al., 2005; Bauer et al., 2008). So far, these findings are based solely on experimental and modeled results. The enormous complexity and poor accessibility of subsurface environments considerably impairs the transferability of simulated data to *in situ* conditions (Griffin et al., 1997). Even though technical innovations remarkably facilitated the collection of sediments and groundwater, scale-adapted sampling without blending the samples and changing the sediment structure and/or groundwater composition still represents a great challenge. The high costs associated with borehole drilling and the installation of high-resolution monitoring wells restrict investigations to a limited number of sites. Small-scale sediment heterogeneities and variability in the biogeochemistry therefore are often neglected and, furthermore, representativeness of the results cannot always be warranted (Haack and Bekins, 2000). In many cases, analysis of soil properties does not comprise a thorough investigation of groundwater chemistry and *vice versa*, though the vast complexity of subsurface processes needs to link soil and groundwater characteristics as well as sediment-microbe interactions.

The work package introduced presents a comprehensive data set comparing the biogeochemistry of sediment and groundwater in a tar oil-contaminated sandy aquifer. Temporally and spatially close sampling intervals allowed a direct comparison of both

sediment and groundwater characteristics. Based on these data, important biotic and abiotic reactions could be specified and localized. In particular, the distribution of natural attenuation processes was investigated, focussing on possible factors limiting and stimulating biodegradation in relation to the sediment structure.

3.2. Site description

The investigated area is a Quaternary sandy aquifer at a former gasworks site in Düsseldorf-Flingern, Germany (Fig. 3.1A). Release of tar oil compounds during operation and break-down of the plant resulted in the development of a contaminant plume with maximum concentrations of > 100 mg l^{-1} of monoaromatic and > 10 mg l^{-1} of polycyclic aromatic hydrocarbons (PAHs). Even though several remediation actions launched since 1996 achieved to remove the major part of the tar oil phases, residual amounts still can be detected in sediments and groundwater, forming a BTEX plume of about 200×40 m in horizontal dimension. For further information on site characteristics see section 2.2.
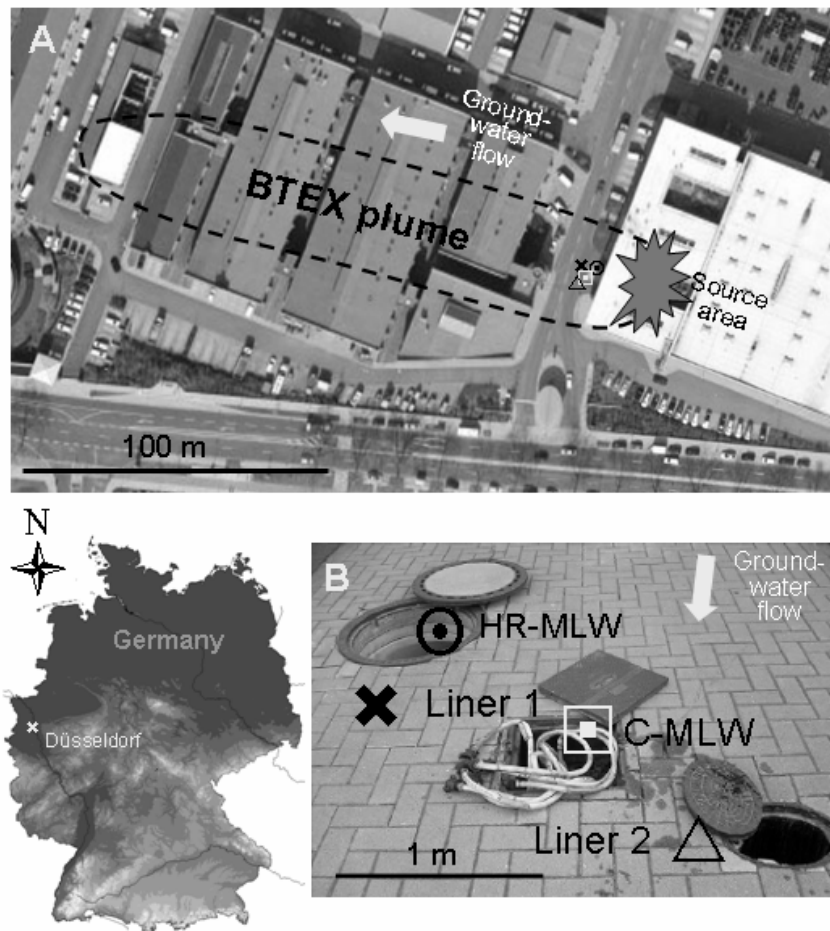
Figure 3.1 A) Schematic overview of the sampling area and B)
the relative distance between the sediment liners.

3.3. Materials and Methods

3.3.1. Groundwater sampling

Water samples were collected in February 2006 from a specially designed high-resolution multi-level well (HR-MLW) at vertical intervals of 2.5 – 10 cm applying extremely slow pumping rates adapted to natural groundwater flow. In order to avoid hydrological shortcuts and disturbance of small-scale gradients, the selected 24 ports were sampled simultaneously using two peristaltic pumps in parallel equipped with pre-conditioned low-sorption fluran tubes (Ismatec, Wertheim, Germany). A detailed description of the HR-MLW as well as information on the sampling procedure and the materials and instruments used is given in section 2.3 and 4.3.

3.3.2. Sediment sampling

One week after sampling groundwater from the high-resolution multi-level well, two boreholes were drilled approximately 0.5 m downgradient and 1.5 m adjacent (diagonal; Fig. 1B) to the HR-MLW by means of hollow-stem auger drilling. Sediment liners were obtained in one meter segments down to a depth of 14 m (Liner 1) and 11 m (Liner 2), respectively. Right after retrieving the sediment liners they were transferred to a big aluminium box and subsampled immediately for a selected set of parameters. During withdrawal of liners and subsampling, the sediments were flushed with argon gas in order to prevent rapid oxidation of reduced soil components.

3.3.3. Sample preparation and analysis

Groundwater was collected in 100 ml pre-washed narrow neck glass bottles and immediately processed for the analysis of a number of biotic and abiotic parameters.
Redox potential, pH and specific conductivity were measured in freshly sampled groundwater using field sensors (WTW, Weilheim, Germany). Fe(II) dissolved in groundwater was determined photometrically from samples immediately fixed with 1 M HCl following the ferrozine assay of Stookey (1970). Dissolved sulfide was also measured photometrically after immediate fixation of the samples with a zinc acetate solution (2 % w/v) using a protocol of Cline (1969), which was modified for small sample volumes.
    Total reduced inorganic sulfur was extracted from sediment samples fixed in 20% (w/v) zinc acetate using HCl-Cr(II) solution (1M Cr(II)-HCl in 12M anoxic HCl), according to the protocol of Ulrich et al. (1997). Under maintenance of anoxic conditions, reduced inorganic sulfur species are converted to hydrogen sulfide during 30 hours of intensive shaking at room temperature. The liberated H_2S is trapped in a 10 % zinc acetate solution and subsequently analyzed according to the method described above.
    Groundwater samples dedicated to the analysis of dissolved mono- and polycyclic aromatic hydrocarbons were amended with NaOH (0.1 M final concentration) to stop biological activity. BTEX concentrations were measured via GC-MS by headspace analysis; the less soluble polycyclic aromatic hydrocarbons (PAH) were determined by liquid injection analysis. Major anions and cations were analyzed by means of ion chromatography (Dionex DC-100, Idstein, Germany). Further details on analytical procedures are given in section 4.3.
    Sediment total organic matter (TOM) was calculated by the loss in weight of dried sediment after combustion of the organic content at 450°C for 4 h. Amorphous, ready available sedimentary iron was extracted in duplicates with 30 ml of 0.5 M HCl from 2 ml of sediment during 24 hours of intensive shaking at room temperature (Heron et al., 1994). Likewise, crystalline iron phases were obtained by 5 M HCl extraction over a period of 21

days. The extracts were processed similar to the groundwater samples as mentioned above. The Fe(III) content was determined after reduction of total iron to Fe(II) using hydroxylamine hydrochloride (HACl) as reductant (see section 2.3). The amount of HACl-reducible Fe(III) was calculated as the difference of Fe(II) determined in the HCl and HACl extracts (Lovley and Phillips, 1987).

Polycyclic aromatic hydrocarbons (PAHs) were extracted from 2 ml of wet sediment with 2 ml acetone during 60 min of intensive shaking at room temperature. An internal standard mixture containing deuterated acenaphthene, chrysene, perylene and phenanthrene species (Internal Standards Mix 25, Ehrenstorfer, Augsburg, Germany) at a final concentration of 25 mg l^{-1} was used for quantification. 1 µl of the acetone phase was directly injected onto a DB5 GC capillary column. Samples were injected at a split ratio of 1:10; the flow rate of the helium carrier gas was 1 ml min^{-1}. The oven temperature initially was held at 40°C for 3 min, then increased at a rate of 9.6°C min^{-1} to 270°C and further increased at a rate of 3.4°C min^{-1} to a final temperature of 310°C and held for 5 min. The MS was operated in the full scan mode, covering masses from 50-500 m z^{-1}.

In situ microbial activity was assessed by determining the enzymatic hydrolysis rates of two fluorogenic substrates, *i.e.* MUF-P (4-methylumbelliferyl phosphate) and MUF-Glc (4-methylumbelliferyl β-D-glucoside) (Freeman et al., 1995; Hendel and Marxsen, 1997). Enzyme assays of both groundwater and sediment samples were performed in 4 ml Supelco glass vials. For each sample, three replicates and one control were prepared. Groundwater was filled into the vials avoiding headspace. Sediment samples were transferred in aliquots of 1 ml into vials, which have been prefilled with anoxic, low-ionic strength (1:500 dilution) freshwater medium (Widdel and Bak, 1992). The substrates MUF-P or MUF-Glc (both Sigma, Taufkirchen, Germany) were added to a final concentration of 225 µM to groundwater samples and 1 mM to sediment samples, respectively. Groundwater samples were incubated at *in situ* temperature (16°C ± 1°C) and the reaction was stopped after 18 hours by addition of ammonium glycine buffer (pH 10.5) at a ratio of 1:10. Enzyme activity within sediment samples was terminated after 22 hours of incubation by adding 100 µl of an alkaline solution (2M NaOH / 0.4M EDTA) to each sample. Controls for background fluorescence were treated analogously, but inactivated with ammonium gylcine buffer prior to starting the incubation. Fluorescence was determined in a luminescence spectrometer (Aminco Bowman Series 2, Thermo Scientific) at 455 nm emission and 365 nm excitation.

3.3.4.   Stable isotope analysis in groundwater

Ratios of deuterium/protium (D/H) and $^{18}O/^{16}O$ of groundwater were determined by dual-inlet mass spectrometry at a precision of ± 1 ‰ for ^{2}H and ± 0.13 ‰ for ^{18}O, respectively. Details on the analysis of groundwater isotopes can be derived elsewhere (Moser and Rauert, 1980; IAEA, 1983).

Stable sulfur ($^{34}S/^{32}S$) and oxygen ($^{18}O/^{16}O$) isotope ratios of sulfate dissolved in groundwater were determined from samples collected in 100 ml vessels containing 10 ml of a 20% (w/v) Zn-acetate solution for precipitation of sulfide. Procedures for the recovery of sulfate and details on isotope measurements are described in detail in section 4.3.

3.4. Results

3.4.1. Distribution of contaminants

The spread of major contaminants, such as benzene, toluene, ethylbenzene and xylenes (BTEX) in groundwater of the investigated aquifer section was restricted to a narrow zone stretching from right below the groundwater table (ca. 6.4 m below land surface [bls] at time of sampling) to a depth of approximately 8 m bls (Fig. 3.2A). Out of the monoaromatic hydrocarbons, toluene constituted the dominant fraction, accounting for about 75 % of the total BTEX mass. No contaminants could be detected in the uppermost sampling port (= capillary fringe) at time of sampling. Only 2.5 cm below, 4.2 mg l^{-1} of BTEX were measured, followed by a vast increase to 58 mg l^{-1} at 6.7 m depth. Subsequently, a steep decline to lowest detectable BTEX concentrations (30 µg l^{-1}) at a depth of 8.1 m bls was found. Concentrations of monoaromatic hydrocarbons thus describe a shallow, vertically thin BTEX plume in this sandy aquifer.

A distribution similar to that of BTEX compounds was found for naphthalene, the major PAH component, which exhibited maximum concentrations of about 16 mg l^{-1} at 6.75 m bls
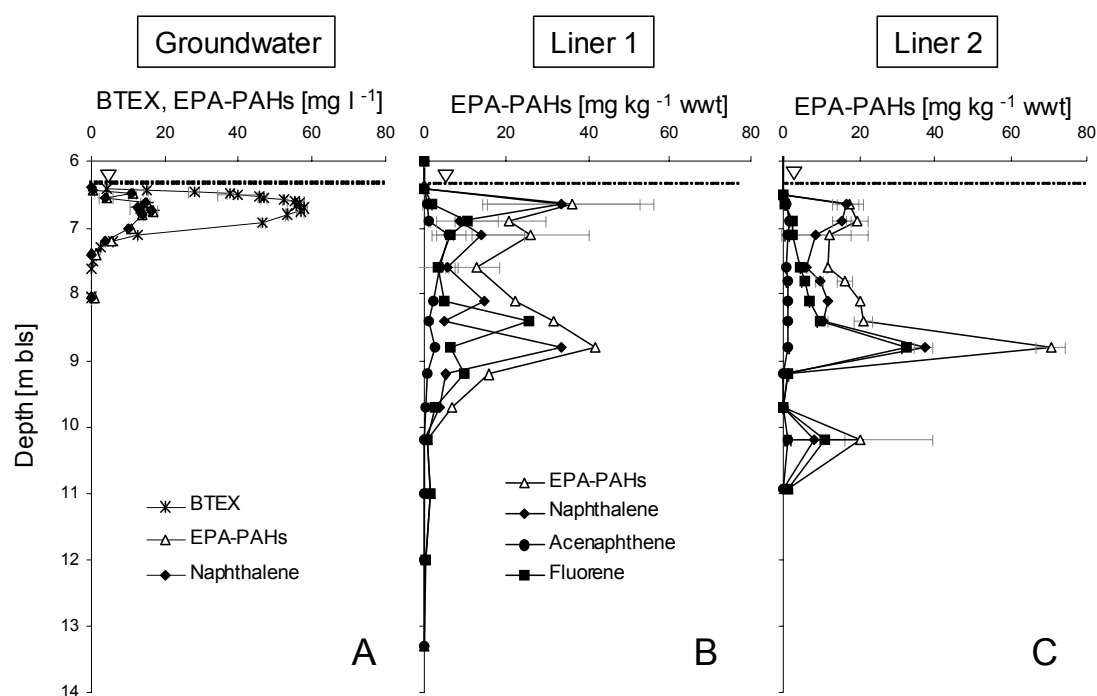
Figure 3.2 Distribution of contaminants in groundwater (A) and sediment samples (B + C). Values represent means of duplicate measurements ± SD.

(Fig. 3.2A). Out of the 16 EPA-PAHs, only acenaphthene and fluorene could further be identified in groundwater with lowest concentrations in the zone of the BTEX plume and slightly increased values further down (> 7 m), but always exhibiting concentrations below 1 mg l^{-1} (data not shown). In comparison to groundwater, sediment samples of Liner 1 (L1) exhibited no detectable amounts of BTEX sorbed to the matrix but two distinct peaks for total PAHs (sum of 16 EPA-PAHs) at 6.65 m and 8.8 m bls (Fig. 3.2B). Both maxima were mainly contributed by naphthalene, with the upper peak located directly within the center of the BTEX plume and the lower one in an area where no BTEX and only small concentrations of PAHs, *i.e.* acenaphthene and fluorene, could be detected in groundwater. Acenaphthene concentrations in sediment of up to 6 mg kg^{-1} wet weight (wwt) were detected at 7.1 m bls, while fluorene was peaking at a depth of 8.4 m with concentrations of 26 mg kg^{-1} wwt. No

other EPA-PAHs were found or, if yet, they were below the detection limit of about 20 µg l^{-1}. The distribution patterns of PAHs within the sediments of Liner 2 were found to be highly similar to that of Liner 1. Nevertheless, maximum concentrations of naphthalene at 6.65 m depth were considerably lower, while fluorene exhibited higher total concentrations compared to Liner 1, reaching > 32 mg kg^{-1} wwt at 8.8 m bls (Fig. 3.2C). Interestingly, a PAH impacted layer was detected in Liner 2 at 10.2 m bls that was not present in Liner 1 sediments (Fig. 3.2 B + C).

3.4.2. Redox-specific parameters

Redox potential (E_h) determined in freshly sampled groundwater revealed the highest value at the uppermost port where water could be withdrawn. With depth, E_h was continuously decreasing, indicating anoxic conditions all across the investigated aquifer section (Fig. 3.3A). A trend opposite to E_h was observed for pH (Fig. 3.3B) and specific conductivity (Fig. 3.3C). Unfortunately, sample volumes sufficient for analysis of these parameters could only be obtained from 10 different depths.
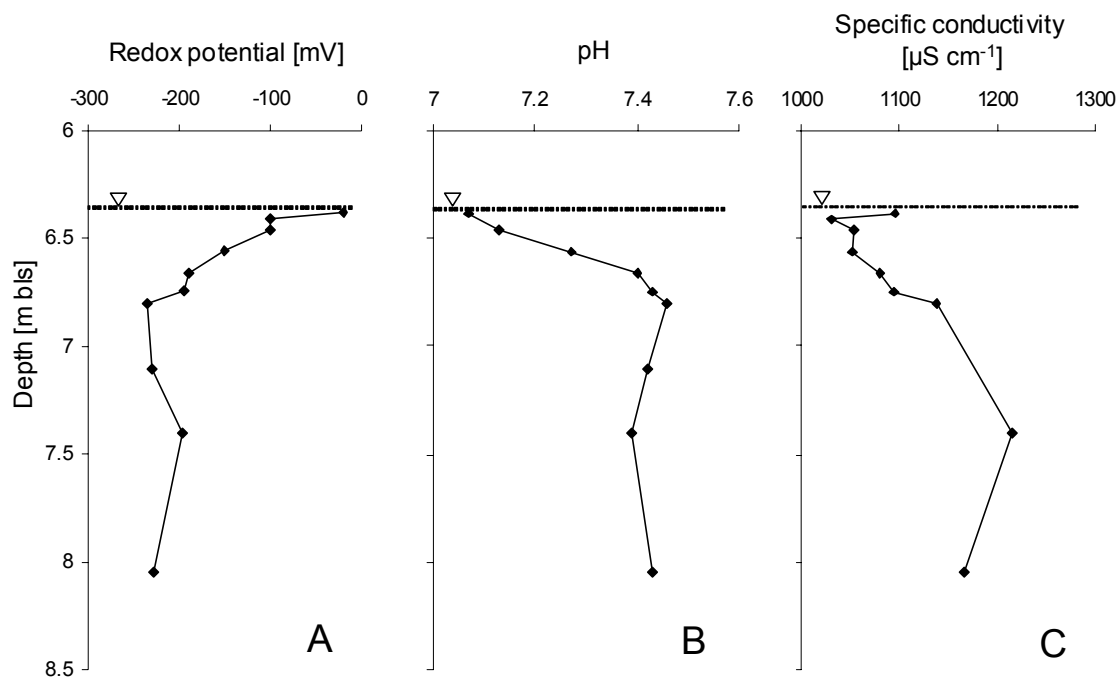
Figure 3.3 Vertical profiles of selected physical-chemical parameters determined in groundwater samples of the HR-MLW.

Dissolved inorganic phosphate was available all across the investigated aquifer section, with minimum concentrations of 70 µg l^{-1} at the water table and peak values of up to 2.1 mg l^{-1} in the plume center (Fig. 3.4D). Determination of nitrate concentrations in groundwater samples failed owing to technical problems. Data of other HR-MLW sampling campaigns, however, indicated nitrate concentrations of less than 1 mg l^{-1} to below detection limit of 0.1 mg l^{-1} all across the investigated aquifer section (data not shown). Sulfate was almost absent in the upper BTEX plume zone, yet its availability increased with declining contaminant mass at the lower plume fringe. At a depth of 7.4 m bls sulfate leveled off to a background concentration of about 120 mg l^{-1}. Concomitant with declining concentrations of organics and
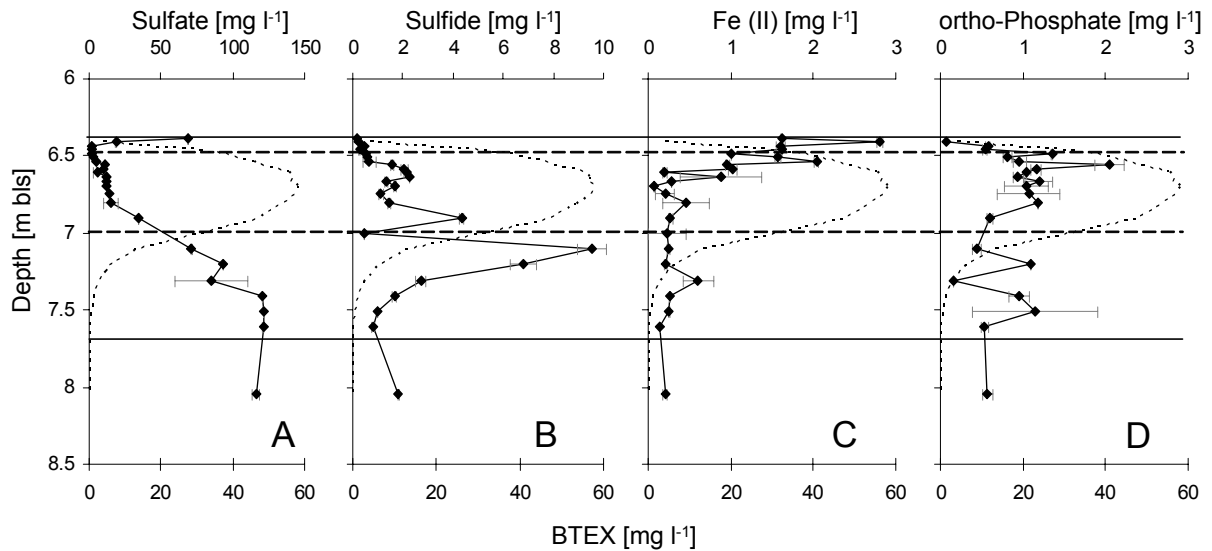
Figure 3.4 Selected gradients of electron acceptors (sulfate), metabolic end products (sulfide, Fe(II)) and nutrients (ortho-phosphate) as determined in groundwater in relation to the BTEX plume (dashed line).

increasing sulfate concentrations at the lower plume fringe distinct sulfide peaks were observed, reaching a concentration of almost 10 mg l^{-1} at 7.11 m bls (Fig. 3.4B). Lower amounts of sulfide were detected in the plume core and scarcely any dissolved sulfide was found within the first decimeters beneath the capillary fringe. There, however, pronounced concentrations of dissolved Fe(II) were measured, followed by a steep decline until more or less stable concentrations of about 0.3 mg l^{-1} were attained at 6.9 m bls (Fig. 3.4C).

Contrary to dissolved ferrous iron, concentrations of ready extractable Fe(II) in the sediment were lowest within the BTEX contamination area but exhibited a pronounced increase with depth, reaching concentrations up to 3.2 g kg^{-1} wwt below 8 m bls (Fig. 3.5 A+B). With the exception of local peaks at 10.2 m (L1) and 9.2 m (L2) bls, the recovery of ready extractable Fe(III) from saturated sediments was lower compared to that of Fe(II). Only low amounts of crystalline Fe(II) were obtained by extraction with 5M HCl; in contrast, concentrations of Fe(III) released by this harsh extraction exhibited clearly higher values of up to 5.5 g kg^{-1} wwt (Fig. 3.5 C+D). The large degree of variability in sediment content indicated by error bars may reflect sampling error as well as sediment heterogeneities.
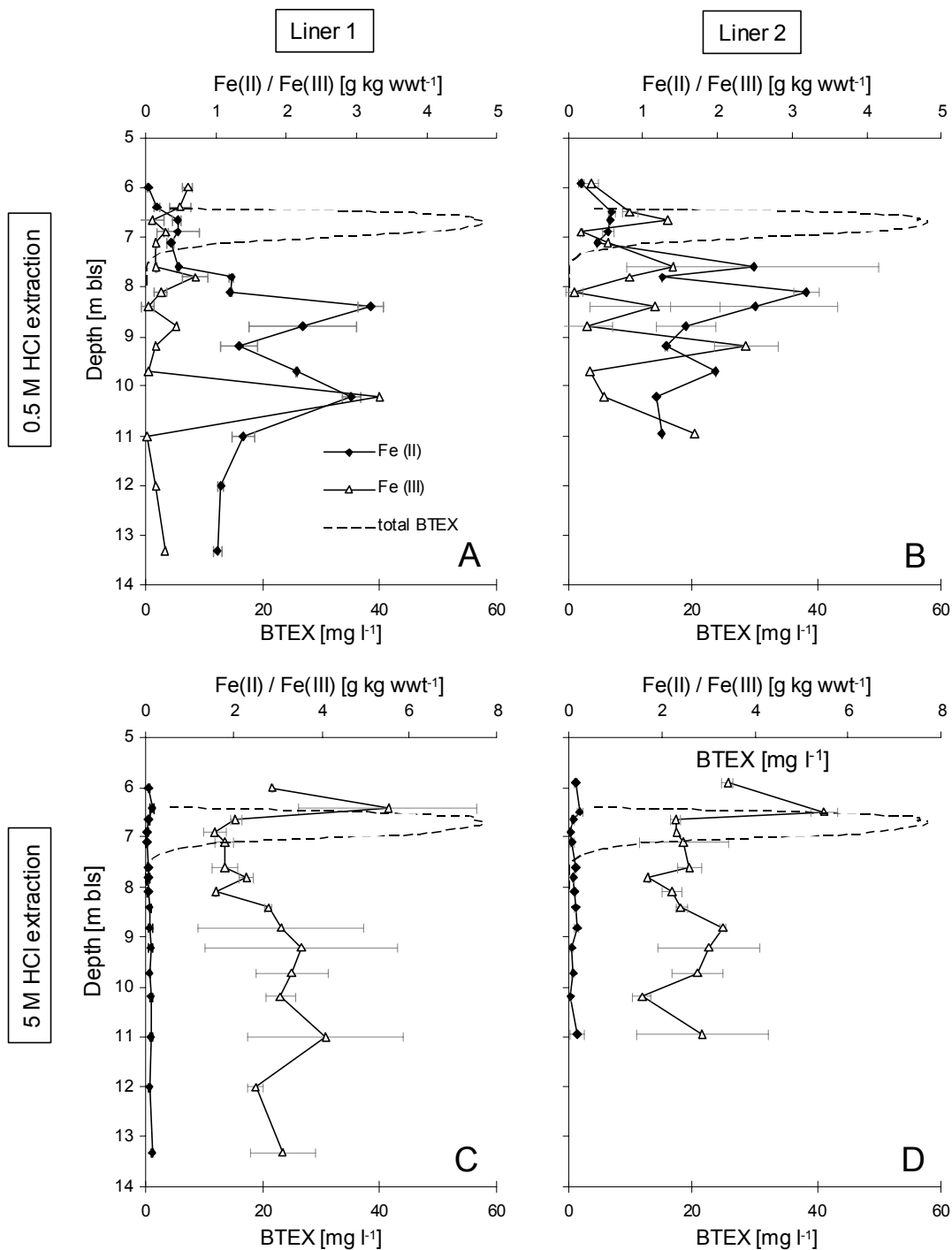
Figure 3.5 Depth profiles of ready available (0.5 M HCl extraction) and crystalline (5 M HCl extraction) iron species in sediment samples of Liner 1 +2 in relation to the BTEX concentration measured in groundwater.

Total reduced inorganic sulfur (TRIS) extracted from sediment samples of Liner 1 revealed concentrations in the range of 0.02 – 0.5 g sulfide per kg (wwt), with pronounced peaks at 7.1 m, 12 m, and elevated values between 9 and 10 m bls (Fig. 3.6A). Unfortunately, no TRIS values are available from Liner 2. Total organic matter (TOM) content in dried sediments of Liner 1 was relatively low, ranging between 0.2 and 0.6 % (dwt) with a mean value of 0.34 % (Fig. 3.6B). A similar distribution was observed in Liner 2 sediments (0.39 % on average), but here a pronounced TOM peak reaching 1.3 % (dwt) was measured at a depth of 11 m bls (Fig. 3.6B).
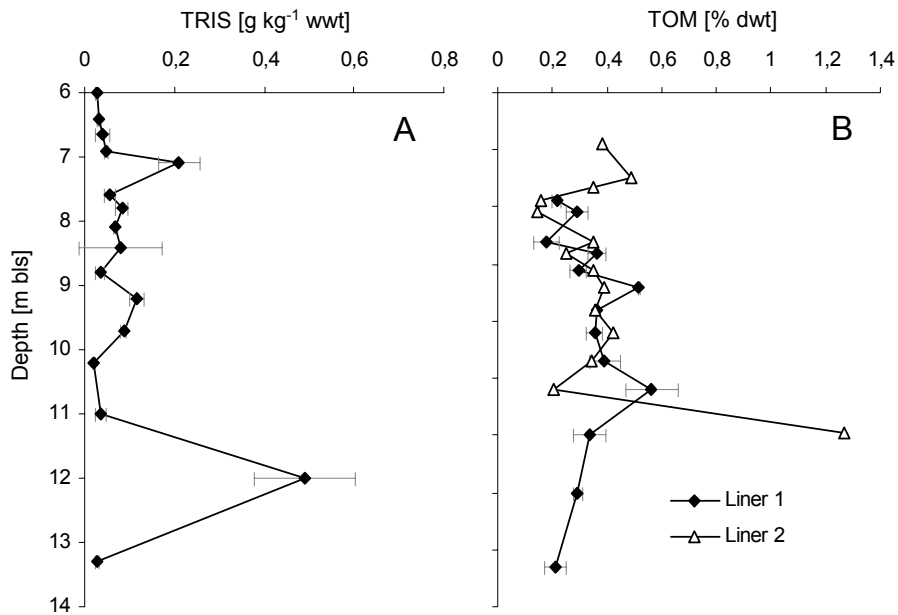
Figure 3.6 Depth profiles of A) total reduced inorganic sulfur (TRIS) and B) total organic matter (TOM) as determined in sediment samples.

3.4.3.   Cell numbers and bioactivity measurements

Total direct cell counts of SybrGreen-stained bacteria (incl. *Archaea*) in sediment samples of Liner 1 exhibited a peak value of ~ 1.5×10^{10} cells kg^{-1} wwt at the upper plume fringe (Fig. 3.7B). With depth, biomass decreased significantly; a small peak was also observed at the lower fringe of the BTEX plume (7.8 m bls).
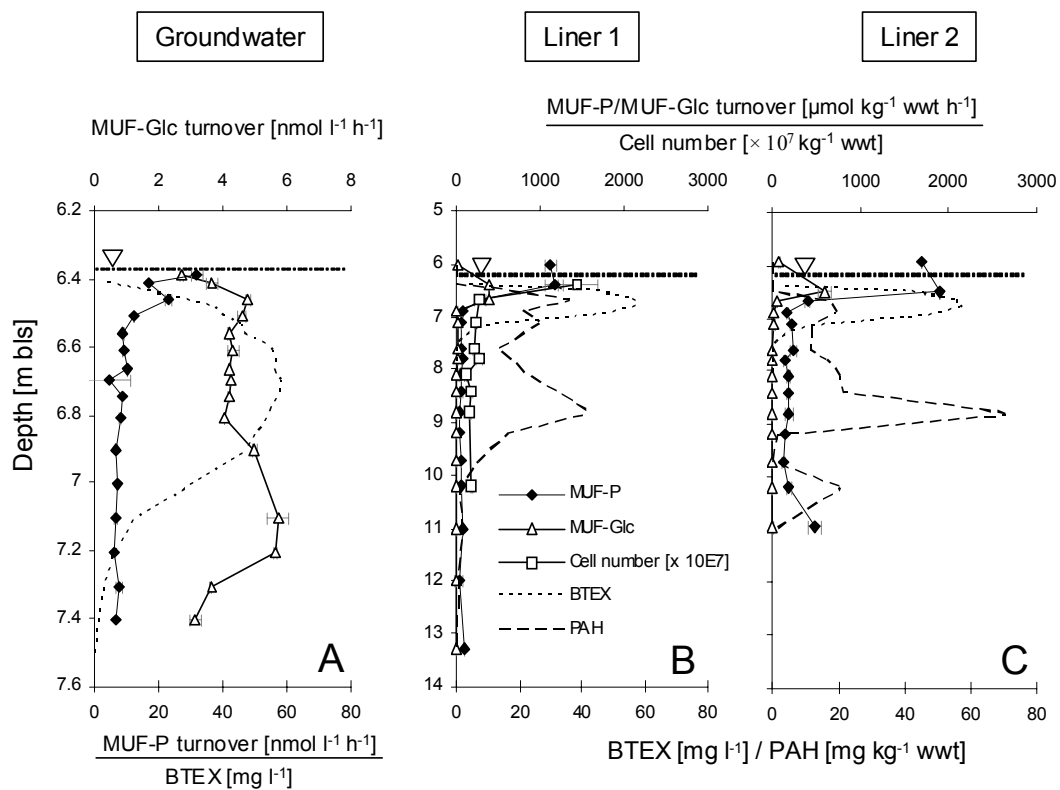
Figure 3.7 Sediment bacterial abundance and selected enzyme activities in groundwater and sediment in relation to BTEX- and PAH-contaminated zones (total cell counts provided by R. Drexel).

Both sediment and groundwater samples exhibited maximum conversion rates for the selected substrates at the uppermost sampling depths. Up to 1.9 mol MUF-P were hydrolysed by phosphatases per kilogram sediment (wwt) and hour in Liner 2, turnover rates in Liner 1 reached maximum values of 1.2 mmol kg^{-1} wwt h^{-1} (Fig. 3.7 B+C). At 6.9 m bls, the activity started to level off at 180 µmol kg^{-1} wwt h^{-1} (Liner 2) and 60 µmol kg^{-1} wwt h^{-1} (Liner 1) on average. Beta-glucosidase activities were comparable for the sediments of both liners according to the individual depth zones, but maximum turnover rates were clearly below those of MUF-P (Fig. 3.7 B+C). The gradient of MUF-P determined in groundwater samples was similar to that observed within the sediments, yet the activity was significantly lower, showing values of max. 32 nmol l^{-1} h^{-1} directly below the water table (Fig. 3.7A), which corresponds to 10.9 nmol kg^{-1} h^{-1} wwt assuming a sediment porosity of 34%. Contrary to sediment samples, enzymatic hydrolysis rates of MUF-Glc in groundwater were more or less similar across the investigated aquifer section with only slightly elevated values at the upper and lower fringe of the BTEX plume (Fig. 3.7A).

3.4.4. Stable isotope measurements

Stable $^{18}O/^{16}O$ and $^{34}S/^{32}S$ isotope ratios of groundwater sulfate originating from the plume center and the lower plume fringe were found significantly enriched in the heavier isotopes when compared to values of samples from the deeper zones of the aquifer (Fig. 3.8A). The isotope ratios in the contaminated zones clearly hinted towards microbial sulfate reduction. However, δ-values [‰] measured at the uppermost sampling ports close to the capillary fringe were distinctly lower and thus also different from the "background" isotope ratios.

With differences of only up to 0.18 ‰ between maximum and minimum $\delta^{18}O$ values and 1.9 ‰ between maximum and minimum $\delta^{2}H$-values, isotope ratios in water exhibited no pronounced differences (Fig. 3.8B). Nevertheless, stable isotope ratios of both elements displayed the same pattern, dividing the groundwater into an isotopically heavier and an isotopically lighter water body.
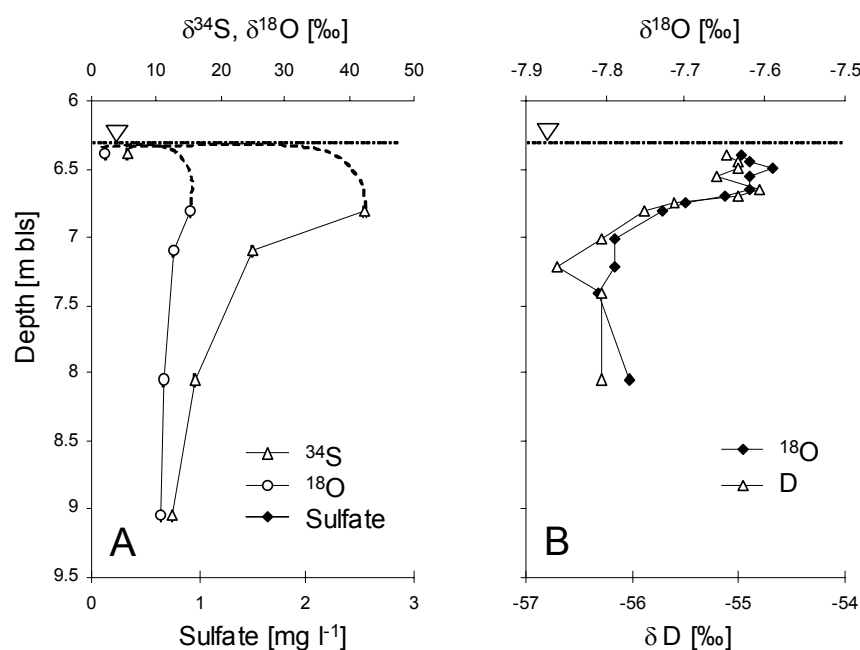
Figure 3.8 Stable isotope ratios of $^{34}S/^{32}S$ and $^{18}O/^{16}O$ of groundwater sulfate and D/H and $^{18}O/^{16}O$ of groundwater.

3.5. Discussion

3.5.1. Heterogeneous distribution of organic contaminants

Analysis of groundwater and sediment samples that were collected at an extraordinary high vertical resolution revealed a very detailed profile showing the distribution of individual contaminants and redox-sensitive parameters across the investigated aquifer section. Steep concentration gradients of benzene, toluene, ethylbenzene and xylene-isomers (BTEX) in groundwater clearly delineated the architecture of the BTEX plume, which was confined to the upside by the groundwater table, thus exhibiting a thin upper plume fringe at the capillary zone. The lower plume border could be delineated by three criteria: first, there was a good agreement between the decreasing gradients of electron donors (*i.e.* BTEX; Fig. 3.2A) and the electron acceptor sulfate (Fig. 3.4A), which came along with a pronounced peak of the metabolic end product sulfide (Fig. 3.4B). Second, molecular analyses of sediment samples revealed the dominance of a highly specialized degrader community of deltaproteobacterial iron and sulfate reducers and fermenting clostridia in the sulfidogenic zone underneath the BTEX plume core (Winderl et al., 2008). Finally, toluene concentrations measured at 7.6 m bls corresponded to experimentally derived threshold toluene concentrations of $10 - 100$ µg l^{-1}, at which oxidation of toluene via sulfate or iron reduction by the bacterial strains TRM1 and *Geobacter metallireducens*, respectively, was observed to stop in batch culture experiments (Schmid, 2004). In contrast to groundwater samples, neither sediments of Liner 1 nor of Liner 2 exhibited measurable BTEX concentrations. According to their differential solubility and sorption behaviour we could distinguish two groups of contaminants at our study site: (i) the monoaromatic BTEX compounds, which were restricted to groundwater samples of the first 1.2 m below the capillary fringe, and (ii) the polycyclic aromatic hydrocarbons (PAHs). The major representative of the latter, *i.e.* naphthalene, was found almost all across the investigated aquifer section in the sediments as well as in groundwater, with pronounced peaks appearing in the area of the BTEX plume and between 8 and 9 m depth (Fig. 3.2). Due to its comparably low molecular weight and high solubility (Eberhardt and Grathwohl, 2002), the distribution and transport of naphthalene in groundwater is quite similar to that of monoaromatic hydrocarbons. In contrast, higher molecular PAHs, according to their complexity and limited solubility, are more recalcitrant to biodegradation and exhibit a higher tendency to adsorb to the sediment matrix. The different solubility and persistence of the PAHs is to a certain degree reflected by the concentration gradients determined in sediments of Liner 1 and Liner 2. Taking into account the inaccuracies associated with the collection of the sediments by liner coring, the differences in the distribution of contaminants may partly be also ascribed to sediment heterogeneities. "Hot spots" of pollutants and preferential flow paths in heterogeneous sediments may additionally foster a diffuse spreading of the contaminants. In the source zone, which is located ~ 15 m upstream of the sampling area, the dense non-aqueous phase liquids (DNAPLs) are likely to seep down due to their higher density and molecular weight. This may explain the accumulation of PAHs in deeper aquifer zones in contrast to the lighter BTEX compounds.

Sorption of PAHs to the sediment matrix is substantially influenced by the presence of organic matter, which is commonly regarded to be negligible in sandy aquifers, where mean organic carbon contents are in the range of only about 0.1 % (Lovley and Chapelle, 1995; Appelo and Postma, 2005). Due to their hydrophobicity, the higher molecular PAHs acenaphthene and fluorene are strongly retained in sediments, and so in the Flingern aquifer, despite the relatively low soil organic carbon content of $0.3 - 0.4$ % (dry weight). Compared to maximal 16 mg l^{-1} of naphthalene dissolved in groundwater (= 5.4 mg per kg soil; see Tab. 3.2), about 6-7 times this amount was found adsorbed to the sediment. Concentrations of acenaphthene were 10-20 times, fluorene concentrations even 100-fold higher in sediments than in groundwater. The relation between adsorbed (C_s) and dissolved concentrations (C_w)

can be expressed by the solid water distribution coefficient K_D of a given compound, according to

$$K_D = \frac{C_s \left[mg\ kg^{-1} \right]}{C_w \left[mg\ kg^{-1} \right]}$$
(eq. 3.1).

In soil-water systems, K_D is also defined by the product of the organic carbon – water distribution coefficient K_{oc} and the fraction of organic compounds in solution f_{oc} (Appelo and Postma, 2005)

$$K_D = K_{oc} \times f_{oc}$$
(eq. 3.2).

Inserting literature K_{oc} values (Tab. 3.1) and measured f_{oc} and C_w from our samples into equations 3.1 and 3.2, the theoretically adsorbed contaminant concentration C_s can be derived. For sediment-associated PAHs, calculated and measured concentrations were in a similar range. As expected, the solubility of the contaminants declined with increasing molecular weight, as can be derived from table 3.2. While measured concentrations of fluorene adsorbed to the sediment exceeded theoretically derived values, the amounts of naphthalene and acenaphthene determined in the sediment were lower compared to theoretical values. Moreover, contrary to calculated maximum toluene concentrations of 59 mg kg^{-1}, neither toluene nor other BTEX compounds were detected in sediment samples of the Flingern site. Obviously, the sorption capacity of the soil matrix was lower than expected, thus rendering monoaromatic hydrocarbons at the investigated aquifer section virtually completely dissolved in groundwater. The discrepancy between calculated and measured concentrations reflects the complexity of sediment-groundwater systems, where dilution, sorption and transport of organic particles are dependent on a variety of parameters, such as molecular weight, temperature, ionic strength or pH. Consequently, calculated values have to be recognized as truly estimates that cannot fully account for *in situ* conditions.

Table 3.1 Sorption properties and aqueous solubilities S_i of selected aromatic hydrocarbons.

Compound	log K_{ow}	log K_{oc}	S_i at 25°C [mg l^{-1}][a]
Toluene	2.69[c]		534.8
Naphthalene	3.36[b]	2.94[b]	31.7
Acenaphthene	3.98[c]	3.66[c]	3.93
Fluorene	4.18[c]	3.86[c]	1.98

S_i = aqueous solubility of organic compound i, K_{ow} = octanol-water coefficient, K_{oc} = organic carbon-water coefficient
[a] Eberhardt and Grathwohl (2002)
[b] Appelo and Postma (2005)
[c] USACE (2002)

Table 3.2 Measured and calculated maximum concentrations of aromatic hydrocarbons in sediment and groundwater of the Flingern aquifer.

Compound	Groundwater [mg l^{-1}][a]	Liner 1 Sediment [mg kg^{-1}]	Liner 2	Calculated[b]
Toluene	45 (15.3)	-	-	59
Naphthalene	16 (5.4)	33.5	37	56
Acenaphthene	0.9 (0.31)	6	1.6	16
Fluorene	0.7 (0.24)	26	32	20

[a] parentheses indicate the corresponding sedimentary concentrations in mg kg^{-1}
[b] theoretical sorbed contaminant concentration calculated from max. contaminant concentrations measured in groundwater

3.5.2. Electron acceptor availability and redox cycling

Despite the recalcitrance of many aromatic contaminants, evidence of biodegradation at the Flingern site, especially of monoaromatic hydrocarbons, was obtained by different biological and geochemical indicators. Biodegradation processes in organically impacted aquifers are suggested to cause significant changes in groundwater and sediment properties, which include: (i) a rapid depletion of the energetically most favourable electron acceptors (*i.e.* oxygen and nitrate) (Anderson and Lovley, 1997; Christensen et al., 2000), (ii) the appearance of metabolites and reaction products (in our case reduced sulfur and iron species as shown in Fig. 3.4 B+C), (iii) increase in pH and alkalinity owing to proton consumption during anaerobic oxidation of organic compounds (Fig. 3.3B), (iv) a decrease in redox potential (Cozzarelli et al., 1999; Christensen et al., 2001) as well as a change in specific conductivity due to the conversion of individual ions such as sulfate (Fig. 3.3C).

3.5.2.1. *Geochemical indicators of sulfate reduction and sulfur cycling processes*

At our site, oxygen and nitrate are likely to be depleted preferentially, thus giving way to energetically less favourable terminal electron accepting processes such as sulfate reduction. At the lower plume fringe, as sulfate decreased from background concentrations of ~ 120 mg l^{-1} to less than 2 mg l^{-1} in the plume core, we observed a significant leap of dissolved sulfide from 1.7 mg l^{-1} up to 9.5 mg l^{-1} (Fig. 3.4 A+B). Regarding reduced sulfur species as potential indicators of sulfate reduction, concentrations of dissolved sulfide hint at maximum bioactivities at the lower plume fringe, but also imply sulfate reduction to take place in the highly contaminated zone between 6.41 m and 6.91 m bls, where dissolved sulfide was still detectable in groundwater at concentrations of > 2 mg l^{-1}.

Analysis of the stable sulfur and oxygen isotope ratios of groundwater sulfate exhibited a significant increase in the plume center and at the lower plume fringe contrary to the lighter isotope ratios measured in sulfate-rich, less contaminated background zones (Fig. 3.8A). As isotope fractionation during bacterial sulfate reduction leads to an enrichment of the heavier ^{34}S and ^{18}O isotopes in the residual sulfate pool (Canfield, 2001), increasing isotope signatures concomitant with decreasing sulfate concentrations in the investigated aquifer section provide direct evidence for microbiological sulfate reduction in the BTEX-impacted zone. Remarkably, the isotope ratios of groundwater sulfate at the upper plume fringe clearly differed from those measured at the lower plume fringe and thus could not unambiguously be related to sulfate reduction. Instead, the sulfate isotope composition rather hinted at intrusion of a different sulfate source, possibly from the unsaturated zone (Anneser et al., 2008; see also section 4.5.2.). Additionally, sulfide as a potential indicator of sulfate reduction was scarce in this area, exhibiting concentrations below 1 mg l^{-1}. In fact, there are different explanations

justifying the lack of sulfide in this zone. One is given by the high concentrations of soluble Fe(II) measured at the uppermost sampling depths (Fig. 3.4C), which are likely to scavenge a major portion of the dissolved sulfide precipitating as FeS (Stumm and Morgan, 1996). Close to the capillary fringe, dissolved sulfide may furthermore serve as reductant for abiotic reduction of iron(III) oxyhydroxides (Cozzarelli et al., 1999; Kostka et al., 2002). Theoretically, sulfate produced during sulfide or pyrite oxidation can again re-enter the sulfur cycle and be subject to further reduction and oxidation processes (Ulrich et al., 2003; Roden et al., 2004).

3.5.2.2.   *Geochemical indicators of iron reduction and iron cycling processes*

Concentrations of ready available Fe(II) extracted from soil samples hint at the occurrence of iron reduction all across the investigated aquifer section, which is not that obvious from Fe(II) gradients measured in groundwater samples. Analogous to sulfur compounds, recycling of iron species is likely to proceed at high rates at the capillary fringe. There, re-oxidation of reduced iron compounds provides electron acceptors, which can be utilized by iron reducing bacteria (Ulrich et al., 1998; Ulrich et al., 2003). Hints on elevated iron reduction in this area are given by increased concentrations of dissolved Fe(II) compared to values measured in deeper zones of the aquifer and higher Fe(II)/sulfide ratios (Fig. 3.9A). A change in the colour of the sediments from brownish-reddish in the iron(III) oxide-rich unsaturated zone to grey-black right after entrance into the saturated aquifer indicates precipitation of iron sulfides, thus providing further evidence for sulfate and iron reduction. Apart from microbial iron reduction, abiotic reductive dissolution of Fe(III) minerals, as mentioned above, may partly be responsible for the elevated Fe(II) concentrations (Cozzarelli et al., 1999; Kostka et al., 2002). Molecular analyses of bacterial DNA extracted from an adjacent, previously drilled sediment liner revealed sequences closely related to genes of *Geobacter* species (Winderl et al., 2007; Winderl et al., 2008). The prevalence of this bacterial strain, which typically classifies a major representative of iron reducing bacteria, provides additional evidence for the importance of microbial iron reduction in this zone.

From a thermodynamic point of view, iron reduction is considered to be energetically more favourable than sulfate reduction (Lovley and Chapelle, 1995). Nevertheless, bacterial iron reduction in organically contaminated porous aquifers is frequently limited by Fe(III) availability, as reported for instance by Albrechtsen and Christensen (1994) and Tucillo et al. (1999). Also at our site, only low amounts of amorphous Fe(III) could be detected in the saturated zone (Fig. 3.5 A+B), and only crystalline Fe(III) species were available at higher concentrations all across the aquifer (Fig. 3.5 C+D). According to Roden and Zachara (1996), some bacteria are capable of using crystalline Fe(III) as electron acceptor. Owing to their stability and inaccessibility, however, these iron minerals are only slowly converted and less attractive to microorganisms (Lovley, 2001), thus giving way to microbial sulfate reduction, as described by Postma and Jakobsen (1996).

Anaerobic oxidation of 1 mg l^{-1} toluene with Fe(III) as electron acceptor is expected to result in the release of 22 mg l^{-1} Fe(II), as can be calculated from equation 3.3 (Wiedemeier et al., 1999):

$$C_7H_8 + 36\ Fe(OH)_3 + 65\ H^+ \rightarrow 7\ HCO_3^- + 36\ Fe^{2+} + 87\ H_2O \qquad \text{(eq. 3.3)}$$
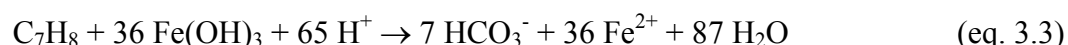
Considering the low concentrations of dissolved Fe(II) measured at our site (Fig. 3.4C), iron reduction is unlikely to be the dominant redox process. On the other hand, compared to total reduced inorganic sulfur (TRIS), about 10 to 100 times higher concentrations of Fe(II) were detected in most sediment samples analysed (Fig. 3.9B, primary x-axis). This may partly be attributed to re-oxidation of the reduced sulfur species during sampling, storing and

extraction procedures. Only in the unsaturated zone, where neither iron nor sulfate reduction are likely to occur, the amount of both compounds was low, exhibiting a $S^{2-}/Fe(II)$ ratio of ~ 1 (Fig. 3.9B, secondary x-axis). Also at the lower plume fringe, the ratio of TRIS compared to Fe(II) was comparatively high, as was the $S^{2-}/Fe(II)$ ratio determined in groundwater samples. The distribution of sulfides in the sediments therefore supports our data from groundwater analysis, which imply increased sulfate reduction at the transition between highly contaminated and less contaminated groundwater. A distinct peak of TRIS (Fig. 3.6.B) and an increased $S^{2-}/Fe(II)$ ratio (Fig. 3.9B) may also indicate pronounced sulfate reduction in sediments at 12 m depth. Unfortunately, groundwater samples were not taken at this depth, thus we cannot link sediment data to groundwater chemistry.

The assumption of increased sulfate reduction at the lower plume fringe is not only supported by steep concentration gradients of sulfate and sulfide, but also by an enrichment of ^{18}O and ^{34}S isotopes in groundwater sulfate, as discussed before. Furthermore, mass balance calculations, which are exemplarily given in section 4.5.2, pointed out the role of sulfate reduction at our study site.

Unlike groundwater samples, however, which provide only a momentary snapshot of the situation *in situ*, sediment analyses as performed in this work allow deeper insights into the history of the aquifer and into long-term processes occurring at a site. The data presented in this study furthermore emphasize the importance of taking into account geochemical cycling of iron species and deposition of mineral precipitates, since these processes may prevent the analytical detection of potential metabolic indicators (e.g. Fe(II) or sulfide) and thus lead to an underestimation of individual redox processes (Roden et al., 2004).

3.5.3. Co-occurrence of redox processes

The ratios of Fe(II) and sulfide as determined in groundwater samples imply an alternating dominance of iron and sulfate reduction with iron reduction dominating within the first 15 cm below groundwater table, while at the lower plume fringe iron reduction seems to
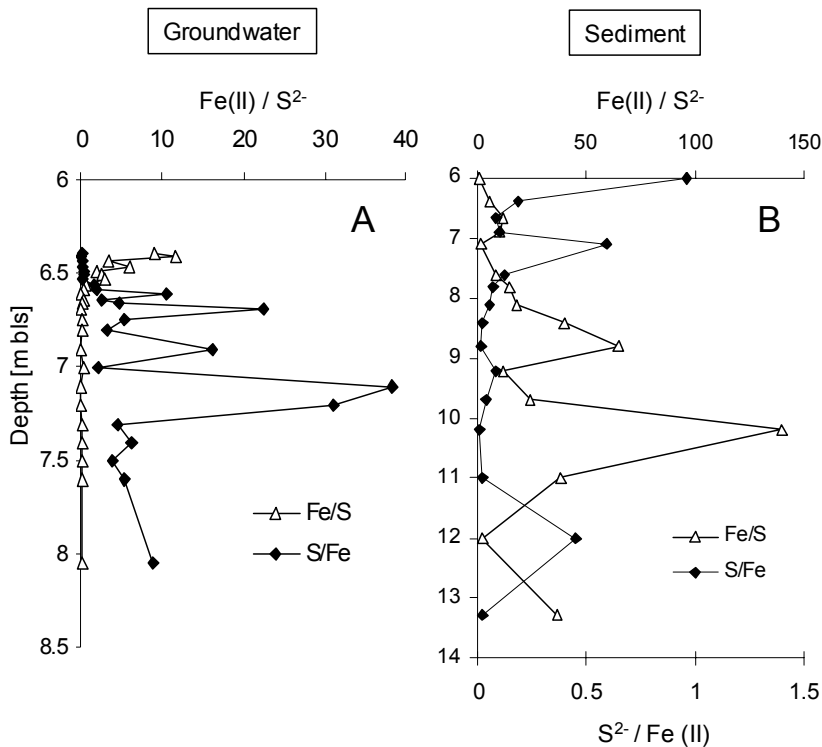
Figure 3.9 Ratios of dissolved ferrous iron and sulfide in A) groundwater samples of the HR-MLW and B) sediments of Liner 1.

be displaced by sulfate reduction (Fig. 3.9A). In fact, it is very likely to find simultaneous iron and sulfate reducing activities near the capillary fringe zone, where possible transient oxic or hypoxic conditions caused by fluctuating hydraulic regimes may promote geochemical cycling of redox species and thus provide a continuous supply of electron acceptors for both iron and sulfate reducers, as described for instance by Cozzarelli et al. (2001) and McGuire et al. (2002) (see also discussion in section 3.5.2). Even though dissolved sulfide was scarce in groundwater samples of the uppermost decimeters below the water table, stable isotope analyses of groundwater sulfate revealed increased $\delta^{34}S$ and $\delta^{18}O$ ratios also in the plume center, where elevated concentrations of dissolved Fe(II) hinted at iron reduction. Co-occurrence of redox processes has been observed at several sites and is also discussed in more detail in the following chapter of this thesis (section 4.5.2; Anneser et al., 2008).

3.5.4. Backtracking the origin of groundwater

Stable environmental isotopes are routinely used as natural hydrological tracers for the identification of flow paths and groundwater sources (Kendall and Caldwell, 1998). In this study, we applied stable isotope ratios of water to see whether the groundwater sampled from the HR-MLW originates from different sources, *i.e.* whether young groundwater from local precipitation and recharge meets older ("inherent") groundwater. Even though the analysis of D/H and $^{18}O/^{16}O$ ratios in water samples of the HR-MLW revealed no significant differences, the δ-values of both isotope pairs changed in depths between 6.7 and 7.1 m bls, apparently dividing the shallow saturated zone into two different water bodies (Fig. 3.8B). Isotope data thus hint at the concurrence of two different water sources, *i.e.* of groundwater transported along the hydraulic gradient ("light" water) and of ("heavy") water infiltrating from the unsaturated zone (Gonfiantini et al., 1998). This latter hypothesis is additionally supported by differences in the stable isotope composition of groundwater sulfate close to the groundwater table, as was discussed in the previous section.

3.5.5. Evaluation of *in situ* bioactivities

In order to assess *in situ* microbial activities, hydrolysis rates of extracellular phosphatases and glucosidases were determined by incubation of sediment and groundwater samples with fluorescently labelled phosphate (MUF-P) and glucoside (MUF-Glc), respectively (Freeman et al., 1995). As expected, maximum bioactivities were detected close to the capillary fringe, where recycling of electron acceptors and mixing with electron donors from the contaminated area create conditions favourable to biodegradation (Sinke et al., 1998; Ronen et al., 2000). Maximum hydrolysis rates of MUF-P and MUF-Glc coincided with highest abundance of sediment bacteria at the upper fringe of the BTEX plume (Fig. 3.7). With an increasing degree of contamination, enzyme activities in sediment and groundwater samples declined rapidly. At the lower plume fringe, bioactivities seemed to be resumed, yet at much lower rates. As phosphatase activities generally increase with microbial phosphate requirements, low biomass abundance (Fig. 3.7B) and high phosphate concentrations in the plume core (Fig. 3.4D) may explain the reduced MUF-P hydrolysis rates. A reverse pattern was observed at the capillary fringe, where much lower concentrations of soluble reactive phosphate in groundwater in parallel to high total cell numbers may have promoted extracellular phosphatase activities.

The observation of 5-6 orders of magnitude higher enzyme activities in sediment compared to groundwater samples can partly be ascribed to the fact that 80 – 99.99 % of the bacteria in aquifers live attached to the sediment matrix (Alfreider et al., 1997; Griebler et al., 2001; Griebler et al., 2002; O'Donnell et al., 2007). Cell numbers and hydrolysis rates assessed from

groundwater samples therefore represent only a small fraction of the entire community biomass and activity. This observation was already demonstrated in a number of studies, where extracellular enzyme activities of sediment-associated communities exceeded those of free-living cells significantly (e.g. Hoppe, 1991; Lehman and O'Connell, 2002). On the other hand, discrepancies in activities between attached and free living cells in organically contaminated sediments have been observed to converge (Griebler et al., 2002). The tremendous differences between groundwater and sediment fractions measured at our site therefore remain unexplained so far.

Zones of enhanced microbial activity matched well zones with highest biomass concentration (Fig. 3.7B). Contrarywise, molecular analysis of sediment samples from an adjacent, previously sampled core at our investigation site (Winderl et al., 2008) exhibited the highest abundance of 16S rRNA gene copies in the plume center, where biodegradation was presumed to be restricted by the toxicity of the contaminants and limited electron acceptor availability. Increased cell numbers in sediment samples collected from the center of contaminant plumes were also reported in previous studies (e.g. Bekins et al., 1999; Ludvigsen et al., 1999). Nevertheless, as discussed in section 4.5.3, at the lower border of the plume core toluene degrader-specific gene sequences were prevailing, thus suggesting enhanced contaminant removal being active in this area (Winderl et al., 2007). Last but not least, biomass and microbial activity data have to be regarded in the light of temporal and spatial dynamics of biogeochemical gradients, which have been observed during a multitude of sampling events and a period of several months (see chapter 5). Apparent contradictory gradients, e.g. high total numbers of attached cells within the highly contaminated zone probably reflect the situation of the past. This can be explained by the observation that biofilms display a kind of memory effect, *i.e.* numbers of attached cells do not change within hours or days (Griebler et al., 2001). Lack of clear correlations between the sediment biomass and geochemical patterns may be attributed to hydraulic changes, which occurred prior to our sampling campaign and which may have become apparent within the sediment communities only after a certain time lag of weeks to months.

3.5.6. Limitations of contaminant natural attenuation

Biodegradation of organic pollutants in aquifers involves numerous complex processes facing a variety of limitations. The toxicity of the contaminant itself or of reaction products and the restricted availability of electron acceptors were already mentioned before. Furthermore, environmental conditions (e.g. pH, temperature, salinity) or the availability of essential nutrients, such as nitrogen or phosphorous, constitute further potentially limiting factors of natural attenuation (Langwaldt and Puhakka, 2000).

Phosphorus, as one essential nutrient for bacterial growth, was assumed not to control biodegradation at our study site owing to the exceptionally high amounts of soluble reactive phosphate detected in the plume center. Limitation of biodegradation by electron acceptor availability, on the other hand, was somehow obvious. Since oxygen and, probably, nitrate are lacking throughout the saturated aquifer, oxidation of the contaminants is dependent on the availability of Fe(III) and sulfate. While ready available ferric oxyhydroxides are scarce in the anoxic aquifer, sulfate is sufficiently disposable in less contaminated zones, but conspicuously depleted in the plume center. In a number of experimental studies and numerical simulations, mixing of electron donors and electron acceptors across geochemical interfaces was suggested to be the major factor controlling natural attenuation in porous media (Prommer et al., 2002; Jose and Cirpka, 2004; Maier and Grathwohl, 2006). Transverse dispersivities in sandy aquifers, which are reported to be in the range of millimeters to centimeters (Klenk and Grathwohl, 2002), are therefore presumably not effective enough to grant sufficient supply of sulfate to the inner plume core, as was exemplarily shown with data of a subsequent sampling

campaign (see section 4.5.3). At several occasions, on the other hand, sulfate was available throughout the plume center, thus hinting towards additional factors controlling biodegradation. With regard to iron reduction, limitation of biodegradation by the comparably poor availability and bad accessibility of ferric iron species is obvious (see section 3.5.2) and is also frequently discussed in literature (Lovley, 1991; Cozzarelli et al., 1999; Tucillo et al., 1999; Christensen et al., 2001).

Ideally, mixing of electron donors and electron acceptors at interfaces results in an instantaneous turnover of the reactants. Since natural attenuation is to a large degree controlled by biokinetics and by mass transfer across physical and biological boundaries (Wick et al., 2001; Johnsen et al., 2005), various cellular mechanisms, e.g. substrate uptake and conversion, may additionally control biodegradation rates. These biokinetic constraints may, for example, be responsible for an overlap of electron donors and electron acceptors, as it was observed in microcosm experiments (Bauer et al., 2008) as well as *in situ* in our case study. Last but not least, low carbon assimilation efficiencies and slow growth rates of groundwater microorganisms and, consequently, low biomass and cell abundances may additionally limit biodegradation in the Flingern aquifer.

3.6. Conclusions

This study demonstrates a fairly good agreement between geochemical and biological data of sediment and groundwater samples. We could, for instance, clearly delineate the BTEX plume and zones of sulfate and iron reduction by comparing gradients of electron donors, electron acceptors, metabolic end products and stable isotope ratios of individual compounds. Likewise, bacterial cell numbers and enzyme activities in sediment and groundwater samples pinpointed zones of increased biodegradation. More than this, comparing sediment and groundwater data revealed correlations and interdependencies that were not obvious from separate, non-comparative analysis of one of the sample types only. This is exemplarily demonstrated for concentrations at the capillary fringe as well as for sulfate and iron reduction. These would have been clearly underestimated if groundwater had been analysed without regard to the chemical composition of the sediment. Unlike groundwater chemistry, which provides only a momentary snapshot of the situation *in situ*, the sediment can be regarded as an "archive" that helps to trace back biogeochemical processes over longer periods and, consequently, to deduce the history of the subsurface environment.

Changing from simplifying "black box" approaches to a "multiple parameter" approach implies a plethora of data that requires thorough and reasonable processing and interpretation. For evaluating and predicting the transport of groundwater pollutants as well as natural attenuation processes, reactive transport models were developed, which meanwhile represent indispensable tools for the conceptualization of remediation strategies. Despite the variety of numerical and analytical solutions existing by now, spatially and temporally appropriate data is still scarce, thus raising the demand for comprehensive site investigations as presented in this study.

3.7. References

Albrechtsen, H.J., and Christensen, T.H. (1994) Evidence for microbial iron reduction in a landfill leachate-polluted aquifer (Vejen, Denmark). *Appl Environ Microbiol* 60: 3920-3925.

Alfreider, A., Krössbacher, M., and Psenner, R. (1997) Groundwater samples do not reflect bacterial densities and activity in subsurface systems. *Water Res* 31: 832-840.

Anderson, R.T., and Lovley, D.R. (1997) Ecology and biogeochemistry of *in situ* groundwater bioremediation. *Adv Microb Ecol* 15: 289-350.

Anneser, B., Einsiedl, F., Meckenstock, R.U., Richters, L., Wisotzky, F., and Griebler, C. (2008) High-resolution monitoring of biogeochemical gradients in a tar oil-contaminated aquifer. *Appl Geochem* 23: 1715-1730.

Appelo, C.A.J., and Postma, D. (2005) *Geochemistry, groundwater and pollution.* Taylor & Francis Group plc., Leiden, NL.

Báez-Cazull, S.B., McGuire, J.T., Cozzarelli, I.M., Raymond, A., and Welsh, L. (2007) Centimeter-scale characterization of biogeochemical gradients at a wetland-aquifer interface using capillary electrophoresis. *Appl Geochem* 22: 2664-2683.

Bamforth, S.M., and Singleton, I. (2005) Bioremediation of polycyclic aromatic hydrocarbons: current knowledge and future directions. *J Chem Technol Biotechnol* 80: 723-736.

Bauer, R.D., Maloszewski, P., Zhang, Y., Meckenstock, R.U., and Griebler, C. (2008) Mixing-controlled biodegradation in a toluene plume - Results from two-dimensional laboratory experiments. *J Contam Hydrol* 96: 150-168.

Bekins, B.A., Godsy, E.M., and Warren, E. (1999) Distribution of microbial physiologic types in an aquifer contaminated by crude oil. *Microb Ecol* 37: 263-275.

Canfield, D.E. (2001) Isotope fractionation by natural populations of sulfate-reducing bacteria. *Geochim Cosmochim Acta* 65: 1117-1124.

Christensen, T.H., Bjerg, P.L., Banwart, S.A., Jakobsen, R., Heron, G., and Albrechtsen, H.-J. (2000) Characterization of redox conditions in groundwater contaminant plumes. *J Contam Hydrol* 45: 165-241.

Christensen, T.H., Kjeldsen, P., Bjerg, P.L., Jensen, D.L., Christensen, J.B., Baun, A. et al. (2001) Biogeochemistry of landfill leachate plumes. *Appl Geochem* 16: 659-718.

Cirpka, O.A. (2005) Effects of sorption on transverse mixing in transient flows. *J Contam Hydrol* 78: 207-229.

Cline, J.D. (1969) Spectrophotometric determination of hydrogen sulfide in natural waters. *Limnol Oceanogr* 14: 454-458.

Cozzarelli, I.M., Herman, J.S., Baedecker, M.J., and Fischer, J.M. (1999) Geochemical heterogeneity of a gasoline-contaminated aquifer. *J Contam Hydrol* 40: 261-284.

Cozzarelli, I.M., Bekins, B.A., Baedecker, M.J., Aiken, G.R., Eganhouse, R.P., and Tuccillo, M.E. (2001) Progression of natural attenuation processes at a crude-oil spill site: I. Geochemical evolution of the plume. *J Contam Hydrol* 53: 369-385.

Eberhardt, C., and Grathwohl, P. (2002) Time scales of organic contaminant dissolution from complex source zones: coal tar pools vs. blobs. *J Contam Hydrol* 59: 45-66.

Freeman, C., Liska, G., Ostle, N.J., Jones, S.E., and Lock, M.A. (1995) The use of fluorogenic substrates for measuring enzyme activity in peatlands. *Plant Soil* 175: 147-152.

Gonfiantini, R., Fröhlich, K., Araguás-Araguás, L., and Rozanski, K. (1998) Isotopes in groundwater hydrology. In *Isotope tracers in catchment hydrology.* Kendall, C., and McDonnell, J.J. (eds): Elsevier Science B. V.

Griebler, C., Mindl, B., and Slezak, D. (2001) Combining DAPI and SYBR Green II for the enumeration of total bacterial numbers in aquatic sediments. *Int Rev Hydrobiol* 86: 453-465.

Griebler, C., Mindl, B., Slezak, D., and Geiger-Kaiser, M. (2002) Distribution patterns of attached and suspended bacteria in pristine and contaminated shallow aquifers studied with an *in situ* sediment exposure microcosm. *Aquat Microb Ecol* 28: 117-129.

Griffin, W.T., Phelps, T.J., Colwell, F.S., and Fredrickson, J.K. (1997) Methods for obtaining deep subsurface microbiological samples by drilling. In *The microbiology of the terrestrial deep subsurface.* Amy, P.S.H., D. L. (ed). Lewis Publishers, Boca Raton, USA.

Haack, S.K., and Bekins, B.A. (2000) Microbial populations in contaminant plumes. *Hydrogeol J* 8: 63-76.

Hendel, B., and Marxsen, J. (1997) Measurement of low-level extracellular enzyme activity in natural waters using fluorigenic model substrates. *Acta Hydrochim Hydrobiol* 25: 253-258.

Heron, G., Crouzet, C., Bourg, A.C.M., and Christensen, T.H. (1994) Speciation of Fe(I I) and Fe(I I I) in contaminated aquifer sediments using chemical extraction techniques. *Environ Sci Technol* 28: 1698-1705.

Hoppe, H.-G. (1991) Microbial extracellular enzyme activity: a new key parameter in aquatic ecology. In *Microbial enzymes in aquatic environments.* Chrost, R.J. (ed). Springer Verlag, New York, USA, pp. 60-83.

IAEA (1983) *Guidebook on nuclear techniques in hydrology.* Vienna.

Johnsen, A.R., Wick, L.Y., and Harms, H. (2005) Principles of microbial PAH-degradation in soil. *Environ Pollut* 133: 71-84.

Jose, S.C., and Cirpka, O.A. (2004) Measurement of mixing-controlled reactive transport in homogeneous porous media and its prediction from conservative tracer test data. *Environ Sci Technol* 38: 2089-2096.

Kendall, C., and Caldwell, E.A. (1998) Fundamentals of Isotope Geochemistry. In *Isotope Tracers in Catchment Hydrology.* Kendall, C., and McDonnell, J.J. (eds). Elsevier Science B.V., Amsterdam, NL, pp. 51-86.

Klenk, I.D., and Grathwohl, P. (2002) Transverse vertical dispersion in groundwater and the capillary fringe. *J Contam Hydrol* 58: 111-128.

Kostka, J.E., Roychoudhury, A., and Van Cappellen, P. (2002) Rates and controls of anaerobic microbial respiration across spatial and temporal gradients in saltmarsh sediments. *Biogeochemistry* 60: 49-76.

Langwaldt, J.H., and Puhakka, J.A. (2000) On-site biological remediation of contaminated groundwater: a review. *Environ Pollut* 107: 187-197.

Lehman, R.M., and O'Connell, S.P. (2002) Comparison of extracellular enzyme activities and community composition of attached and free-living bacteria in porous medium columns. *Appl Environ Microbiol* 68: 1569-1575.

Lovley, D.R. (1991) Dissimilatory Fe(III) and Mn(IV) reduction. *Microbiol Rev* 55: 259-287.

Lovley, D.R. (2001) Anaerobes to the rescue. *Science* 293: 1444-1446.

Lovley, D.R., and Phillips, E.J. (1987) Rapid Assay for Microbially Reducible Ferric Iron in Aquatic Sediments. *Appl Environ Microbiol* 53: 1536-1540.

Lovley, D.R., and Chapelle, F.H. (1995) Deep subsurface microbial processes. *Rev Geophys* 33: 365-381.

Ludvigsen, L., Albrechtsen, H., Ringelberg, D.B., Ekelund, F., and Christensen, T.H. (1999) Distribution and composition of microbial populations in a landfill leachate contaminated aquifer (Grindsted, Denmark). *Microb Ecol* 37: 197-207.

Maier, U., and Grathwohl, P. (2006) Numerical experiments and field results on the size of steady state plumes. *J Contam Hydrol* 85: 33-52.

Maier, U., Rügner, H., and Grathwohl, P. (2007) Gradients controlling natural attenuation of ammonium. *Appl Geochem* 22: 2606-2617.

Mayer, K.U., Benner, S.G., Frind, E.O., Thornton, S.F., and Lerner, D.N. (2001) Reactive transport modeling of processes controlling the distribution and natural attenuation of phenolic compounds in a deep sandstone aquifer. *J Contam Hydrol* 53: 341-368.

McGuire, J.T., Long, D.T., Klug, M.J., Haack, S.K., and Hyndman, D.W. (2002) Evaluating behavior of oxygen, nitrate, and sulfate during recharge and quantifying reduction rates in a contaminated aquifer. *Environ Sci Technol* 36: 2693-2700.

McGuire, J.T., Smith, E.W., Long, D.T., Hyndman, D.W., Haack, S.K., Klug, M.J., and Velbel, M.A. (2000) Temporal variations in parameters reflecting terminal-electron-accepting processes in an aquifer contaminated with waste fuel and chlorinated solvents. *Chemical Geology* 169: 471-485.

Moser, H., and Rauert, W. (1980) *Isotopenmethoden in der Hydrologie.* Gebrüder Borntraeger, Berlin-Stuttgart.

O'Donnell, A.G., Young, I.M., Rushton, S.P., Shirley, M.D., and Crawford, J.W. (2007) Visualization, modelling and prediction in soil microbiology. *Nat Rev Microbiol* 5: 689-699.

Postma, D., and Jakobsen, R. (1996) Redox zonation: equilibrium constraints on the Fe (III)/SO$_4^{2-}$ reduction interface. *Geochim Cosmochim Acta* 60: 3169-3175.

Prommer, H., Barry, D.A., and Davis, G.B. (2002) Modelling of physical and reactive processes during biodegradation of a hydrocarbon plume under transient groundwater flow conditions. *J Contam Hydrol* 59: 113-131.

Prommer, H., Tuxen, N., and Bjerg, P.L. (2006) Fringe-controlled natural attenuation of phenoxy acids in a landfill plume: integration of field-scale processes by reactive transport modeling. *Environ Sci Technol* 40: 4732-4738.

Rahman, M.A., Jose, S.C., Nowak, W., and Cirpka, O.A. (2005) Experiments on vertical transverse mixing in a large-scale heterogeneous model aquifer. *J Contam Hydrol* 80: 130-148.

Roden, E.E., and Zachara, J.M. (1996) Microbial reduction of crystalline iron(III) oxides: influence of oxide surface area and potential for cell growth. *Environ Sci Technol* 30: 1618-1628.

Roden, E.E., Sobolev, D., Glazer, B., and Luther, G.W. (2004) Potential for microscale bacterial Fe redox cycling at the aerobic-anaerobic interface. *Geomicrobiol J* 21.

Ronen, D., Scher, H., and Blunt, M. (2000) Field observations of a capillary fringe before and after a rainy season. *J Contam Hydrol*: 103-118.

Ronen, D., Graber, E.R., and Laor, Y. (2005) Volatile organic compounds in the saturated-unsaturated interface region of a contaminated phreatic aquifer. *Vadose Zone Journal* 4: 337-344.

Schmid, N. (2004) Contaminant threshold concentrations in bacterial mineralization of individual petroleum hydrocarbons. MSc thesis. In *Institute for Geoscience, Center for Applied Geoscience (ZAG)*: Eberhard Karls University Tübingen, Germany.

Sinke, A.J.C., Dury, O., and Zobrinst, J. (1998) Effects of a fluctuating water table: column study on redox dynamics and fate of some organic pollutants. *J Contam Hydrol*: 231-246.

Stookey, L.L. (1970) Ferrozine - a new spectrophotometric reagent for iron. *Anal Chem* 42: 779-781.

Stumm, W., and Morgan, J.J. (1996) *Aquatic Chemistry*: John Wiley & Sons Inc, New York.

Tucillo, M.E., Cozzarelli, I.M., and Herman, J.S. (1999) Iron reduction in the sediments of a hydrocarbon-contaminated aquifer. *Appl Geochem* 14: 655-667.

Tuxen, N., Albrechtsen, H.J., and Bjerg, P.L. (2006) Identification of a reactive degradation zone at a landfill leachate plume fringe using high resolution sampling and incubation techniques. *J Contam Hydrol* 85: 179-194.

Ulrich, G.A., Krumholz, L.R., and Suflita, J.M. (1997) A Rapid and Simple Method for Estimating Sulfate Reduction Activity and Quantifying Inorganic Sulfides. *Appl Environ Microbiol* 63: 4626.

Ulrich, G.A., Breit, G.N., Cozzarelli, I.M., and Suflita, J.M. (2003) Sources of sulfate supporting anaerobic metabolism in a contaminated aquifer. *Environ Sci Technol* 37: 1093-1099.

Ulrich, G.A., Martino, D., Burger, K., Routh, J., Grossman, E.L., Ammerman, J.W., and Suflita, J.M. (1998) Sulfur cycling in the terrestrial subsurface: commensal interactions, spatial scales, and microbial heterogeneity. *Microb Ecol* 36: 141-151.

USACE (2002) Soil Vapor Extraction and Bioventing. In *Engineering and Design*: US Army Corps of Engineers.

Wick, L.Y., Colangelo, T., and Harms, H. (2001) Kinetics of mass transfer-limited bacterial growth on solid PAHs. *Environ Sci Technol* 35: 354-361.

Widdel, F., and Bak, F. (1992) Gram negative mesophilic sulfate reducing bacteria. In *The Prokaryotes. A handbook on the biology of bacteria: ecophysiology, isolation, identification, and applications*. Balows, H.G.T.A., Dwarkin, M., Harder, W., and Schleifer, K.H. (eds): Springer, New York, pp. 3352-3378.

Wiedemeier, T.H., Rifai, H.S., Newell, C.J., and Wilson, J.T. (1999) *Natural Attenuation of Fuels and Chlorinated Solvents in the Subsurface*: John Wiley & Sons, New York.

Winderl, C., Schaefer, S., and Lueders, T. (2007) Detection of anaerobic toluene and hydrocarbon degraders in contaminated aquifers using benzylsuccinate synthase (bssA) genes as a functional marker. *Environ Microbiol* 9: 1035-1046.

Winderl, C., Anneser, B., Griebler, C., Meckenstock, R.U., and Lueders, T. (2008) Depth-resolved quantification of anaerobic toluene degraders and aquifer microbial community patterns in distinct redox zones of a tar oil contaminant plume. *Appl Environ Microbiol* 74: 792-801.

4. High-resolution monitoring of biogeochemical gradients in a tar oil-contaminated aquifer

4.1. Introduction

Several hundred thousand groundwater sites worldwide are organically contaminated and scheduled for cleanup, which is associated with immense efforts and costs. This has stimulated the evaluation of the potential of natural attenuation (NA) in contaminated aquifers and the development of bioremediation strategies. Although natural attenuation is on the way to become an accepted strategy when dealing with impacted sites, there is still a need for reliable methods to identify and monitor occurrence, distribution and extent of biodegradation *in situ*.

Monoaromatic and polycyclic aromatic hydrocarbons represent an important class of contaminants being part of gasoline, tar oil and other petroleum products. The high water solubility of the BTEX (*i.e.* benzene, toluene, ethylbenzene, xylenes) and the toxicity impose a specific significance onto these substances regarding polluted aquifers. Introduced into the aquifer, the pollutants partly dissolve from the non-aqueous phase liquids (NAPL) and are transported with groundwater flow, forming an organic contaminant plume (Christensen et al., 2000). Typically, natural attenuation processes then lead to the development of a quasi-stationary plume where NAPL dissolution rates equal removal rates of the solutes in the plume. In such mature (stable) hydrocarbon plumes elimination of the contaminants by abiotic processes, such as sorption/desorption or volatilization may be negligible. Instead, dilution by diffusion and dispersion controls the distribution and microbially mediated degradation is considered to be the dominant process responsible for a net reduction in mass flow of contaminants (Christensen et al., 2001).

In porous aquifers, where laminar flow prevails, longitudinal and transverse dispersion represent the dominant mixing processes (Cirpka et al., 1999). Therefore, at the fringes of organic contaminant plumes mixing of anoxic polluted groundwater with oxic pristine groundwater results in the concurrence of electron donors (organic contaminants) and electron acceptors such as oxygen, nitrate, and sulfate and conditions beneficial for biodegradation are created. Thus, the degradation potential for various electron donors like aromatic hydrocarbons is absent or limited inside the plume, but excellent in the plume fringe area (van Breukelen and Griffioen, 2004). A few studies reported enhanced biodegradation rates at these zones, which are generally displayed by steep biogeochemical gradients (Davis et al., 1999; Spence et al., 2001; McGuire et al., 2005; Tuxen et al., 2006; Rees et al., 2007). Progress in understanding of NA processes now requires detailed information on these gradients and on the spatial distribution of biodegradation (Lerner et al., 2000 ; Thornton et al., 2001 ; van Breukelen & Griffioen, 2004 ; Kappler et al., 2005).

The increasing awareness of the role of gradients for evaluating redox processes is reflected in a repeated claim for scale-adapted sampling (Smith et al., 1991; Wilson et al., 2004). However, the definition of the relevant scale highly depends on the environment as well as on the issue of investigation (Haack and Bekins, 2000). While in the open ocean a scale of tens of meters may be appropriate, only a millimeter resolution is sufficient to capture the steep biogeochemical gradients in marine surface sediments, and the analysis of cell-cell interactions and gradients within biofilms asks for even more sophisticated tools capable of recording concentration profiles at µm- to nm-scales (Kappler et al., 2005). Already decades ago, Ronen et al. (1987) and Pickens et al. (1978) observed significant variations in concentrations of electron acceptors and contaminants along a vertical aquifer cross section at the centimeter and decimeter scale, respectively. More recent studies demonstrated that the appropriate scale for sampling in porous aquifers may range between centimeters and meters in dependence to sediment texture and hydraulic conductivity (Smith et al., 1991; Bjerg et al.,

1995; Postma and Jakobsen, 1996; Jakobsen and Postma, 1999; Lerner et al., 2000; Thornton et al., 2001; van Breukelen and Griffioen, 2004; Wilson et al., 2004; Salminen et al., 2006; Scholl et al., 2006; Báez-Cazull et al., 2007). To complement these data, reactive transport models suggest the width of the mixing zone at the fringe of contaminant plumes in porous aquifers to be in the range of millimeters up to decimeters (Klenk and Grathwohl, 2002).

The intention of the present study was to evaluate the geochemical gradients at the fringe of a BTEX plume by means of a new multi-level sampling well designed for the extraction of groundwater at an extraordinary high vertical resolution of 2.5 – 33 cm. The new information gained from small-scale vertical distribution patterns of selected biogeochemical parameters is highlighted in comparison to results from a conventional multi-level well with 0.5 - 1m screening intervals. Moreover, the data of the high-resolution multi-level well are discussed with regard to redox processes involved in biodegradation and the distribution of microbial activities across the anoxic hydrocarbon plume undergoing natural attenuation. The study raises evidence for additional limitations of biodegradation in contaminant plumes besides the control by hydrodynamic mixing, *i.e.* mainly transverse dispersion.

4.2. Site description

The study site was a Quaternary sand and gravel aquifer at a former gasworks site (Düsseldorf - Flingern) in the river Rhine valley, Western Germany. Across a thickness of about 10 m the sediments show a relatively homogeneous composition and permeability (mean $k_f = 1 \times 10^{-3}$ m s^{-1}), which is interrupted by thin gravel inclusions only in deeper layers (> 12 m below land surface (bls)). In about 15 m bls the aquifer is confined by low permeable Tertiary fine sand layers (Fig. 4.1). Groundwater in this section of the aquifer follows a hydraulic gradient of about 6 ‰ from east towards west with a velocity of 0.1 - 2 m d^{-1}.

From 1893 until 1967, benzene, gas, coke, and different tar oil components were produced on an area of about 170,000 m^2. Production processes, but also destructions during World War II and finally the deconstruction of the plant in 1968 led to the release of monoaromatic and polycyclic aromatic hydrocarbons into the sediments and groundwater over a period of at least 30 years. Consequently, a predominantly anoxic contaminant plume of about 600 m length and 100 m width, consisting mainly of benzene, toluene, ethylbenzene, xylenes (BTEX), as well as naphthalene and acenaphthene, developed (Wisotzky and Eckert, 1997; Eckert, 2001). Several remediation actions launched in 1996, including soil excavation, hydraulic barriers, pump & treat measurements, and *in situ* biostimulation successfully removed the major part of the tar oil phases from the source zone and reduced the size of the BTEX plume to 200 m × 40 m in dimension with a thickness of only 1 – 2 m (Fig. 4.1). The maximum concentration of BTEX (with toluene constituting the main contaminant) decreased from originally more than 100 mg l^{-1} to 20 mg l^{-1} on average, while total PAH concentrations remained more or less constant at ~ 10 mg l^{-1} (Eckert, 2001). The excavated soil areas were re-filled with sand and gravel. Concrete sealings across wide areas of the former gasworks site prevent intrusion of rainwater into the sediment and aquifer, thus weakening the relevance of direct recharge.
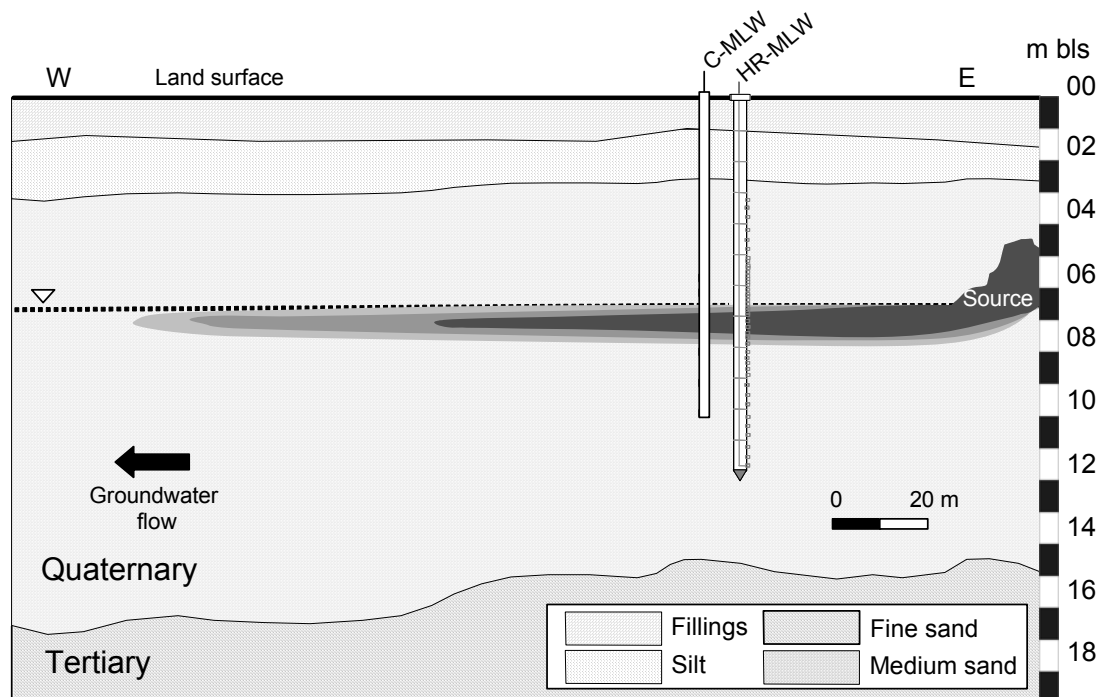
Figure 4.1 Cross section through the investigated aquifer depicting the geologic situation and the approximate location of the high-resolution multi-level well (HR-MLW) and the adjacent conventional multi-level well (C-MLW) in relation to the contaminant distribution; bls = below land surface.

4.3. Materials and methods

4.3.1. High-resolution multi-level groundwater well

In order to obtain groundwater samples at a high vertical resolution across the fringe and center zones of the contaminant plume, a novel high-resolution multi-level well (MLW) was designed with a sampling resolution of down to 2.5 cm. The well was assembled of 12 single units, each consisting of a high-density polyethylene (HDPE) tube of 1 m length and 15 cm outer diameter, so the total length of the well was 12 m (Fig. 4.2A). At pre-selected depths, small filter units (sintered bronze silencers, Norgren, UK) were inserted at distances of either 2.5 cm (high resolution, HR), 10 cm (middle resolution, MR) or 33 cm (low resolution, LR) from each other (Fig. 4.2 B-D). Each filter unit was connected to a peristaltic pump via a stainless steel capillary (1 mm inner diameter; Fig. 4.2 C+E) that was inserted tightly through a rubber stopper into the filter port. Depth distribution of the sampling ports and the degree of spatial resolution were chosen according to the approximate location of the plume center. This information was gained from sampling a conventional multi-level well with 2-inch filter elements (0.5 – 1 m screening intervals) in the direct vicinity (1 m distance) of the high-resolution MLW (Fig. 4.1).

Hollow-stem auger drilling was applied prior to installation of the high-resolution MLW. After insertion of the well and removal of the supporting steel pipes the sediment was allowed to collapse, thus providing a perfect embedding of the filter ports in the aquifer sediments and preventing hydraulic shortcuts from artificial filter sands. The sediment liners obtained from borehole drilling were processed anoxically for analyses of biogeochemical parameters, as described in section 3.3.

57
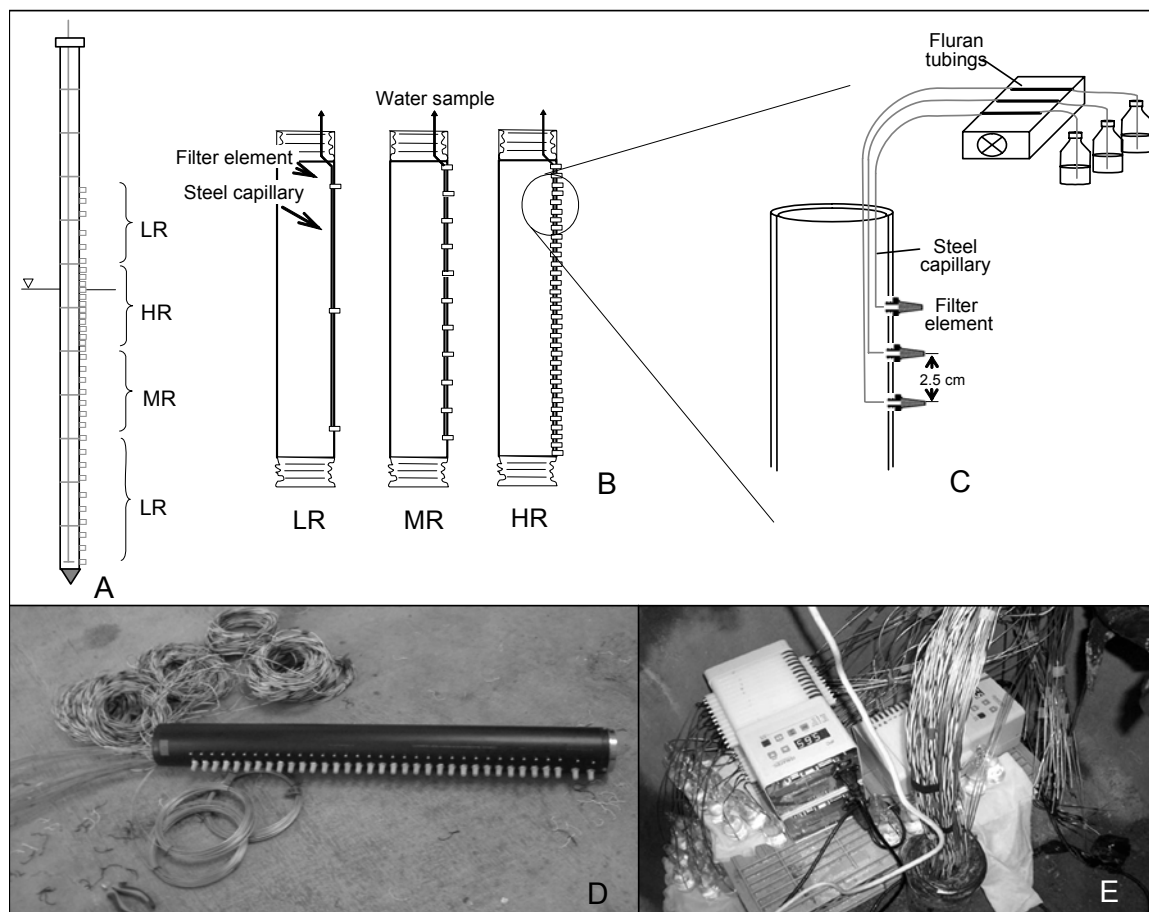
Figure 4.2 Schematic drawings of the high-resolution multi-level well; A) arrangement of the modules in the mounted well; B) modules with filter screen intervals of 33 cm (low resolution; LR), 10 cm (middle resolution; MR) and 2.5 cm (high resolution; HR); C) detailed view of filter screens and sampling equipment assembly; D) photograph of a HR-module; E) view on sampling equipment assembly in the manhole of the well.

4.3.2. Groundwater sampling

After the introduction of the high-resolution MLW in June 2005 the well was left for three months of acclimatization before a first sampling campaign was performed in September 2005. The data presented in this work stem from our fourth groundwater sampling campaign in August 2006. A selection of ports was chosen for sampling in order to obtain (1) a highly-resolved profile (2.5-10 cm) across the putative plume center and fringes and (2) a less resolved (10-33 cm) vertical profile of the Quaternary aquifer down to a depth of 10 m below land surface (bls). For sampling, the selected steel capillaries were connected to multi-channel peristaltic pumps (IPC-N or IPC) using 2-stopper Fluran HCA tubes (both Ismatec, Wertheim, Germany). Previous pumping tests with different tube materials suggested Fluran tubings to be most suitable for hydrocarbon sampling from anoxic systems with respect to gas permeability and sorption of aromatic hydrocarbons (see section 2.4.1 and Anneser et al., 2008). In order to avoid volatilization of contaminants and re-oxidation of reduced components such as sulfide and ferrous iron the Fluran tubes and sample bottles were bridged by short steel capillaries, which were submerged to the bottom of the sampling vessels (100 ml narrow neck glass bottles; Fig. 4.2E).

For comparison, groundwater of a conventional MLW 1 m apart from the new high-resolution MLW was collected four weeks later. Here, samples were drawn by use of a multi-channel suction pump at a rate of several liters per minute.

In order to prevent mixing of waters from different depths, the filter screens were sampled simultaneously both for the high-resolution and the conventional MLW.

4.3.3. Sample preparation and analysis

4.3.3.1. Dissolved and sedimentary metabolites and ions

Groundwater aliquots for analysis of dissolved sulfide, Fe(II), major anions, and cations as well as aromatic hydrocarbons were subsampled directly from the bottom of the sample vessels and treated immediately in order to avoid oxidation and volatilization of analytes. For sulfide determination, 200 µl of sample were fixed in duplicates in 1 ml of a 2 % (w/v) zinc acetate solution, following in principle the protocol of Cline (1969). For quantification of Fe(II), 100 µl of groundwater were fixed in 900 µl 1M HCl in 1.5 ml Eppendorf tubes. The amount of Fe(II) was measured photometrically by the ferrozine assay (Stookey, 1970). Samples for sulfide and Fe(II) analyses were further processed and photometrically measured on site.

During drilling of the new high-resolution MLW sediment liners were taken for analysis of different hydrogeochemical parameters. For determination of sedimentary sulfide, the core samples were brought into argon-gas flooded plastic bags and frozen at -20°C until preparation. After freeze drying the soil samples were ground and homogenised. The sulfide-sulfur was measured after combustion at 550°C infra-red spectroscopically as SO_2 (Combustion Furnace CS 5500, Ströhlein, Germany).

Sedimentary iron was extracted from 2 ml sample aliquots with 30 ml of 0.5 M HCl (ready extractable iron) or 5 M HCl (crystalline iron), respectively, during 24 hours or 21 days of intensive shaking at room temperature. Concentrations of Fe(II) were measured as described above. The Fe(III) content from sediment samples was obtained by complete reduction of the total iron to Fe(II) with hydroxylamine hydrochloride solution in 1 M HCl (10% w/w). Samples of 100 µl, which had been incubated in 0.5 M or 5 M HCl as described above, were added to 900 µl of hydroxylamine solution, incubated for 20 min at room temperature, and measured by the ferrozine assay. The Fe(III) concentration was derived from the difference between total iron content and concentrations of Fe(II).

For BTEX analysis, a sample volume of 3 ml was transferred into 10 ml headspace GC vials and amended with 300 µl of 1M NaOH (final concentration 0.1 M) to stop biological activity. Vials were sealed with gas tight polytetrafluoroethylene (PTFE) septa. Samples dedicated to the analysis of polycyclic aromatic hydrocarbons (PAH) were filled into 15 ml glass vials (Supelco/Sigma-Aldrich, Munich, Germany) and closed avoiding headspace with PTFE-coated screw caps. BTEX and PAH samples were stored at 4°C in the dark until further analysis.

The leftover of the 50 - 100 ml groundwater samples was filtered through a 0.45 µm pore size filter, placed on ice, and the following day used for the analysis of major anions and cations by ion chromatography on a Dionex DC-100 device (Dionex, Idstein, Germany) and for determination of dissolved inorganic and organic carbon using a Sievers* 900 Portable TOC analyser (GE Analytical Instruments, Boulder, USA).

Redox potential (E_H), pH, and electrical conductivity were measured in freshly sampled groundwater using field sensors (WTW, Weilheim, Germany).

4.3.3.2.   Mono- and polycyclic aromatic hydrocarbons

Contaminant concentrations (BTEX and PAHs) were determined with a Trace DSQ GC-MS instrument (Thermo Electron, Dreieich, Germany) equipped with a Combi PAL autosampler (CTC Analytics, Zwingen, Switzerland).

For headspace analysis of BTEX compounds, 250 µl of gas sample were injected at a split ratio of 1:10 onto a DB5 capillary column (J & W Scientific, Folson, CA, USA). Helium was used as carrier gas at a flow rate of 1 ml min^{-1}. The oven temperature was as follows: 40°C for 1 min, then temperature was increased at a rate of 15°C min^{-1} to 200°C and, in a second ramp, at a rate of 25°C min^{-1} to a final temperature of 300°C, where it was held for 1.33 min. The MS was operated in the selected ion mode (SIM). For quantification of BTEX, standards of different concentrations were prepared in methanol and an internal standard, containing fluorobenzene and 1,4-dichlorobenzene (EPA 524 Internal Standard Mix, Supelco, Bellefonte, PA, USA), was added to each sample and to the standards at a final concentration of 0.67 µg ml^{-1}.

PAHs were extracted from 13 ml groundwater samples during 60 min of intensive shaking with 500 µl of cyclohexane. An internal standard mix containing deuterated acenaphthene, chrysene, perylene, and phenanthrene (Internal Standards Mix 25, Ehrenstorfer, Augsburg, Germany) was used for quantification of priority PAH species as defined by the US Environmental Protection Agency (EPA-PAHs). 1 µl of the cyclohexane phase was injected onto a DB5 column. Samples were injected at a split ratio of 1:10, flow rate of the helium carrier gas was 1 ml min^{-1}. The oven temperature initially was held at 40°C for 3 min, then increased at a rate of 9.6°C min^{-1} to 270°C and further increased at a rate of 3.4°C min^{-1} to a final temperature of 310°C and held for 5 min. The MS was operated in the full scan mode, covering masses from 50-500 m z^{-1}.

Sampling and analyses of groundwater from the conventional MLW were performed by an external analytical lab. The following parameters were analyzed according to norms of the German Institute for Standardization (DIN-standard procedures), European Organization for Standardization (EN-standard procedures) and the International Organization for Standardization (ISO-standard procedures): pH (DIN38404-5, 1984-01), electrical conductivity (EN27888, 1993-11), sulfide (photometrically), sulfate, nitrate (both ISO10304-2, 1996-11), BTEX (DIN38407-9, 1991-05) and EPA-PAH (ISO17993, 2003).

4.3.3.3.   Bacterial cell numbers

For the enumeration of bacterial cell numbers, 15 ml aliquots of groundwater samples were fixed with glutardialdehyde solution (25%) to a final concentration of 2.5% and stored at 4°C. For staining of the cells fixed groundwater samples were amended with the fluorescent DNA dye SYBR green I (Molecular probes, Invitrogen, Karlsruhe, Germany) at a ratio of 1:10,000. After 15 min of staining, samples were filtered onto a 0.2 µm black polycarbonate filter (Millipore) and rinsed once with 10 ml of cell-free sterile water. Subsequently, the filter was removed from the filtration tunnel and embedded in flourescent oil on a microscope slide. Cells were counted with a Zeiss Axiolab microscope at 1000 × magnification (filter set: Zeiss, Ex 450-490 nm, FT 505 nm, LP 520 nm), using a counting grid. Further details on bacterial direct counts are described elsewhere (Griebler et al., 2001; Griebler et al., 2002).

4.3.3.4.   Sulfate isotope ratios

Isotopic measurements on groundwater sulfate were performed for samples obtained from the high-resolution multi level well. For determination of stable sulfur and oxygen isotope ratios in residual sulfate, groundwater was pumped into 100 ml vessels containing 10 ml of a 20% (w/v) Zn-acetate solution for precipitation of sulfide. Prior to sulfate analysis, samples were filtered through 0.45 µm pore size syringe filters (Millipore, Schwalbach,

Germany) in order to remove sulfide. Subsequently, sulfate was precipitated as $BaSO_4$ by addition of $3 - 5$ ml 10% $BaCl_2$. The precipitate was recovered by centrifugation. After complete conversion of $BaSO_4$ to SO_2 via high temperature combustion (1000°C) with WO_2 and V_2O_5, isotope analysis was performed on an isotope ratio mass spectrometer (IRMS Thermo Electron MAT 253) coupled to an elemental analyzer (EA-EuroVector). For measurements of $\delta^{18}O$ in sulfate, $BaSO_4$ was pyrolized at 1450°C in a discharge chamber (ConFloIII-Interface) and isotope analysis was conducted by subsequent IRMS (Holt, 1991).

Sulfur and oxygen isotope ratios are reported in parts per thousand (‰) using the conventional delta-notation (δ):

$$\delta_{sample}(‰) = \frac{\left(R_{sample} - R_{std}\right)}{R_{std}} \times 1000 \qquad\qquad \text{(eq. 4.1)},$$

where R is the $^{34}S/^{32}S$ or the $^{18}O/^{16}O$ ratio of the sample and the standard, respectively. $\delta^{34}S$ values are reported relative to Canon Diablo Triolite (V-CDT) and $\delta^{18}O$ values relative to Vienna Standard Mean Ocean Water (V-SMOW). Two international reference materials, NBS-127 and OGS, as well as several lab-internal standards were repeatedly measured to ensure accuracy. Reproducibility was $\pm$ 0.2 ‰ for $\delta^{34}S$ measurements of sulfate and $\pm$ 0.5 ‰ for $\delta^{18}O$ measurements of sulfate.

4.4. Results

4.4.1. Optimization of the sampling procedure

After installation, the newly constructed high resolution groundwater well was tested considering possible hydraulic shortcuts and appropriate pumping rates in relation to the deviation of analyte concentrations. In order to obtain water samples representative for a distinct vertical aquifer section, the pumping rate and the volume of water samples had to be minimized. Given a filter radius of 0.5 cm and a total intended sampling radius of 1.5 cm and assuming furthermore a mean groundwater flow velocity of 1 m d^{-1} (Schmitt et al., 1998) and a porosity of 30%, the incoming horizontal flow towards the sampling radius accounts for about 50 ml d^{-1}. Apart from the low sample volume derived by this procedure, pumping at such low rates showed that reactive chemical species (e.g. Fe(II) or sulfide) interacted with each other or with the steel surface of the capillary during transport to the surface. Furthermore, collection of such small water volumes in open vessels comprises the risk of loosing the major fraction of volatile compounds via volatilization. Preceeding pumping tests applying stepwise increased pumping rates revealed highest and constant measurable concentrations of analytes at about 1 ml min^{-1} (data not shown). Consequently, collection of a total amount of $50 - 200$ ml of sample simultaneously withdrawn from the different ports at a maximum pumping rate of $v_{max} = 1.4$ ml min^{-1} was compromised. Prior to sample collection, pre-pumping over night at rates comparable to natural flow velocities (0.014 ml min^{-1} and 0.057 ml min^{-1} for IPC-N and IPC pumps, respectively) and subsequent twofold exchange of the 'stagnant' water in the filter ports, capillaries and tubings at highest pumping rates were performed.

4.4.2. Spatial variation in groundwater geochemistry

Sampling of the conventional multi-level well (C-MLW) with a spatial resolution of 0.5 - 1 m revealed vertical concentration profiles of individual BTEX compounds. Highest

concentrations were located at the uppermost sampling port in the saturated zone at 6.5 m bls. Subsequently, a decline in concentrations was observed with depth, and at the sampling point at 8 m bls BTEX concentrations fell below detection limits. This is exemplarily shown for toluene, *o*-xylene, and ethylbenzene (Fig. 4.3A+B). The picture drawn from these data indicated a plume with a vertical thickness of about 1.5 m. Comparing these data with concentration profiles derived from the high-resolution MLW (HR-MLW), which is located one meter apart from the C-MLW, revealed up to one order of magnitude higher concentrations for individual contaminants. The higher resolution also resulted in a clear picture of the distribution of contaminants with steep concentration gradients detected at the upper and lower plume fringe. From these data a vertical plume thickness of only 0.8 m was derived for BTEX and naphthalene (Fig. 4.3A-C). Of the 16 EPA-PAHs naphthalene, acenaphthene and fluorene could be measured within the HR-MLW, but only naphthalene and acenaphthene were detected within the C-MLW. While naphthalene, which constituted the main component, showed a distribution pattern similar to the monoaromatic hydrocarbons, acenaphthene and fluorene exhibited an opposite trend with lowest concentrations in the upper parts of the aquifer (Fig. 4.3C).
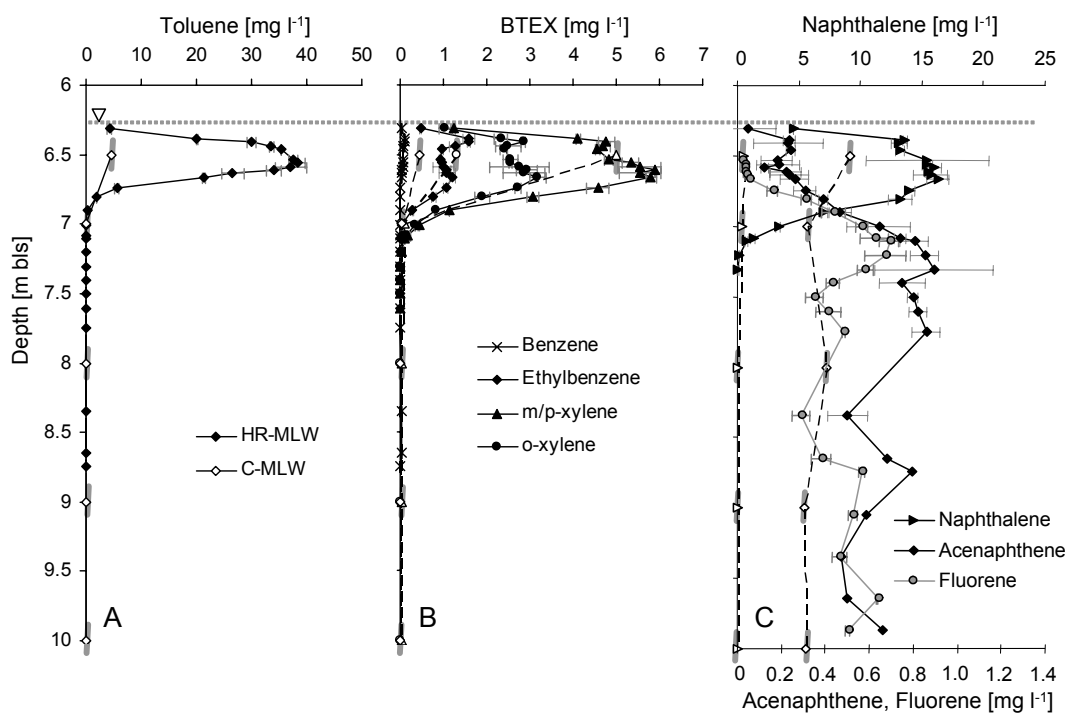
Figure 4.3 Selected vertical gradients for monoaromatic (A + B) and polyaromatic (C) hydrocarbons, as obtained from high-resolution sampling (black symbols). Values obtained from the conventional multi-level well (C-MLW) are depicted in white symbols. Values represent means of duplicate measurements ± SD; C-MLW data represent single measurements.

The spatial distribution of selected hydrochemical parameters is shown as concentration-depth profiles in Fig. 4.4. Without exception, the high-resolution sampling revealed most pronounced variations with depth in the zone of the contaminant plume. The entire aquifer section investigated lacked detectable amounts of dissolved oxygen (data not shown), which was clearly reflected by the very low redox values (Fig. 4.4A). The most reduced area of the aquifer matched the zone of highest contaminant concentrations. In this case, the results obtained from C-MLW samples were found misleading, showing slightly positive redox values all across the saturated zone. The differences between data from low

and high-resolution sampling were less pronounced regarding pH and specific conductivity. However, the C-MLW was not appropriate to reflect the steep gradients of both pH and specific conductivity present at the upper plume fringe (Fig. 4.4B+C). While the pH patterns followed in general the distribution of the contaminants, the conductivity mirrored sulfate concentrations (Fig. 4.4C and Fig. 4.5B). Peak concentrations of dissolved organic carbon (DOC) occurred in the zone of highest contamination (Fig. 4.4E). A similar picture was obtained for the dissolved inorganic (DIC) and the total dissolved carbon (TDC; Fig. 4.4F). For the conventional MLW only DOC values were available, showing elevated values at 6.5 and 7 m bls (Fig. 4.4E) without capturing the plume shape.
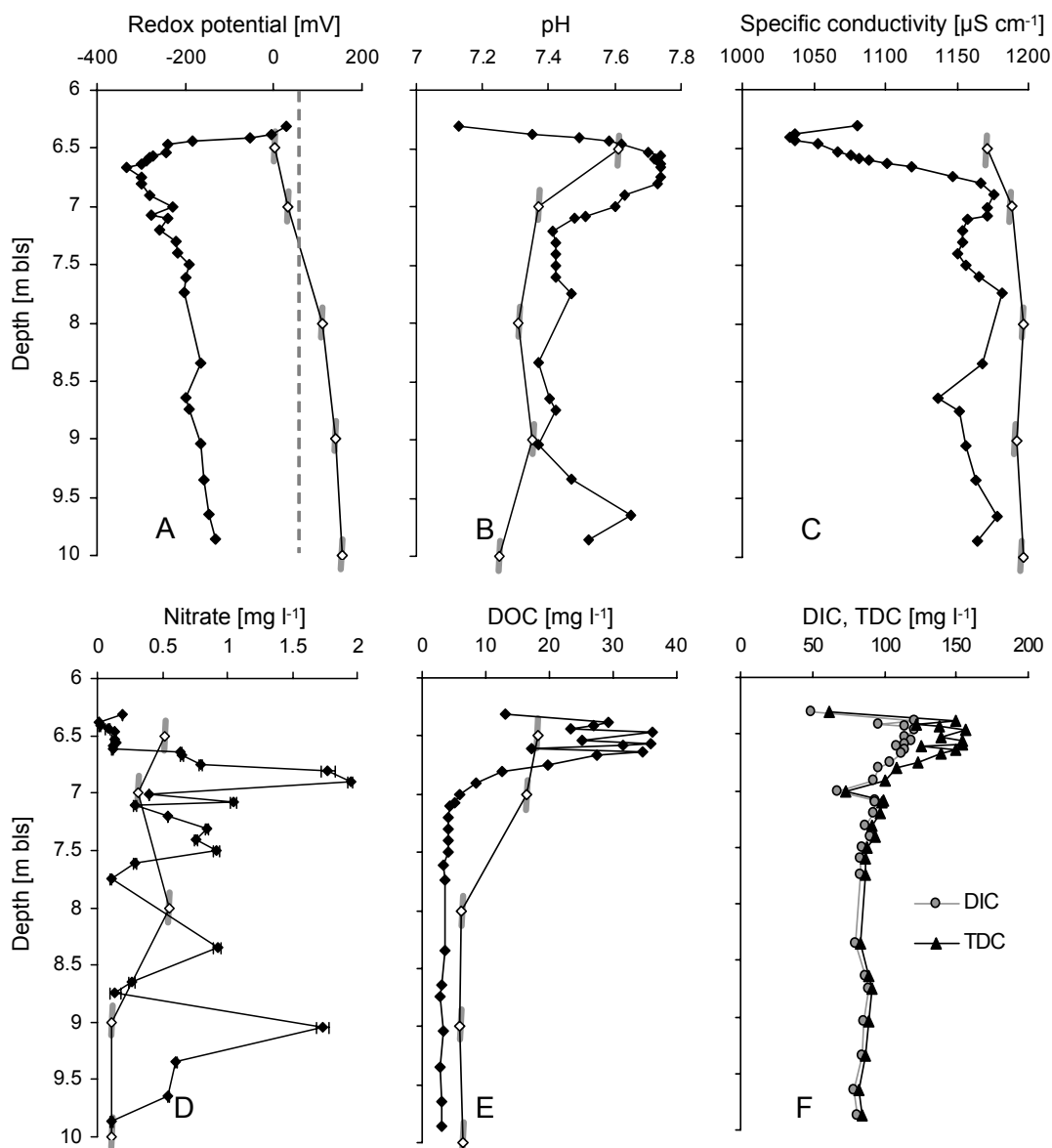
Figure 4.4 Vertical profiles of selected physical and chemical parameters determined in groundwater samples from the high-resolution multi-level well with a resolution of 2.5 – 33 cm (black symbols), and a conventional multi-level well with a resolution of 0.5 – 1 m (white symbols); for DIC and TDC, no data were available from the conventional multi-level well; the transition to oxidized conditions in A) is delineated by the dashed line. Values represent single measurements, except nitrate concentrations, which represent means of duplicate measurements ± SD.

4.4.3. Distribution of electron acceptors and metabolic end products

Considering the distribution of terminal electron acceptors available for biodegradation of organic contaminants, it can first be stated that no oxygen was found in groundwater samples from the HR-MLW (data not shown). Concentrations of nitrate were found to range close to the detection limit of 0.1 mg l^{-1} in the plume core. A first peak with depth was observed at the lower plume fringe, reaching 2 mg l^{-1}. In the less contaminated areas further small but distinct peaks < 2 mg l^{-1} were found (Fig. 4.4D). High sulfate concentrations of about 200 mg l^{-1} occurred in less and non-contaminated areas of the investigated aquifer. Looking at our high-resolution vertical profile, the core of the contaminant plume was almost depleted in sulfate (Fig. 4.5B). The corresponding plume core sample from the C-MLW exhibited > 100 mg l^{-1} sulfate (Fig. 4.5B). High resolution data of sulfide showed one pronounced peak of more than 8 mg l^{-1} at the lower plume fringe, while Fe(II) was found highest at the upper and lower inner fringe as well as right below the plume together with small sulfide peaks (Fig. 4.5C and D).
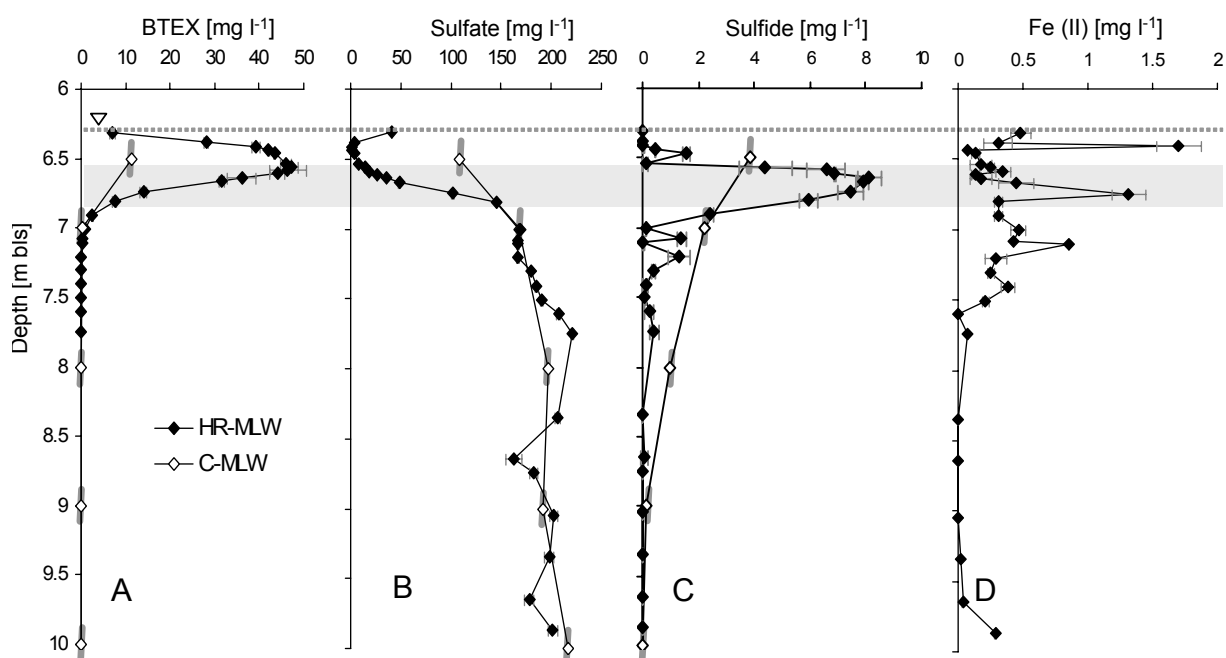
Figure 4.5 Prevailing redox processes across the contaminant plume as assumed from the distribution of contaminants (A), individual electron acceptors (sulfate; B) and metabolic end products (sulfide, Fe(II); C+D). Values represent means of duplicate measurements ± SD; C-MLW data represent single measurements.

Iron values obtained from analysis of the sediment liners, which were collected prior to the installation of the HR-MLW exhibited concentrations of ready extractable ferrous iron (0.5M HCl extraction for 24h) of 0.6 to 1 g kg^{-1} wet weight (wwt) in the area of the plume, followed by a sudden increase to nearly 4 g kg^{-1} wwt below a depth of 7.3 m bls (Fig. 4.6A). Easy extractable ferric iron was only found in sediments of the unsaturated zone and at the first sampling point within the saturated zone at 6.4 m bls. Iron bound in the minerals (extracted with 5M HCl during 21 days on a rotary shaker) showed a different picture. Here, the ferrous iron fraction within the contaminated and less contaminated saturated sediments fell in the upper mg kg^{-1} range (max. 130 mg kg^{-1}), while ferric iron values showed concentrations of about 2 - 5 g kg^{-1} wwt (Fig. 4.6A).

Sediment-bound sulfide was found in the plume core and at the lower plume fringe zone at concentrations of 200 to 300 mg kg^{-1} (Fig. 4.6B) as well as in sediments between 8.8 and

11.2 m bls. In soil samples where both ferrous iron and sulfide were measured, the Fe(II) to sulfide ratio was between 3 and 18 (data not shown).
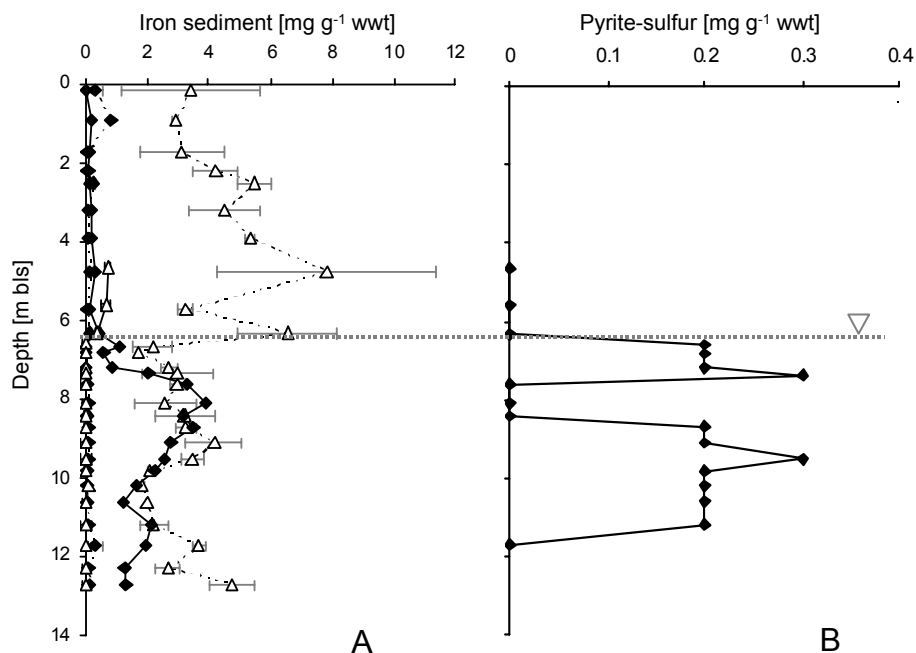
Figure 4.6 A) Vertical profiles of ready extractable Fe(II) (diamonds) and Fe(III) (triangles) (solid lines) and cristalline ferric and ferrous iron (dashed lines) and B) pyrite-sulfur as determined from freshly collected sediment samples. Dotted line indicates the position of the groundwater table at time of sampling. Values represent means of duplicate measurements ± SD.

4.4.4. Bacterial sulfate reduction

In order to qualitatively proof microbially mediated sulfate reduction, the stable isotope ratios of both $^{34}S/^{32}S$ and $^{18}O/^{16}O$ in sulfate were determined. Unfortunately, groundwater sulfate concentrations in samples from the upper plume fringe and the plume core were not sufficient for isotope analysis. Nevertheless, the data clearly showed a significant enrichment of both $\delta^{34}S$ and $\delta^{18}O$ concomitant with decreasing sulfate concentrations entering the plume from below (Fig. 4.7A).

4.4.5. Vertical distribution of suspended bacteria

The bacterial biomass suspended in groundwater as determined by direct cell counts was found most pronounced directly at the groundwater table, which brings together the capillary fringe and the area of the upper plume fringe. A further increase in cell numbers was detected at the lower plume fringe and once again at a deeper zone between 8.7 and 9.4 m bls (Fig. 4.7B). Lowest values were present in plume core samples.
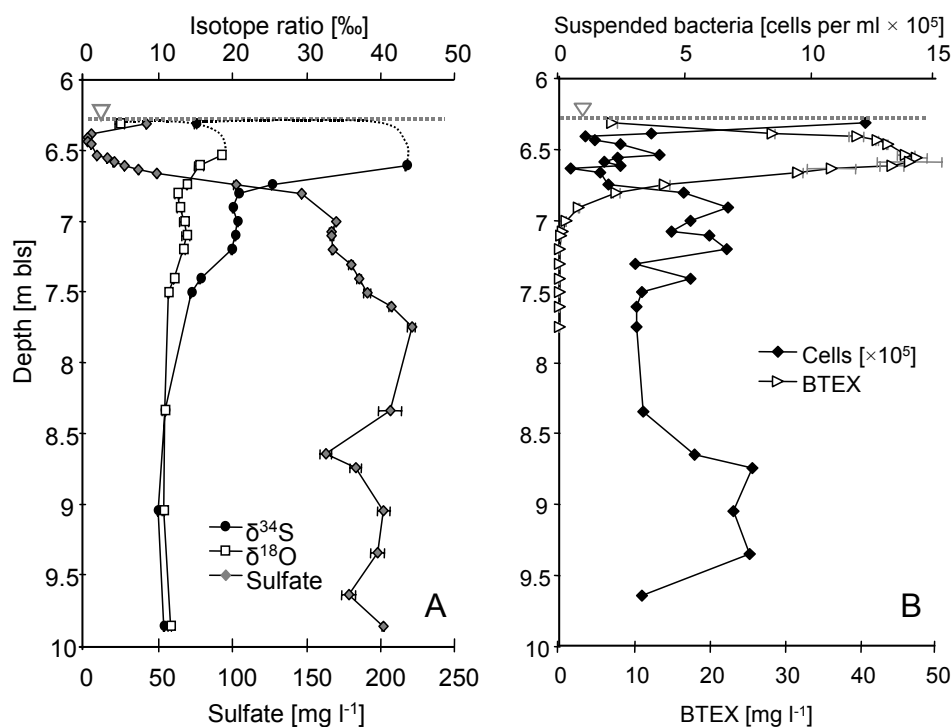
Figure 4.7 A) Ratios of $\delta^{34}S$ and $\delta^{18}O$ of sulfate from selected sampling depths. The dashed lines indicate the progression of the two isotope curves, as suggested from data of other sampling events; B)cross gradients of total numbers of suspended cells (single measurements) and total BTEX concentrations (mean values of duplicates ± SD) as obtained from high-resolution sampling.

4.5. Discussion

4.5.1. The relevance of scale-adapted groundwater sampling

For a detailed understanding of natural attenuation processes and the evaluation of potential limiting factors, knowledge on the occurrence and distribution of biogeochemical gradients and microbial activities is crucial. Thus, the need for sampling adapted to the scale of processes and gradients is obvious.

Decades ago, pioneering work in this field was done by Ronen et *al.* (1987) and Pickens et *al.* (1978) who reported on significant variations in concentrations of electron acceptors and contaminants across a vertical aquifer section at the centimeter and decimeter scale, respectively. Since then, the importance of high-resolution sampling in groundwater studies has been claimed frequently (e.g. Smith et al., 1991), but, nevertheless, the number of high resolution studies is still limited (Smith et al., 1991; Bjerg et al., 1995; Davis et al., 1999; Lerner et al., 2000; Spence et al., 2001; Thornton et al., 2002; Kota et al., 2004; van Breukelen and Griffioen, 2004; Wilson et al., 2004; Salminen et al., 2006; Scholl et al., 2006; Tuxen et al., 2006; Báez-Cazull et al., 2007).

First of all, we have to raise the question: what does high resolution mean? In order to study natural attenuation processes within a phenol contaminated sandstone aquifer, Lerner and co-workers installed multi-level wells that allowed for groundwater sampling at 1m vertical intervals (Lerner et al., 2000). Given the extraordinary thickness of the plume of 60 m and a fringe zone of 2 m in width, the applied sampling resolution was exceptionally high and successfully captured the sharp biogeochemical gradients and significant spatial variations of different parameters across the plume (Thornton et al., 2001). However, as mentioned initially, transverse dispersion acts in the range of millimeters to decimeters depending on grain size distribution, sediment heterogeneity and flow velocity, but is in theory independent

from the total plume thickness. Moreover, if it is assumed that biodegradation in the plume is not only controlled by hydrodynamic mixing, which was suggested by several hints (see below), the extension of the fringe zone is also a matter of distance from the source. Therefore, in many other cases, the steep biogeochemical gradients in the fringe zones remained unresolved applying a 1 m vertical sampling resolution. A sampling interval of 1 m was also applied for investigations of a porous aquifer contaminated with waste fuels and solvents in order to statistically evaluate the effects of recharge events on redox processes (McGuire et al., 2005). Chemical changes occurring after recharge through the saturated zone lead to a measurable shift in the availability and relevance of individual terminal electron acceptors. However, the fate of the electron acceptors introduced by recharge could not be resolved appropriately with the applied sampling technique and therefore remained rather speculative. This accentuates the need for adaptation of the sampling resolution to the environmental conditions. In a recent study at a landfill leachate-affected wetland, groundwater samples were obtained at a resolution of 0.5 – 1 cm by use of passive diffusion samplers ("peepers"). Across a 50 cm vertical profile, mixing interfaces were characterized by steep biogeochemical gradients that allowed for evaluation of dominant redox processes (Báez-Cazull et al., 2007). Additionally, push & pull tests were performed in order to assess kinetic controls on sulfate reduction and the role of biogeochemical cycling processes at transition zones (Kneeshaw et al., 2007). These are just a few examples, which demonstrate that the appropriate scale for sampling in porous aquifers may vary between centimeters and meters in dependence to sediment texture and hydraulic conductivity. To complement the available studies, reactive transport models suggest transverse dispersion and thus the width of the mixing zones harbouring steep biogeochemical gradients to be in the range of millimeters up to decimeters (Klenk and Grathwohl, 2002).

The urgent demand for high-resolution sampling could nicely be demonstrated by our investigations of the homogeneous sandy tar oil-contaminated aquifer in Düsseldorf. We sampled a vertical cross section through a hydrocarbon plume with a spatial resolution of 0.5 to 1 m (conventional multi-level well; C-MLW) and 2.5 to 33 cm (high-resolution multi-level well; HR-MLW), respectively. The comparison of vertical profiles of selected chemical species, *i.e.* contaminants, electron acceptors and metabolites, revealed steep small-scale biogeochemical gradients in the centimeter range across the contaminant plume that could in no way be traced by the already relatively good resolution of the C-MLW of 50 cm. As an example, 50 cm resolution sampling underestimated maximum concentrations of selected hydrocarbon compounds, such as toluene, *o*-xylene, ethylbenzene, and naphthalene, in the plume center by 60 to 95 %, or in other cases, as shown for acenaphthene, overestimated the present concentrations 3-fold (Fig. 4.3C). The low-resolution sampling resulted in an averaging of small-scale concentrations and destruction of steep gradients. This was mainly caused by sampling water at high pumping rates through long filter screens and large pumping tubes - potential errors associated with most routinely applied multi-level wells. BTEX concentrations derived from the C-MLW in our case indicated a plume thickness of about 1.5 m, while the actual plume width assumed from the HR-MLW accounted for only 0.8 m. A similar picture is obtained for most of the parameters measured (Fig 4.3 and Fig. 4.5). Likewise, overestimation of the plume thickness may hamper the estimation of source location. Using the formula of Harleman and Rumer (1963)

$$\frac{C(x, y)}{C_0} = \frac{1}{2} erfc\left(\frac{y}{\sqrt{4\alpha_T x}}\right)$$

$\hspace{6cm}$ (eq. 4.2),

where C_0 is the source concentration, $C(x, y)$ corresponds to 0.1 C_0 at the respective sampling depth, x is the distance to the source and y is half of the plume width, and assuming a

transverse dispersivity of $\alpha_T = 0.1$ cm for our sandy aquifer top zone and a homogeneous sediment, a given plume width of 0.8 m as derived from the HR-MLW reveals an approximate calculated distance of the sampling site from the source of about 15 m. The 1.5 m plume width obtained from the C-MLW would indicate the source to be 50 m upgradient.

4.5.2. Hydrogeochemical patterns and distribution of electron accepting processes

Previous investigations performed at the sandy tar oil-contaminated Düsseldorf aquifer suggested biodegradation to be primarily associated with sulfate and iron reduction (Wisotzky and Eckert, 1997; Eckert, 2001). These earlier findings were clearly supported by our high-resolution study. Additionally, our data now allowed the allocation of redox processes to distinct zones and provided first detailed insights into the distribution and spatial variability of electron acceptors and metabolic end products.

A first noticeable pattern observed was the decline in contaminant mass accompanied by a steep sulfate gradient at the transition between the BTEX plume and ambient groundwater. Groundwater sulfate was found almost depleted in the plume center. This strongly indicates sulfate reduction being involved in hydrocarbon degradation. Stable isotope analysis on groundwater sulfate represents a powerful tool to identify bacterial sulfate reduction in groundwater (e.g. Einsiedl and Mayer, 2005). Elevated $\delta^{34}S$ and $\delta^{18}O$ values in residual sulfate in concert with H_2S concentrations of up to several mg l^{-1} indicated sulfate reduction occurring across the lower plume fringe (Fig. 4.7A). However, at the upper plume fringe the situation was slightly different. Isotope ratios different from those below a depth of 6.5 m (plume core) were found at the uppermost sampling port. There, sulfate was depleted to about 50 mg l^{-1}, but nevertheless lacked a signature characteristic for sulfate reduction (Fig. 4.8), i.e. no enrichment in the heavier isotopes $\delta^{34}S$ and $\delta^{18}O$ was observable. The discrepancy in isotope ratios, however, is rather attributed to infiltration of another sulfate source, for instance by recharge from the unsaturated zone than to lacking sulfate reduction.

Figure 4.8 Plotting isotope ratios of $\delta^{34}S$ and $\delta^{18}O$ versus 1/sulfate concentration indicates a different source of sulfate for the uppermost sampling port, whereas the dotted and dashed lines connect isotope values belonging to an identical sulfate source. Values represent means of duplicate measurements $\pm$ SD.

In order to get a better conception of the role of sulfate reduction in contaminant degradation, we performed some simple back-of-the-envelope calculations with toluene as the dominant model electron donor, according to the following equation:

$$C_7H_8 + 4.5\ SO_4^{2-} + 3\ H_2O \rightarrow 2.25\ HS^- + 2.25\ H_2S + 7\ HCO_3^- + 0.25\ H^+ \qquad \text{(eq. 4.3)}$$
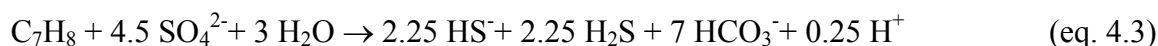
Assuming that the difference in sulfate between the background concentration and the amount measured at each individual sampling point in the contaminant plume reflects the amount of sulfate that was used as electron acceptor for toluene degradation, we can reconstruct the

theoretical original toluene concentration dissolved in groundwater. Granted a background sulfate concentration of about 200 mg l^{-1} at our sampling site (the high values are caused by building rubble fillings upstream of our study site), this gives a bell-shaped toluene curve with maximum concentrations in the plume core of > 80 mg l^{-1}, which is close to the maximum concentrations of about 100 mg l^{-1} measured nearby the putative source (data not shown). Distinctly lower measured toluene concentrations of up to 40 mg l^{-1} therefore clearly hint at high sulfate reduction activities. On the other hand, if we assume perfect mixing of the sulfate into each zone of the plume, up to 48 mg l^{-1} toluene (*i.e.* the total toluene concentration measured at the site) theoretically could have been oxidized with sulfate as electron acceptor. The high residual toluene concentrations in the plume center therefore probably result from poor availability of sulfate, which is caused by insufficient mixing of electron donors and electron acceptors. In contrast, low contaminant concentrations at the plume fringe are attributed to enhanced mixing caused by transverse dispersion. Improving mixing in these sediments, for instance by implementation of artificial heterogeneities, could therefore significantly improve natural attenuation. Without removal of the contaminant source, however, this would result only in a shortening of the total plume length but not in a reduction of the period of contamination.

Apart from sulfate reduction, alternative terminal electron accepting processes have to be considered to be active at our investigation site. As mentioned before, iron reduction was suggested to be involved additionally to sulfate reduction in contaminant degradation at the Flingern site (Wisotzky and Eckert, 1997; Eckert, 2001). High-resolution data indeed revealed elevated concentrations of dissolved Fe(II) in the top zone of the aquifer from the groundwater table down to a depth of about 7.5 m bls, peaking in the upper and lower plume fringe zone at about 1.7 mg l^{-1} and lowest values in the plume core (Fig. 4.5D). Below a depth of 7.5 m Fe(II) values dropped to background concentrations in the lower µg l^{-1} range. The concomitant presence of dissolved sulfide and ferrous iron at some depths indicated that either small FeS particles affected water analysis or sulfate and iron reduction rates exceeded kinetics of FeS precipitation or other abiotic reactions. The ratio of dissolved ferrous iron to sulfide exhibited a clear dominance of Fe(II) in the outer upper and lower plume fringe, while the inner plume fringes as well as the plume core showed a sulfide to Fe(II) ratio of > 5.

The partial depletion of ready available ferric iron in the contaminated zone hints towards iron reduction. Considering a total extractable amount of sedimentary Fe(II) of $0.6 - 4$ g kg^{-1} we can re-calculate the theoretically oxidized toluene concentration according to the following equation:

$$C_7H_8 + 36\ Fe(OH)_3 + 65\ H^+ \rightarrow 7\ HCO_3^- + 36\ Fe^{2+} + 87\ H_2O \qquad \text{(eq. 4.4)}$$
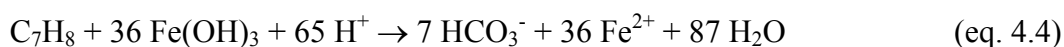
Consequently, the Fe(II) extracted from contaminated sediments may have been precipitated during oxidation of up to 180 mg kg^{-1} toluene. Analoguously, sedimentary sulfide concentrations of $200 - 300$ mg kg^{-1} correspond to the oxidation of up to 188 mg kg^{-1} toluene. Taking into account the continuous transportation of up to 100 mg l^{-1} BTEX at a groundwater flow of $0.1 - 2$ m d^{-1} through the sediments over a period of several decades, the relatively low concentrations of precipitates imply biodegradation rates occuring at this site to be very low. On the other hand, about one ton of iron slags is annually disposed from the Flingern site. Consequently, considerable amounts of iron are supposably eluted with groundwater flow and therefore not taken into account for iron reduction processes.

Overlapping redox zones in contaminant plumes, *i.e.* the concomitant occurrence of dissolved Fe(II) and sulfide in groundwater samples, as observed at our site, have also been reported in previous studies (Thornton et al., 2001; McGuire et al., 2002). According to the partial equilibrium approach, as postulated by Jakobsen and Postma (1999), the rate limiting fermentative step in redox reactions is independent from the type of terminal electron

acceptor. The co-occurrence of e.g. methanogenesis and sulfate reduction may rather be attributed to the bioavailability of electron acceptors or the formation of microenvironments (Bjerg et al., 1995). Therefore, competitive exclusion of redox processes caused by energetic constraints and, consequently, the formation of well separated redox zones, as often suggested (Lovley, 1995, 2001), does not necessarily evolve.

Redox data obtained from groundwater samples indicated aerobic biodegradation to be negligible, with possible exception of the uppermost sampling port close to the capillary fringe, where traces of oxygen may have been available from time to time originating from diffusion and groundwater recharge from the unsaturated zone (Fig. 4.4A). With depth, a strong decrease in redox potential implied highly reduced (anoxic) conditions within the plume. Nitrate was found at only low concentrations at the lower plume fringe and below. It is suggested that nitrate, available at background concentrations of about 10-20 mg l^{-1} in ambient groundwater, is readily consumed for oxidation of organic contaminants or reduced species, e.g. sulfide or Fe(II) (Eckert and Appelo, 2002). The small amounts of nitrate arriving at our sampling well (max. 2 mg l^{-1}) may contribute only to an evanescent degree to contaminant removal, since, under optimal conditions, 5 mg l^{-1} of nitrate are required for oxidation of 1 mg l^{-1} toluene:

$$C_7H_8 + 0.2H^+ + 7.2\ NO_3^- \rightarrow 7\ HCO_3^- + 3.6\ N_2 + 0.6\ H_2O \qquad \text{(eq. 4.5)}$$
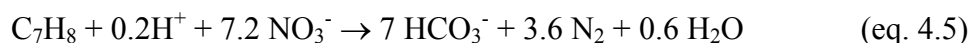
Likewise, only minor importance was ascribed to contaminant removal via manganese reduction, owing to the relatively low concentrations of reduced Mn^{2+} (< 1mg l^{-1}) measured within the conventional MLW (data not shown). Contaminant loss may partly be accredited also to volatilization or sorption, whereas the latter is, considering an average total organic matter content in the sediment of only ~ 0.45 % (wwt), supposed to be exiguous.

4.5.3. Mixing-controlled biodegradation at the plume fringe – hot spot of microbial activity

Numerous studies report enhanced microbial abundances and activities in the transition zone of two layers of different geological origin (e.g. Mc Mahon et al., 1992; Ulrich et al., 1998; Krumholz, 2000). A similar picture displaying increased biomass, biodegradation rates and consequently steep biogeochemical gradients was obtained for the fringes of organic contaminant plumes either from mathematical modelling (Cirpka et al., 1999; Prommer et al., 2006), experimental lab data (Thullner et al., 2004; Tuxen et al., 2006; Bauer et al., 2008; Rees et al., 2007), and field studies (Cozzarelli et al., 1999; Davis et al., 1999; Ludvigsen et al., 1999; Spence et al., 2001; van Breukelen and Griffioen, 2004; McGuire et al., 2005). Additionally, a number of studies reported biodegradation in the plume center to be limited by toxicity of the contaminants or depletion of electron acceptors, while enhanced degradation rates were found at the plume fringe (e.g. Mayer et al., 2001; Pickup et al., 2001; Thornton et al., 2001; Takahata et al., 2006).

The effect of mixing interfaces at transition zones on the biodegrader community was studied in microcosm experiments using sediments from a phenoxy-acid herbizides-contaminated landfill (Tuxen et al., 2006). Sediment samples obtained at 5 cm vertical intervals exhibited steep geochemical gradients at the transition of contaminated and uncontaminated aquifer. An increased biodegradation potential found within this zone could
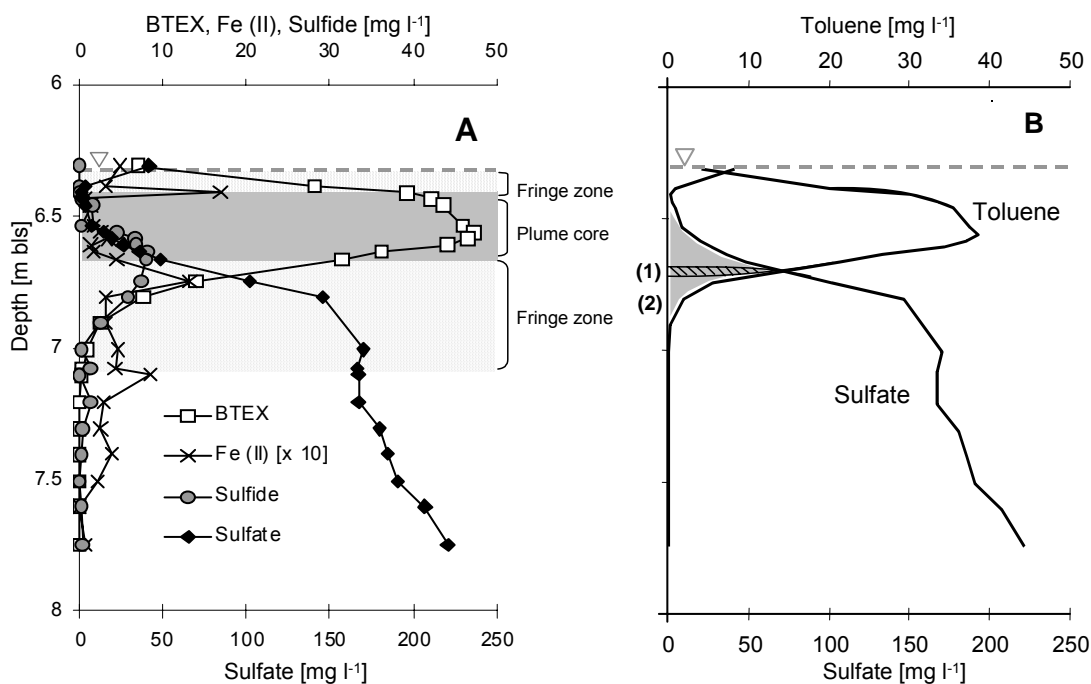
Figure 4.9 A) Conceptual drawing of the plume core and the upper and lower fringes according to the gradients of total BTEX, dissolved sulfate, sulfide and Fe(II); B) assuming an instantaneous biodegradation exclusively limited by transverse dispersion almost no overlap of electron donor and acceptor is expected (1), while a broad overlap is observed *in situ* (2). For further explanation see text.

be correlated to a proliferating number of degraders. The role of transverse mixing at that site was estimated by use of numerical transport models and compared to data determined in the field (Prommer et al., 2006). The simulated data agreed fairly well with the conditions prevailing *in situ*, thus validating the conceptual plume fringe model of mixing-controlled biodegradation. An extensive study of mixing-controlled aerobic and anaerobic biodegradation in toluene plumes was undertaken by Bauer and co-workers (2008). High-resolution sampling in two-dimensional flow-through aquifer microcosms proved plume fringes to be hot spots of biodegradation, driven by hydrodynamic mixing in porous media. However, this paper also explained that although mixing was the driving process for biodegradation, overlapping zones of electron acceptor and electron donor may be found at the plume fringes and thus implied additional limiting factors to be present (Bauer et al., 2008).

Similar patterns were found at our investigation site. First, steep and small-scale opposing gradients for organic contaminants, the electron acceptors sulfate and ferric iron as well as the metabolic end products sulfide and ferrous iron at the upper and lower plume fringe clearly hinted at increased biodegradation activities. The assumption of enhanced bioactivities at the plume fringe was additionally supported by bacterial cell counts, which exhibited lowest numbers in the highly contaminated core and an increase in biomass at the plume fringes (Fig. 4.7B), and compound-specific stable isotope analysis of sulfate (Fig. 4.7A) and toluene (see section 5.3.3). Additionally, molecular analysis of the sediment microbial communities revealed that based on real time PCR analysis almost 50% of all cells carried the functional gene for anaerobic toluene degradation in the area of the lower plume fringe (Winderl et al., 2008). On the other hand, the high-resolution data revealed overlapping gradients of electron donors and electron acceptors, as exemplarily shown for sulfate and toluene in Fig. 4.9A. This contradicts an instantaneous bioreaction exclusively limited by hydrodynamic mixing, as frequently assumed in model simulations (e.g. Borden and Bedient, 1986; Ham et al., 2004), which would result in complete sulfate depletion in the plume core

and only a small zone of overlap (Fig. 4.9B). It seems that the phenotypical time scale of other reactions or processes lags behind the time scale of transport (advection and dispersion; Bauer et al., 2008). This does not imply that reaction rate constants of biodegradation are too low. Additional limitations in our case may be imposed by (i) transient hydraulic conditions or recharge events resulting in high temporal dynamics of the contaminant distribution, (ii) biokinetic constraints and the number of active degraders, (iii) availability of substrates limited by microscale diffusion, and (iv) inhibition of degradation caused by toxicity (see discussions in Thornton et al., 2001; Salminen et al., 2006; Scholl et al., 2006; Bauer et al., 2008). A few parameters indicate significant biodegradation also to occur in the plume center, with sulfate reduction as the most prominent reaction. The total depletion of sulfate in the plume center identifies the core as an important sinc. This is additionally supported by the isotopic composition of sulfate. Although not explicitly seen in the groundwater data from August 2006, which are presented in this study (Fig. 4.7A), analyses from other sampling dates showed isotopic enrichment of sulfate within the plume core zone (sections 3.5.2.1 and 5.3.3). Likewise, the DIC gradient reflecting CO_2 production during contaminant oxidation exhibits highest values in the plume center and an increase concomitant with decreasing amounts of aromatic hydrocarbons (Fig. 4.4F).

There may be situations where maximum biodegradation is found in the plume center. Contrary to our hypothesis, bioactivity at the fringe of a landfill leachate plume in the Netherlands was found to be decreased. Reactive transport modeling studies using PHREEQC-2 showed that secondary redox reactions of reduced species (e.g. re-oxidation of methane and ferrous iron) probably controlled biodegradation by reducing the availability of energetically favourable electron acceptors, such as oxygen, nitrate and sulfate. Hence, biodegradation was restricted to methanogenic activities within higher contaminated zones of the plume (van Breukelen and Griffioen, 2004). Secondary redox reactions are likely to occur to a certain degree also at our site. Nevertheless, the individual pools of electron donors, electron acceptors and associated reduced species indicate that consumption of electron acceptors is primarily coupled to direct oxidation of the contaminants (Fig. 4.5). However, there is an interesting aspect regarding the composition of the microbial community along the vertical transect across the BTEX plume, which was shown to be dominated by a highly specific toluene degrader community at the fringe zone of the plume (Winderl et al., 2008). Phylogenetic analyses assigned this group to *Geobacter*-related deltaproteobacteria, which are generally well-known iron reducers (Lovley, 1997). The simultaneous activity of individual redox processes, as also observed at our study site is supported by other field studies (Postma and Jakobsen, 1996; McGuire et al., 2002). It may either imply non-competitive co-occurrence of different microorganisms with different physiology or the prevalence of "allrounder" organisms that both proliferate under iron and sulfate reducing conditions. Despite the higher theoretical energy yield obtained from iron reduction (Christensen et al., 2000), low concentrations and availability as well as reduced reactivity of iron oxides in the sediment may render sulfate reduction dominant over iron reduction (Blodau et al., 1998). At our site, we speculate that at the upper plume fringe coinciding with the capillary fringe amorphous iron oxides are continuously recycled by oxidation during groundwater table fluctuations and iron reduction might be prominent, therefore. At the lower plume fringe the role of sulfate and iron reduction seemed to alternate (Fig. 4.9A). In the anoxic plume center, however, availability of reactive iron oxides was low, implying that sulfate reduction was most prominent.

Even though sulfide was not detected in the uppermost sampling ports, sulfate reduction probably also took place at the upper plume fringe. Scavenging of sulfide by re-oxidation or FeS-precipitation as well as volatilization of H_2S may lead to a significant underestimation of sulfate reduction based on free sulfide concentrations. Even though the sediment analyses

performed in this study unfortunately were not able to distinguish between different iron minerals, siderite may analoguously constitute an important sink of Fe(II).

4.6. Conclusions and outlook

The comparison of data obtained by means of a conventional multi-level well with a spatial sampling resolution of 0.5 to 1 m and a novel high-resolution multi-level well achieving a vertical sampling resolution of 2.5 to 33 cm demonstrated steep biogeochemical gradients in the centimeter scale across a BTEX plume in a sandy aquifer. High-resolution sampling revealed also individual small-scale redox zones as well as pronounced microbial biomass and activity at the plume fringe. Together with other parameters, these findings support the role of the fringes of contaminant plumes as zones of high biodegradation activities. However, overlapping gradients of both high concentrations of contaminants and electron acceptors indicate that biodegradation at this site is not solely mixing-controlled but additional biotic or abiotic factors have to be considered as limiting parameters for biodegradation, which remain to be elucidated. However, it is obvious that the biodegradation activity is not limited by trivial factors such as phosphorous or nitrogen availability.

4.7. References

Anneser, B., Richters, L., and Griebler, C. (2008) Application of high-resolution groundwater sampling in a tar oil–contaminated sandy aquifer. Studies on small-scale abiotic gradients. In *Adavances in subsurface pollution of porous media: indicators, processes and modelling.* Candela, L., Vadillo, I., and Elorza, F.J. (eds): Taylor & Francis / Balkema, Leiden, NL.

Báez-Cazull, S.B., McGuire, J.T., Cozzarelli, I.M., Raymond, A., and Welsh, L. (2007) Centimeter-scale characterization of biogeochemical gradients at a wetland-aquifer interface using capillary electrophoresis. *Appl Geochem* 22: 2664-2683.

Bauer, R.D., Maloszewski, P., Zhang, Y., Meckenstock, R.U., and Griebler, C. (2008) Mixing-controlled biodegradation in a toluene plume - Results from two-dimensional laboratory experiments. *J Contam Hydrol* 96: 150-168.

Bjerg, P.L., Rügge, K., Pedersen, J.K., and Christensen, T.H. (1995) Distribution of redox-sensitive groundwater quality parameters downgradient of a landfill (Grindsted, Denmark). *Environ Sci Technol* 29: 1387-1394.

Blodau, C., Hoffmann, S., Peine, A., and Peiffer, S. (1998) Iron and sulfate reduction in the sediments of acidic mine lake 116 (Brandenburg, Germany): rates and geochemical evaluation. *Water Air Soil Pollut* 108: 249-270.

Borden, R.C., and Bedient, P.B. (1986) Transport of dissolved hydrocarbons influenced by reaeration and oxygen limited biodegradation: 1. Theoretical development. *Water Res Research* 22: 1973-1982.

Christensen, T.H., Bjerg, P.L., Banwart, S.A., Jakobsen, R., Heron, G., and Albrechtsen, H.-J. (2000) Characterization of redox conditions in groundwater contaminant plumes. *J Contam Hydrol* 45: 165-241.

Christensen, T.H., Kjeldsen, P., Bjerg, P.L., Jensen, D.L., Christensen, J.B., Baun, A. et al. (2001) Biogeochemistry of landfill leachate plumes. *Appl Geochem* 16: 659-718.

Cirpka, O.A., Frind, E.O., and Helmig, R. (1999) Numerical simulation of biodegradation controlled by transverse mixing. *J Contam Hydrol* 40: 159-182.

Cline, J.D. (1969) Spectrophotometric determination of hydrogen sulfide in natural waters. *Limnol Oceanogr* 14: 454-458.

Cozzarelli, I.M., Herman, J.S., Baedecker, M.J., and Fischer, J.M. (1999) Geochemical heterogeneity of a gasoline-contaminated aquifer. *J Contam Hydrol* 40: 261-284.

Davis, G.B., Barber, C., Power, T.R., Thierrin, J., Patterson, B.M., Rayner, J.L., and Quinglong, W. (1999) The variability and intrinsic remediation of a BTEX plume in anaerobic sulfate-rich groundwater. *J Contam Hydrol* 36: 265-290.

DIN38404-5 (1984-01) Deutsche Einheitsverfahren zur Wasser-, Abwasser- und Schlammuntersuchung; Physikalische und physikalisch-chemische Kenngrößen (Gruppe C); Bestimmung des pH-Wertes (C 5). In: DIN Deutsches Institut für Normung e. V; Beuth Verlag, Berlin, Germany.

DIN38407-9 (1991-05) Deutsche Einheitsverfahren zur Wasser-, Abwasser- und Schlammuntersuchung; Gemeinsam erfaßbare Stoffgruppen (Gruppe F); Bestimmung von Benzol und einigen Derivaten mittels Gaschromatographie (F 9). In: DIN Deutsches Institut für Normung e. V; Beuth Verlag, Berlin, Germany.

Eckert, P. (2001) Untersuchungen zur Wirksamkeit und Stimulation natürlicher Abbauprozesse in einem mit gaswerksspezifischen Schadstoffen kontaminierten Grundwasserleiter. In *Bochumer Geologische und Geotechnische Arbeiten*. Bochum: PhD thesis, Ruhr-Universität Bochum, Germany, p. 123.

Eckert, P., and Appelo, C.A.J. (2002) Hydrogeochemical modeling of enhanced benzene, toluene, ethylbenzene, xylene (BTEX) remediation with nitrate. *Water Res Res* 38: 1-11.

Einsiedl, F., and Mayer, B. (2005) Sources and processes affecting sulfate in a karstic groundwater system of the Franconian Alb, southern Germany. *Environ Sci Technol* 39: 7118-7125.

EN27888 (1993-11) Wasserbeschaffenheit; Bestimmung der elektrischen Leitfähigkeit (ISO 7888:1985); Deutsche Fassung EN 27888:1993. In: DIN Deutsches Institut für Normung e. V; Beuth Verlag, Berlin, Germany.

Griebler, C., Mindl, B., and Slezak, D. (2001) Combining DAPI and SYBR Green II for the enumeration of total bacterial numbers in aquatic sediments. *Int Rev Hydrobiol* 86: 453-465.

Griebler, C., Mindl, B., Slezak, D., and Geiger-Kaiser, M. (2002) Distribution patterns of attached and suspended bacteria in pristine and contaminated shallow aquifers studied with an *in situ* sediment exposure microcosm. *Aquat Microb Ecol* 28: 117-129.

Haack, S.K., and Bekins, B.A. (2000) Microbial populations in contaminant plumes. *Hydrogeol J* 8: 63-76.

Ham, P.A.S., Schotting, R.J., Prommer, H., and Davis, G.B. (2004) Effects of hydrodynamic dispersion on plume lengths for instantaneous bimolecular reactions. *Adv Water Res* 27: 803-813.

Harleman, D.R.F., and Rumer, R.R. (1963) Longitudinal and lateral dispersion in an isotropic porous medium. *J Fluid Mech* 16: 385-394.

Holt, B.D. (1991) *Oxygen Isotopes.* New York: Wiley.

ISO10304-2 (1996-11) Wasserbeschaffenheit - Bestimmung der gelösten Anionen mittels Ionenchromatographie - Teil 2: Bestimmung von Bromid, Chlorid, Nitrat, Nitrit, Orthophosphat und Sulfat in Abwasser (ISO 10304-2:1995); Deutsche Fassung EN ISO 10304-2:1996. In: DIN Deutsches Institut für Normung e. V; Beuth Verlag, Berlin, Germany.

ISO17993 (2003) Wasserbeschaffenheit - Bestimmung von 15 polycyclischen aromatischen Kohlenwasserstoffen (PAK) in Wasser durch HPLC mit Fluoreszenzdetektion nach Flüssig-Flüssig-Extraktion. (ISO 17993:2002). In: DIN Deutsches Institut für Normung e. V; Beuth Verlag, Berlin, Germany.

Jakobsen, R., and Postma, D. (1999) Redox zoning, rates of sulfate reduction and interactions with Fe-reduction and methanogenesis in a shallow sandy aquifer, Rømø, Denmark. *Geochim Cosmochim Acta* 63: 137-151.

Kappler, A., Emerson, D., Edwards, K., Amend, J.P., Gralnick, J.A., Grathwohl, P. et al. (2005) Microbial activity in biogeochemical gradients - new aspects of research. *Geobiology* 3: 229-233.

Klenk, I.D., and Grathwohl, P. (2002) Transverse vertical dispersion in groundwater and the capillary fringe. *J Contam Hydrol* 58: 111-128.

Kneeshaw, T.A., McGuire, J.T., Smith, E.W., and Cozzarelli, I.M. (2007) Evaluation of sulfate reduction at experimentally induced mixing interfaces using small-scale push-pull tests in an aquifer-wetland system. *Appl Geochem, in press*.

Kota, S., Barlaz, M.A., and Borden, R.C. (2004) Spatial heterogeneity of microbial and geochemical parameters in gasoline contaminated aquifers. *Practice periodical of hazardous, toxic and radioactive waste management*: 105-118.

Krumholz, L.R. (2000) Microbial communities in the deep subsurface. *Hydrogeol J* 8: 4-10.

Lerner, D.N., Thornton, S.F., Spence, M.J., Banwart, S.A., Bottrell, S.H., Higgo, J.J. et al. (2000) Ineffective natural attenuation of degradable organic compounds in a phenol-contaminated aquifer. *Ground Water* 38: 922-928.

Lovley, D.R. (1995) Bioremediation of organic and metal contaminants with dissimilatory metal reduction. *J Ind Microbiol* 14: 85-93.

Lovley, D.R. (1997) Microbial Fe(III) reduction in subsurface environments. *FEMS Microbiol Rev* 20: 305-313.

Lovley, D.R. (2001) Anaerobes to the rescue. *Science* 293: 1444-1446.

Ludvigsen, L., Albrechtsen, H., Ringelberg, D.B., Ekelund, F., and Christensen, T.H. (1999) Distribution and composition of microbial populations in a landfill leachate contaminated aquifer (Grindsted, Denmark). *Microb Ecol* 37: 197-207.

Mayer, K.U., Benner, S.G., Frind, E.O., Thornton, S.F., and Lerner, D.N. (2001) Reactive transport modeling of processes controlling the distribution and natural attenuation of phenolic compounds in a deep sandstone aquifer. *J Contam Hydrol* 53: 341-368.

Mc Mahon, P.B., Chapelle, F.H., Falls, W.F., and Bradley, P.M. (1992) Role of microbial processes in linking sandstone diagenesis with organic rich clays. *J Sed Petrol* 62: 1-10.

McGuire, J.T., Long, D.T., and Hyndman, D.W. (2005) Analysis of recharge-induced geochemical change in a contaminated aquifer. *Ground Water* 43: 518-530.

McGuire, J.T., Long, D.T., Klug, M.J., Haack, S.K., and Hyndman, D.W. (2002) Evaluating behavior of oxygen, nitrate, and sulfate during recharge and quantifying reduction rates in a contaminated aquifer. *Environ Sci Technol* 36: 2693-2700.

Pickens, J.F., Cherry, J.A., Grisak, G.E., Merritt, W.F., and Risto, B.A. (1978) A mulitlevel device for groundwater sampling and piezometric monitoring. *Ground Water* 16: 322-327.

Pickup, R.W., Rhodes, G., Alamillo, M.L., Mallinson, H.E., Thornton, S.F., and Lerner, D.N. (2001) Microbiological analysis of multi-level borehole samples from a contaminated groundwater system. *J Contam Hydrol* 53: 269-284.

Postma, D., and Jakobsen, R. (1996) Redox zonation: equilibrium constraints on the Fe (III)/SO_4^{2-} reduction interface. *Geochim Cosmochim Acta* 60: 3169-3175.

Prommer, H., Tuxen, N., and Bjerg, P.L. (2006) Fringe-controlled natural attenuation of phenoxy acids in a landfill plume: integration of field-scale processes by reactive transport modeling. *Environ Sci Technol* 40: 4732-4738.

Rees, H.C., Oswald, S.E., Banwart, S.A., Pickup, R.W., and Lerner, D.N. (2007) Biodegradation processes in a laboratory-scale groundwater contaminant plume assessed by fluorescence imaging and microbial analysis. *Appl Environ Microbiol* 73: 3865-3876.

Ronen, D.M., Magaritz, M., Gvirtzman, H., and Garner, W. (1987) Microscale chemical heterogeneity in groundwater. *J Hydrol* 92: 173-178.

Salminen, J.M., Hanninen, P.J., Leveinen, J., Lintinen, P.T., and Jørgensen, K.S. (2006) Occurrence and rates of terminal electron-accepting processes and recharge processes in petroleum hydrocarbon-contaminated subsurface. *J Environ Qual* 35: 2273-2282.

Schmitt, R., Langguth, H.-R., and Püttmann, W. (1998) Abbau aromatischer Kohlenwasserstoffe und Metabolitenbildung im Grundwasserleiter eines ehemaligen Gaswerksstandorts. *Grundwasser* 2: ^78-86.

Scholl, M.A., Cozzarelli, I.M., and Christenson, S.C. (2006) Recharge processes drive sulfate reduction in an alluvial aquifer contaminated with landfill leachate. *J Contam Hydrol* 86: 239-261.

Smith, R.L., Harvey, R.W., and LeBlanc, D.R. (1991) Importance of closely spaced vertical sampling in delineating chemical and microbiological gradients in groundwater studies. *J Contam Hydrol* 7: 285-300.

Spence, M.J., Bottrell, S.H., Higgo, J.J., Harrison, I., and Fallick, A.E. (2001) Denitrification and phenol degradation in a contaminated aquifer. *J Contam Hydrol* 53: 305-318.

Stookey, L.L. (1970) Ferrozine - a new spectrophotometric reagent for iron. *Anal Chem* 42: 779-781.

Takahata, Y., Kasai, Y., Hoaki, T., and Watanabe, K. (2006) Rapid intrinsic biodegradation of benzene, toluene, and xylenes at the boundary of a gasoline-contaminated plume under natural attenuation. *Appl Microbiol Biotechnol* 73: 713-722.

Thornton, S.F., Lerner, D.N., and Davison, R.M. (2002) Groundwater monitoring. In *Encyclopedia of Environmetrics.* El-Shaarawi, A.H., and Piegorsch, W.W. (eds). Chichester: John Wiley & Sons, Ltd, pp. 960-974.

Thornton, S.F., Quigley, S., Spence, M.J., Banwart, S.A., Bottrell, S., and Lerner, D.N. (2001) Processes controlling the distribution and natural attenuation of dissolved phenolic compounds in a deep sandstone aquifer. *J Contam Hydrol* 53: 233-267.

Thullner, M., Schroth, M.H., Zeyer, J., and Kinzelbach, W. (2004) Modeling of a microbial growth experiment with bioclogging in a two-dimensional saturated porous media flow field. *J Contam Hydrol* 70: 37-62.

Tuxen, N., Albrechtsen, H.J., and Bjerg, P.L. (2006) Identification of a reactive degradation zone at a landfill leachate plume fringe using high resolution sampling and incubation techniques. *J Contam Hydrol* 85: 179-194.

Ulrich, G.A., Martino, D., Burger, K., Routh, J., Grossman, E.L., Ammerman, J.W., and Suflita, J.M. (1998) Sulfur cycling in the terrestrial subsurface: commensal interactions, spatial scales, and microbial heterogeneity. *Microb Ecol* 36: 141-151.

van Breukelen, B.M., and Griffioen, J. (2004) Biogeochemical processes at the fringe of a landfill leachate pollution plume: potential for dissolved organic carbon, Fe(II), Mn(II), NH_4^+, and CH_4 oxidation. *J Contam Hydrol* 73: 181-205.

Wilson, R.D., Thornton, S.F., and Mackay, D.M. (2004) Challenges in monitoring the natural attenuation of spatially variable plumes. *Biodegradation* 15: 359-369.

Winderl, C., Anneser, B., Griebler, C., Meckenstock, R.U., and Lueders, T. (2008) Depth-resolved quantification of anaerobic toluene degraders and aquifer microbial community patterns in distinct redox zones of a tar oil contaminant plume. *Appl Environ Microbiol* 74: 792-801.

Wisotzky, F., and Eckert, P. (1997) Sulfat-dominierter BTEX-Abbau im Grundwasser eines ehemaligen Gaswerksstandortes. *Grundwasser* 2: 11-20.

5. The hidden dynamics of biogeochemical processes in an organically contaminated porous aquifer

5.1. Introduction

Geobiologists searching for bioactivities in subsurface environments are well advised to look for gradients, which typically form at sea water – fresh water interfaces, at the transition between surface water and groundwater or the fringes of contaminant plumes. The transport of substances across physical-chemical boundaries by mixing processes is commonly regarded as the rate controlling mechanism for many geochemical and biological reactions (Thornton et al., 2001; Klenk and Grathwohl, 2002; Prommer et al., 2006; Maier et al., 2007). Generally, metabolic activities at these zones are reflected by steep gradients of electron donors, electron acceptors and metabolic end products that arise at different spatial scales. The diffusive boundary layer surrounding bacterial cells, for instance, extends about 10-fold the diameter of the cell and reveals gradients in the scale of micrometers to millimeters (Jørgensen, 1998). Geochemical or lithological transition zones, such as sulfate/methane interfaces in deep marine sediments of the Pacific Ocean, have been observed to stimulate redox processes and to cause changes in the microbial composition, which can be observed on a cm-scale (Parkes et al., 2005). Dense hypersaline interfaces at deep-sea haloclines, which act as barriers for nutrients sinking down the water column and therefore create an attractive nutrient-rich environment for microorganisms, even stretch across several decimeters to meters (van der Wielen et al., 2005; Daffonchio et al., 2006). With a rate of only a few centimeters per year, advection and diffusion-controlled mixing processes in subseafloor sediments are reported to proceed very slowly, while at hot spots, such as hydrothermal vents, the distribution of terminal electron accepting processes can change by several orders of magnitude within centimeters and minutes (Jørgensen and Boetius, 2007).

Biotic and abiotic patterns across interfaces have been subject of intensive studies in various types of environments, such as lake sediments and the subsea floor, during the last years. So far, however, only little is known about the dynamics of gradients and interfaces in groundwater systems. Often, these are threatened by pollution with aromatic hydrocarbons, which may be released by accidental spills or careless handling of organic compounds such as tar oil and solvents during production or manufacturing processes. In order to cleanup such poorly accessible, anaerobic environments, the capability of microorganisms to degrade a range of organic contaminants is increasingly recognized. In porous aquifers, the supply of electron donors and electron acceptors is primarily controlled by hydrodynamic dispersion, *i.e.* transverse mixing and diffusion at transition zones, such as the capillary fringe or the fringe of an organic contaminant plume (Klenk and Grathwohl, 2002; Maier et al., 2007). Although it is often suggested, plumes in aquifers are not static. Transient flow conditions caused by hydraulic changes or high-conductivity lenses have been reported to cause plume meandering and increased convection (Werth et al., 2006; Bauer et al., submitted). This, in turn, leads to a displacement and moving of transition zones and consequently to an enlargement of the mixing area, thus affecting the scale of biogeochemical gradients (Rahman et al., 2005). However, the impact of transient hydraulic conditions on the distribution of redox processes and, above all, on the biodegradation capacity is poorly understood by now, not least owing to the difficulties tainted with scale-adapted groundwater sampling (Anneser et al., 2008b; Anneser et al., 2008a). In fact, we still need to bring in some light concerning the mechanisms driving biodegradation in the subsurface, thus rendering microbial communities and their ecological interactions as well as the impacts of spatial and temporal variabilities a black box to modelers and ground water resource managers (Fredrickson and Fletcher, 2001).

In this study, we offer fascinating insights into the small-scale distribution of biogeochemical gradients in a tar oil-contaminated porous aquifer and highlight the yet unrecognized spatial and temporal dynamics of redox processes within the contaminant plume.

5.2. Materials and methods

5.2.1. High-resolution groundwater sampling

The investigation site is a Quaternary, relatively homogenous sandy aquifer at the former gasworks plant in Düsseldorf-Flingern (Germany), which is heavily contaminated with mono- and polycyclic aromatic hydrocarbons. Groundwater was sampled from a high-resolution multi-level well at vertical intervals of 2.5 – 33 cm using a peristaltic pump. Low pumping rates and simultaneous sampling of all connected ports minimized the risk of mixing groundwater from different depths. Sorption and volatilization of aromatic hydrocarbons was minimized by use of pre-saturated fluran tubes (Ismatec, Wertheim, Germany) and immediate preservation of the samples using appropriate methods. For more details on the study site and the sampling methods see Anneser et al. 2008 a+b as well as sections 2.3 and 4.3.

5.2.2. Contaminant concentration and groundwater chemistry

For the analysis of monoaromatic hydrocarbons groundwater samples were amended with 1 M NaOH (final concentration 0.1 M) to stop biological activity. After addition of an internal standard (EPA 524 Internal Standard Mix, Supelco, Bellefonte, PA, USA) at a final concentration of 0.67 µg ml^{-1}, the volatile contaminant fraction was quantified from the headspace on a GC-MS analyzer (Trace DSQ, Thermo Electron, Dreieich, Germany), which was equipped with a DB5 capillary GC-column (J & W Scientific, Folson, CA, USA). Sulfate was determined by ion chromatography after filtration of the water samples through a 0.45 µm syringe filter. Dissolved sulfide and ferrous iron were analyzed photometrically following in principle the protocols of Cline (1969) and Stookey (1970), respectively. Further details on the analytical procedures of the individual parameters are given in section 4.3.3 and Anneser et al. (2008b).

5.2.3. Determination of cell numbers and productivity

Water samples dedicated to total bacterial cell counts were fixed with glutardialdehyde solution (final concentration 2.5 %) and stained with the DNA dye SYBR green I (Molecular Probes, Invitrogen, Karlsruhe, Germany), which was added at a ratio of 1:10,000. After filtration onto 0.2 µm polycarbonate filters (Millipore, Germany), bacterial cells were enumerated by fluorescence microscopy at 1000 × magnification, as described elsewhere (Griebler et al., 2001; Griebler et al., 2002).
Bacterial carbon production (BCP) was estimated via the incorporation of [^{3}H]-leucine by adapting protocols of Kirchman (1993). Radioactively labelled [^{3}H]-leucine (165 Ci mmol^{-1}, 1 mCi ml^{-1}, GE Healthcare) was added directly in the field to triplicates of 15 ml groundwater at a final concentration of 10 nM, which corresponded to the saturation concentration determined in preceding experiments. In parallel, groundwater samples fixed with formaldehyde (3.7% final concentration) prior to substrate addition were run as controls. Samples were incubated at *in situ* temperatures (± 1°C) in thermoboxes. Label incorporation was determined to be linear for at least 10 hours. After 4-6 hours, the incubation was stopped

with formaldehyde and samples were stored at 4°C in darkness till further analysis. Later, samples were treated with ice-cold trichloroacetic acid (TCA) at a final concentration of 5% and placed on ice for 15 min. Prior to and after sample filtration, cellulose nitrate filters (0.2 μm, Whatman) were rinsed with ice-cold MQ water and ice-cold 5% TCA solution. After filtration, filters were placed into scintillation vials and dried for 1 hour at room temperature before being dissolved in 1 ml ethylacetate, followed by shaking for 1 h. After the addition of a scintillation cocktail (Ultima Gold XR), samples were stored overnight at 4°C in the dark and subsequently subjected to liquid scintillation counting on a Tri-Carb 1600 TR (Perkin Elmer). Counts were manually corrected for quenching using a predetermined quench curve and a machine counting efficiency program. The actual incorporation of label into proteins was determined to be 10% of the total bacterial [^{3}H]-leucine uptake. Incorporation rates were converted to bacterial carbon production (BCP) using the following conversion equation (Kirchman and Ducklow, 1993):

$$\text{BCP [g]} = \text{mol Leu}_{inc} \times 100 / 7.3 \times 131.2 \times 0.86 \times 2 \qquad \text{(eq. 5.1)}$$

mol Leu$_{inc}$	= Leu incorporation rate [mol l^{-1} h^{-1}]
100/7.3	= mol% Leu in protein fraction
131.2	= molecular weight of Leu [g mol^{-1}]
0.86	= ratio of cellular carbon to protein
2	= correction factor for isotope dilution

5.2.4. Stable isotope analyses

Samples dedicated to sulfate isotope analysis were fixed with 20 % Zn-acetate solution in order to prevent re-oxidation of dissolved sulfide during groundwater sampling and sample storage. Details on the analytical procedure and on calculations of the sulfate isotope ratios are given in section 4.3.3 and in Anneser et al. (2008b).

Toluene isotope ratios were measured on a Trace GC analyzer (Thermo Finnigan, San Jose, CA), which was coupled to an isotope ratio mass spectrometer (Thermo Finnigan MAT, Bremen, Germany). Upstream the GC-IRMS system, a purge & trap concentrator (Tekmar LSC 3100) was connected to a liquid autosampler (Tekmar AQUAtek 70, Tekmar-Dohrmann, Mason, OH). Details on the analytical procedure and on calculations of the carbon isotope ratios can be derived from Zwank et al. (2003).

5.3. Results and discussion

5.3.1. Biogeochemical indicators of biodegradation

By means of a novel high-resolution multi-level well, biogeochemical gradients were recorded in the centimeter-range at temporal intervals of three to five months over a period of almost two years. Allocation of bioactive zones was possible by comparison of steep vertical profiles of redox-sensitive parameters. Redox potential, for instance, exhibited a significant decrease towards strongly reduced values in the plume core, which typically can be observed during anaerobic biodegradation of organic compounds (Christensen et al., 2001). A more or less inverse behaviour was observed for pH, which showed a pronounced increase with depth, possibly due to electron consuming reactions (Fig. 5.1A). Concentration profiles of aromatic hydrocarbons allowed to distinguish two zones of contamination: (1) gradients of the monoaromatic hydrocarbons benzene, toluene, ethylbenzene and xylenes (BTEX) delineated a
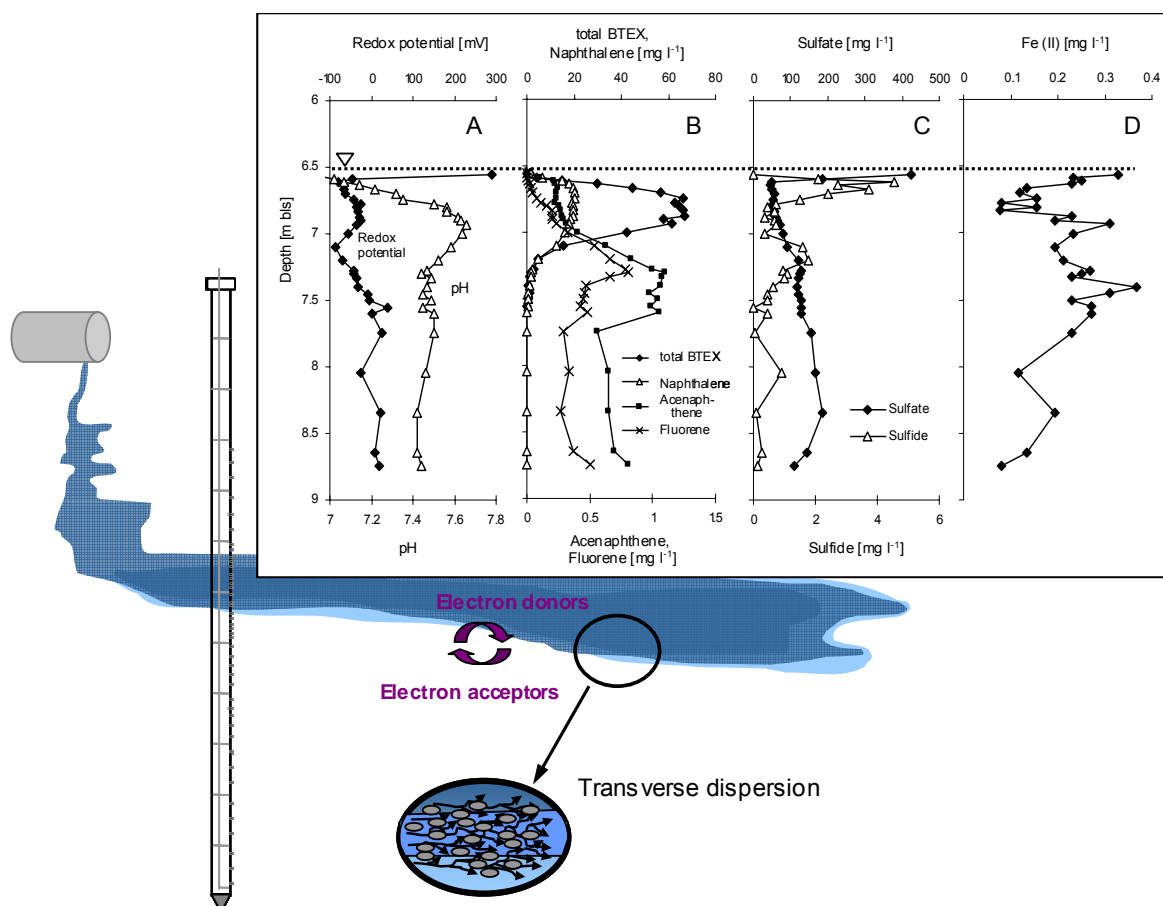
Figure 5.1 Transverse dispersion at the upper and lower plume fringe resulted in the formation of steep physical-chemical gradients, which are indicative of dominant redox processes (here shown exemplarily at results of a sampling campaign performed in February 2007).

BTEX plume, which contained toluene as main constituent and which was restricted to an area of less than 1 m in thickness right beneath the groundwater table (Fig. 5.1B). (2) In contrast, the zone impacted by higher molecular polycyclic aromatic hydrocarbons (PAHs) stretched all across the investigated aquifer, exhibiting an accumulation of the contaminants with depth, yet at significantly lower concentrations compared to the BTEX compounds (Fig. 5.1B).

As can be seen in Fig. 5.1C, sulfate decreased from background concentrations of about 150 mg l^{-1} to less than 50 mg l^{-1} in the center of the BTEX plume. At the same time, pronounced sulfide production was observed at the upper and lower plume fringe (Fig. 5.1C). Assuming sulfide as a reaction product of sulfate reduction, these peaks may be indicative of increased bioactivity at the plume fringe. To a minor degree, iron reduction as a further important redox process of biodegradation is likely to take place all across the investigated aquifer section, particularly at the upper and lower plume fringe, as suggested by the gradient of dissolved Fe(II) (Fig. 5.1D). Hints on iron reduction at this site were also given by the distribution of sedimentary iron species, which is illustrated elsewhere in detail (Anneser et al., 2008b; sections 3.4.2 and 4.4.3). In addition, molecular analyses of the sediments revealed the prevalence of toluene degrader-specific gene sequences closely related to those of the iron reducing *Geobacter* species (Winderl et al., 2007; Winderl et al., 2008).

5.3.2. Migration of biogeochemical gradients

Between September 2005 and May 2007, six sampling campaigns were performed at intervals of three to five months. In the course of the first four sampling dates (September 2005 till August 2006), the hydraulic head at our sampling site exhibited only minor changes at about 6.36 m (± 5 cm) below land surface (bls) (Fig. 5.2). Nevertheless, considerable variations in the vertical plume expansion could be observed. This is impressively demonstrated by the sequence of BTEX gradients in relation to the water table, as depicted in Figure 5.2. In May 2006, for instance, maximum BTEX concentrations of 69 mg l^{-1} were measured at a depth of 6.56 m bls. Three months later, the maximum peak concentration accounted for only 47 mg l^{-1}. Defining the plume center as the area comprising > 50 % of the maximum toluene concentration, the vertical expansion of the plume core at the same time shrinked by half its original size from 0.4 m to 0.2 m. More than this, the shape of the vertical concentration patterns sometimes displayed a sharp peak (September 2005) but changed towards a belly-shaped form a few months later. At our last sampling date in May 2007, the BTEX plume assumed a peaked shape again (Fig. 5.2). Taking into account the comparatively modest fluctuations of the water table during that period, the variations in the vertical and horizontal dimension of the BTEX plume unveiled the amazing natural dynamics in our contaminated groundwater system.

Remarkably, the changes in the distribution of contaminants were reflected by respective fluctuations of individual redox-sensitive geochemical gradients, as illustrated in Fig. 5.2 at the example of sulfate and sulfide. Concomitant with decreasing contaminant concentrations, sulfate availability declined, exhibiting nearly depletion in the plume center. Parallely, the lower fringe of the BTEX plume was steadily accompanied by pronounced sulfide peaks, thus indicating that biodegradation activities preferentially took place in this zone.

It is exciting to follow the main sulfide peaks over time in their vertical position in relation to the upper and lower fringes of the contaminant plume. Throughout the sampling period from September 2005 until May 2006, the zone of high dissolved sulfide concentrations was distinguished by one to three peaks of different size, which were located between 6.6 and 7.5 m bls, stretching from the plume center across the lower plume fringe. Concomitant with a shrinking of the plume's thickness by August 2006, the large single sulfide peak (7.1 m bls) accounting for 13 mg l^{-1} in May 2006 seemed collapsed, leaving only a tiny fraction behind in August 2006, while the main sulfide peak shifted upwards, following the steep BTEX gradient.

Then, between August 2006 and February 2007, a pronounced decrease of the groundwater table by 25 cm lead to a downward shift of the entire plume. Simultaneously, an increase of the maximum BTEX load by about 43 % was observed (Fig. 5.2). Owing to this downward movement, the upper plume fringe literally "slipped" into the sulfate reduction zone that had established at the lower boundary of the BTEX plume recorded in August 2006. After this shift the plume was found again expanded downwards, bringing back sufficient amounts of contaminants. Nonetheless, the sulfide peak in 7.2 m bls still had not recovered, but the former main peak of August 2006, now located at the upper fringe of the plume, was much smaller too. The curve illustrating the hydraulic head (groundwater table) proves a continuous decrease between the August 2006 and February 2007 sampling survey. Thus, neither stable hydraulic conditions nor new zones exhibiting high amounts of dissolved sulfide could be established in this period (Fig. 5.2).
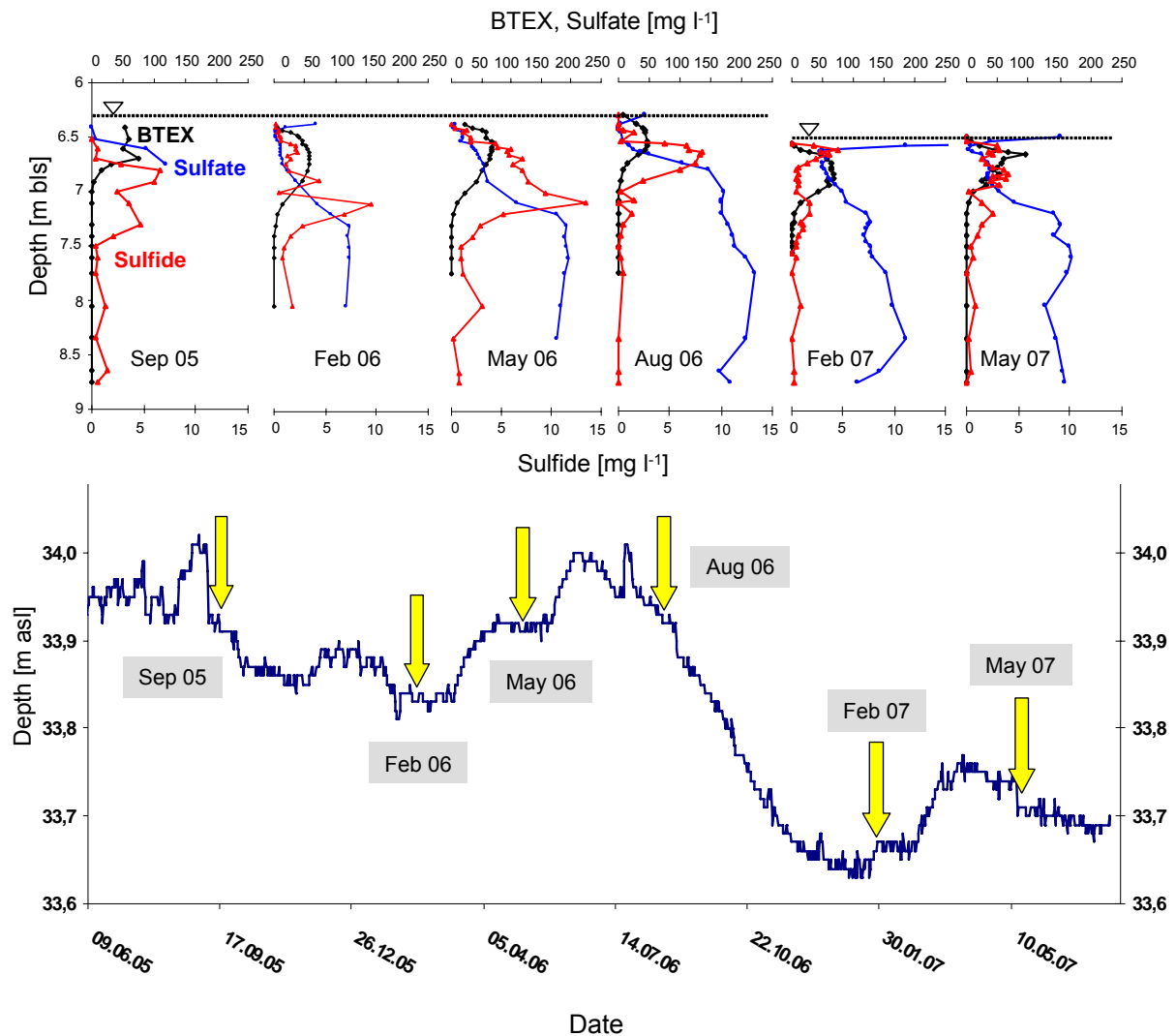
Figure 5.2 Considerable fluctuations in the distribution of BTEX, sulfate and sulfide were observed even at relatively constant hydraulic conditions (Sep 05 – Aug 06, Feb 07 – May 07). Pronounced sulfide peaks at the lower plume fringe followed the plume dynamics unless the sulfate reducer community was strongly disturbed by a drastic hydraulic change between Aug 06 and Feb 07. The hydraulic head measured in a neighbouring monitoring well, as depicted in the lower graph, corresponds to the vertical position of the water table of the HR-MLW (m bls = meters below land surface; m asl = meters above sea level).

Maximum sulfide concentrations, which were suddenly found at the upper plume fringe in February 2007, implied that sulfate reducing activities now lagged behind the plume dynamics. Obviously, it took the degrader community months to cope with the changed situation. After slowing down their sulfate reducing activities, as it is suggested by increased BTEX concentrations and lower sulfide concentrations in February 2007, resumption of the original activities may be indicated by the re-establishing sulfide peak at the lower plume fringe. With an upward movement of the lower plume fringe in May 2007 the distribution of dissolved sulfide changed again: the lower sulfide peak was still present and the upper one still located at the upper fringe, yet further reduced in size. Now, however, we could observe a third peak developing at the new position of the lower plume fringe.

It has to be added that these patterns, as described here, exclusively reflect the information gained from groundwater samples, so far neglecting sediment information. Previous investigations at the Flingern aquifer suggested iron reduction to occur in parallel to

sulfate reduction, yet to a lower extent (Eckert, 2001; Anneser et al., 2008b). To a certain degree, the sulfide produced may be captured and precipitated in the form of FeS or it may be re-oxidized at the expense of Fe(III) dissolution, as discussed in section 3.5.2. However, the high amounts of sulfide that came along with decreasing sulfate concentrations corroborate our assumption that the gradients detected in the groundwater are attributed to microbial sulfate reduction rather than to abiotic reactions.

As the sampling area is extensively sealed, the impact of local recharge on the position of the water table is considered to be insignificant. Hence, the oscillations of the water table could not directly be correlated to atmospheric conditions. It is speculative whether the expansion and shrinking of the plume and the migration of the gradients is correlated to seasonal fluctuations. Rising water tables not only cause a dilution and, consequently, reduced toxicity of the contaminants; above all, mixing with water from the unsaturated zone provides fresh electron acceptors and nutrients and thus improves conditions for biodegradation. Consequently, a slightly elevated groundwater table in August 2006 compared to the months before and after, concomitant with an increase in temperature of up to 3°C (data not shown) within the upper 1.5 m of the saturated zone, may have promoted bioactivities during summer and thus effected a reduction in total BTEX mass.

5.3.3.   Resilience and adaptive capacity of groundwater bacteria

The fact that sulfide peaks moved up and down, collapsed but partly remained for some while and newly formed again, steadily following the electron donor and electron acceptor gradients indicates the potential for sulfate reduction being present in the attached aquifer microbial communities all over the investigated vertical cross section. The data imply that at least on a long-term basis of several months individual physiological groups and activities within microbial communities are initialized and establish pronounced biodegradation activities.

The adaptive capacity of the biodegrader community is reflected by vertical profiles of the stable isotope ratios of toluene ($^{13}C/^{12}C$) and groundwater sulfate ($^{34}S/^{32}S$), which provide in the first instance evidence of microbially mediated anaerobic toluene oxidation (Fig. 5.3A) or, respectively, sulfate reduction (Fig. 5.3B) (see Anneser et al., 2008b). Independent from the vertical movements of the upper plume fringe, steep gradients of the respective δ-values indicating enhanced bioactivities were always located at the transition contaminated-uncontaminated groundwater. In the plume center, on the other hand, no shifts in isotope ratios hinting at toluene degradation were detectable, while, at the same time, strongly enriched ^{34}S values suggested sulfate reduction to be active in this zone. These putatively contradictory patterns may be explained by masking effects. To obtain a pronounced $^{13}C/^{12}C$ isotope shift in the residual fraction of toluene, more than 50% of the total compound fraction needs to be degraded (Meckenstock et al., 2004). In consequence, the high toluene concentrations in the plume center at least partly mask the occurrence of biodegradation. Vice versa, the low amounts of residual sulfate in the plume center are likely to be enriched in the heavier ^{34}S isotope contrary to isotopically lighter "background" sulfate. Moreover, sulfate measured in groundwater close to the capillary fringe revealed isotope ratios different from those determined in groundwater of deeper, less contaminated zones. This may hint at different origins of groundwater sulfate, which may, for instance, infiltrate with recharge from the unsaturated zone (see Anneser et al., 2008b).
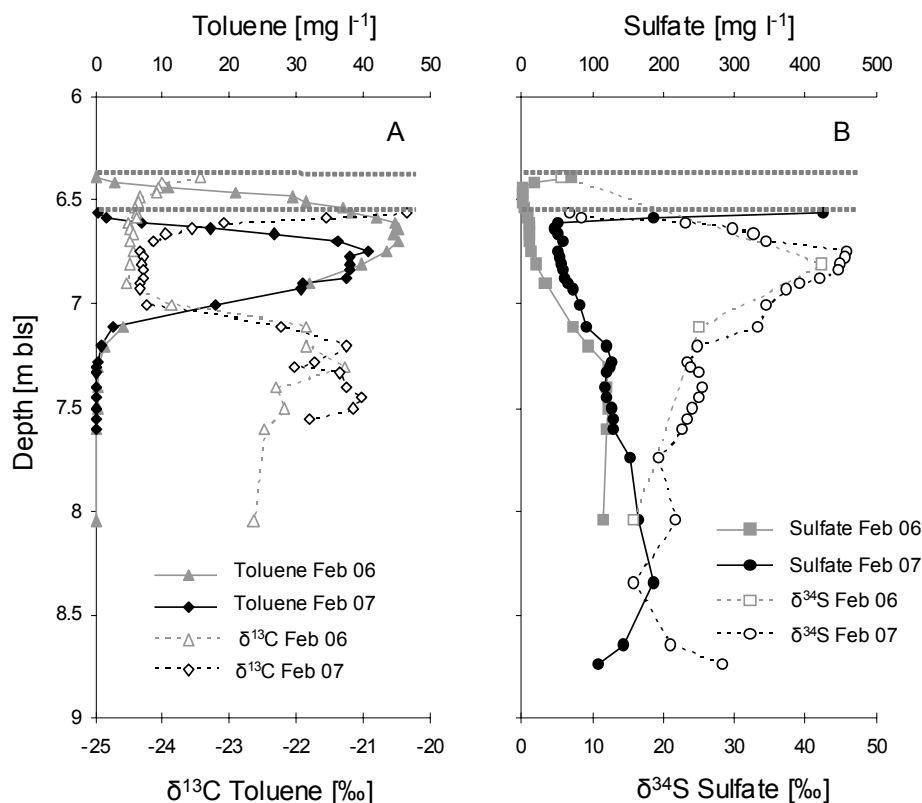
Figure 5.3 Increasing stable isotope ratios of toluene ($\delta^{13}C$) and groundwater sulfate ($\delta^{34}S$) concomitant with a decline in the respective substrate concentrations provided qualitative evidence for microbially mediated biodegradation.

Interestingly, gradients of $\delta^{13}C$ and $\delta^{34}S$ suggest biodegradation to proceed without significant restrictions even after the drop of the water table between August 2006 and February 2007, whereas sulfide peaks imply a shift of the "sulfidogenic" zone from the lower towards the upper plume fringe, accompanied by an apparent decrease in sulfide production.

Regarding the observed dynamics of the redox conditions, the question arises: *what* changes? Is it just a permanent switch-on and -off of metabolic pathways that controls bioactivities? Or are changes in the concentration of contaminants and metabolites attributed to variations of bacterial densities or activities? Are sulfate reducers able to actively follow their nutrient source and to re-establish within a few weeks?

Even under putatively optimal lab conditions many groundwater microorganisms are characterized by very slow reproduction rates of weeks to months (Mailloux and Fuller, 2003). Furthermore, only up to 10 % of the subsurface microorganisms are found free-living in the groundwater, while the majority resides attached to the soil matrix and therefore cannot readily move from one location to another (Bekins et al., 1999; Lehman and O'Connell, 2002). It is therefore more likely that the hydrological and geochemical changes at our site hit an already pre-adapted community, which was activated upon the altered conditions (Prosser et al., 2007). The resulting temporary "boost" in bioactivity may be reflected by an increased sulfide production. While the supposable highly diverse microbial community at the upper plume fringe obviously maintained its major processes by functional redundancy (see subsequent discussion), the specialized population in the sulfidogenic zone was visibly retarded in bioactivity. Upon resuming their activity, however, the bacteria apparently

prepared to take ahead the capillary fringe community, as can be inferred from slightly increased sulfide and biomass gradients obtained in May 2007 (Fig. 5.2 and Fig. 5.4).

In order to account for the bulk of bacteria attached to soil particles, the population dynamics were evaluated from the analysis of sediment samples obtained in June 2005 and February 2006, respectively. Molecular analyses of sediment samples, which were obtained in June 2005 prior to installation of the HR-MLW, revealed maximum total cell numbers in the zone of highest contamination, whereas the ratio of toluene degrader-specific gene sequences was found to dominate in the sulfidogenic zone underneath the plume core (Winderl et al., 2008). In sediments collected eight months later and ~0.5 m distant from the first sampling site, the distribution of bacterial sequences was similar to that of the first sediment liners, but shifted against each other as a consequence of temporal and spatial fluctuations (Pilloni & Lueders, personal communication). Consequently, it can be stated that long-term dynamics, as observed in groundwater at our study site, also applied for sediment-associated microbial communities.

Total cell numbers within groundwater samples revealed slight but significant variations corresponding well to the plume fringe concept, which assumes maximum bioactivities and biomass at the fringes of an organic contaminant plume (Bauer et al., 2008a). Maximum biomass was detected directly beneath the capillary fringe (Fig. 5.4), where recharge presumably provided supply of "fresh" nutrients and created conditions beneficial to both anaerobic and aerobic as well as contaminant degrading and non-degrading microorganisms. While an increasing concentration of toxic pollutants caused a decrease in biomass, the transition to less contaminated groundwater at the lower plume fringe obviously provided more favourable conditions again, which is indicated by a small but distinct increase in cell numbers. On the other hand, an increase in biomass is not necessarily correlated to enhanced bioactivity. This becomes evident if cell numbers and productivity data determined in February 2007 and May 2007 are compared. Even though cell numbers were relatively high in February, incorporation of ^{3}H-labeled leucine was by a factor of 6 lower after the drastic water table shift when compared to data obtained three months later (Fig. 5.4). This observation emphasizes the call for considering both cell numbers and bioactivity in order to properly describe *in situ* biogeochemical interactions, as was also claimed by Röling (2007) in a recent study.

Lowered carbon production concomitant with a decreasing sulfide concentration, as observed in February 2007 (Fig. 5.2 and Fig. 5.4), imply that the hydraulic fluctuations exhibited strong effects on microbial communities of certain layers and resulted in a delay of bioactivities. According to Torsvik et al. (2002), strong disturbances exerting selective pressure on microbial communities are likely to generate a less diverse but highly specialized population of r-strategists, which overgrows the less adapted rivalry. This may apply for the sulfidogenic zone underneath the BTEX plume, where a relatively poor diversity of specialized toluene degraders was revealed by molecular analyses of sediment samples (Winderl et al., 2008). The capillary fringe, on the other hand, which forms the transition between saturated and unsaturated zone and therefore is permanently subject to moderate changes, exhibited a considerably higher microbial diversity. This observation fits well to the "intermediate disturbance theory", which states that minor perturbations are likely to cause shifts in the microbial community composition or even lead to an increase rather than to a loss in biodiversity (Griebler and Lueders, 2008).

Can we conclude from our findings that the contaminant degraders are in fact more resilient to fluctuations than can be assumed at first sight? According to Botton et al. (2006), resilience denotes the persistence of relationships within a system, *i.e.* the ability of a

community to maintain specific functions. Highly diverse microbial communities often harbour a variety of metabolic pathways, thus providing functional redundancy. A varying abundance of species with similar ecological functions grants the persistence of a specific feature by functional overlap and therefore represents a form of "biological insurance". At our site, a greater diversity was revealed at the upper compared to the lower plume fringe, where a highly specialized but less diverse community of sulfate and iron reducers prevailed (Winderl et al., 2008). Hence, it can be speculated that functional redundancy of the highly diverse microbial community at the upper zone of the aquifer buffered the effects of the hydraulic change and prevented an interruption of the metabolic activities. In comparison, the adaptive capacity of the specialized community detected at the lower plume fringe was significantly lower, thus delaying resumption of the original status.
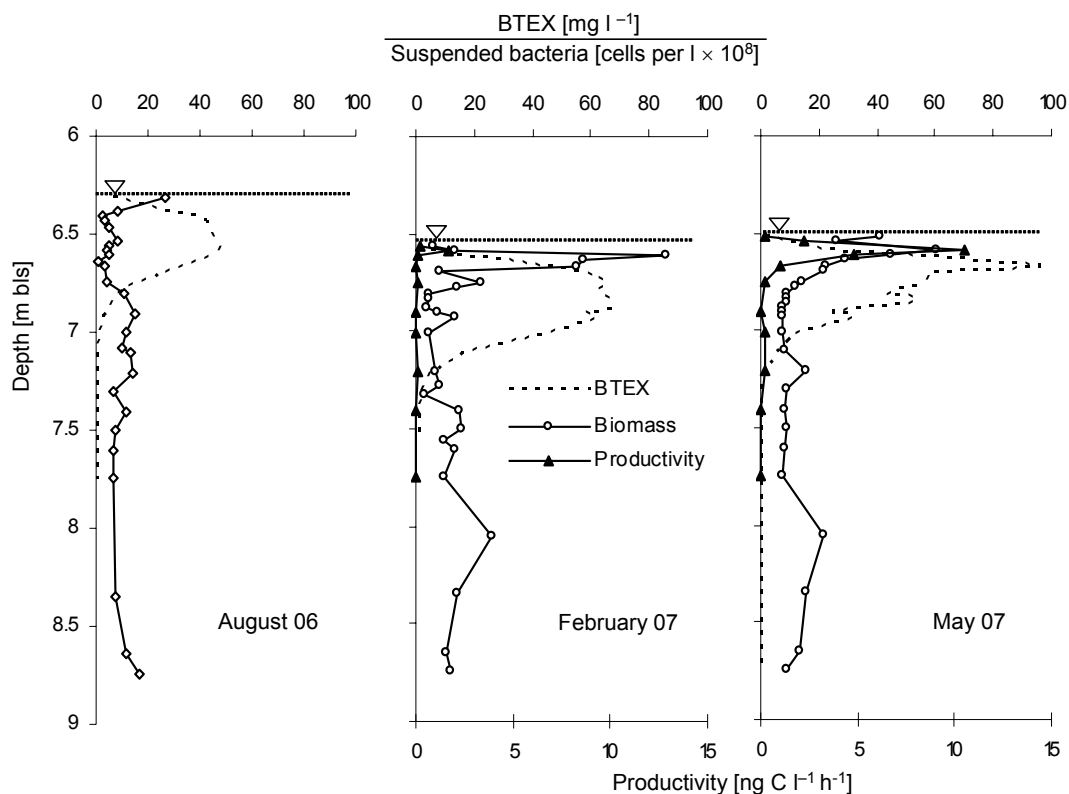
Figure 5.4 Dynamics of biotic variables in relation to the BTEX plume. Maximum cell numbers and carbon production were found at the capillary fringe, while lowest cell numbers were located in the plume core.

5.4. Conclusions

Above all, the small-scale gradients and their spatial and temporal dynamics as observed in this study point towards the high complexity of biodegradation processes taking place in a tar oil-contaminated porous aquifer. In this mostly considered stable environment we could demonstrate astonishing, unexpected dynamics in the centimeter to decimeter scale, bearing severe consequences for contaminant turnover. By now, such empirical data are rare, although their integration into site-specific reactive transport models is crucial for reliable calculations of contaminant transport and fate, which therefore often remain quite speculative. Improving the predictability of plume development will facilitate the implementation of guidelines for sanitation liables and environmental authorities and will foster the acceptance of natural attenuation as a cost-efficient alternative to technical remediation approaches.

5.5. References

Anneser, B., Richters, L., and Griebler, C. (2008a) Application of high-resolution groundwater sampling in a tar oil–contaminated sandy aquifer. Studies on small-scale abiotic gradients. In *Adavances in subsurface pollution of porous media: indicators, processes and modelling.* Candela, L., Vadillo, I., and Elorza, F.J. (eds), Taylor & Francis / Balkema, Leiden, NL.

Anneser, B., Einsiedl, F., Meckenstock, R.U., Richters, L., Wisotzky, F., and Griebler, C. (2008b) High-resolution monitoring of biogeochemical gradients in a tar oil-contaminated aquifer. *Appl Geochem* 23: 1715-1730.

Bauer, R.D., Maloszewski, P., Zhang, Y., Meckenstock, R.U., and Griebler, C. (2008a) Mixing-controlled biodegradation in a toluene plume - Results from two-dimensional laboratory experiments. *J Contam Hydrol* 96: 150-168.

Bauer, R.D., Rolle, M., Eberhardt, C., Grathwohl, P., Bauer, S., Kolditz, O. et al. (2008b) Enhanced biodegradation by hydraulic heterogeneities in petroleum hydrocarbon plumes. submitted to *J Contam Hydrol*.

Bekins, B.A., Godsy, E.M., and Warren, E. (1999) Distribution of microbial physiologic types in an aquifer contaminated by crude oil. *Microb Ecol* 37: 263-275.

Botton, S., van Heusden, M., Parsons, J.R., Smidt, H., and van Straalen, N. (2006) Resilience of microbial systems towards disturbances. *Crit Rev Microbiol* 32: 101-112.

Christensen, T.H., Kjeldsen, P., Bjerg, P.L., Jensen, D.L., Christensen, J.B., Baun, A. et al. (2001) Biogeochemistry of landfill leachate plumes. *Appl Geochem* 16: 659-718.

Cline, J.D. (1969) Spectrophotometric determination of hydrogen sulfide in natural waters. *Limnol Oceanogr* 14: 454-458.

Daffonchio, D., Borin, S., Brusa, T., Brusetti, L., van der Wielen, P.W., Bolhuis, H. et al. (2006) Stratified prokaryote network in the oxic-anoxic transition of a deep-sea halocline. *Nature* 440: 203-207.

Eckert, P. (2001) Untersuchungen zur Wirksamkeit und Stimulation natürlicher Abbauprozesse in einem mit gaswerksspezifischen Schadstoffen kontaminierten Grundwasserleiter. In *Bochumer Geologische und Geotechnische Arbeiten*. PhD thesis, Ruhr-Universität Bochum, Germany, p. 123.

Fredrickson, J.F., and Fletcher, M.M. (2001) *Subsurface Microbiology and Biogeochemistry.*: John Wiley & Sons, Inc.

Griebler, C., and Lueders, T. (2008) Microbial diversity in groundwater ecosystems. *Freshwater Biology*.

Griebler, C., Mindl, B., and Slezak, D. (2001) Combining DAPI and SYBR Green II for the enumeration of total bacterial numbers in aquatic sediments. *Int Rev Hydrobiol* 86: 453-465.

Griebler, C., Mindl, B., Slezak, D., and Geiger-Kaiser, M. (2002) Distribution patterns of attached and suspended bacteria in pristine and contaminated shallow aquifers studied with an *in situ* sediment exposure microcosm. *Aquat Microb Ecol* 28: 117-129.

Jørgensen, B.B. (1998) Life in the diffusive boundary layer. In *The Benthic Boundary Layer*. Boudreau, B.P., and Jørgensen, B.B. (eds). Oxford: Oxford University Press, pp. 348-373.

Jørgensen, B.B., and Boetius, A. (2007) Feast and famine-microbial life in the deep-sea bed. *Nat Rev Microbiol* 5: 770-781.

Kirchman, D.L. (1993) Leucine incorporation as a measure of biomass production by heterotrophic bacteria. In *Handbook of methods in aquatic microbial ecology*. Kemp, P.F., Cole, J.J., Sherr, B.F., and Sherr, E.B. (eds). Lewis Publishers, New York, USA.

Kirchman, D.L., and Ducklow, H.W. (1993) Estimating conversion factors for the thymidine and leucine methods for measuring bacterial production. In *Handbook of methods in aquatic microbial ecology*. Kemp, P.F., Cole, J.J., Sherr, B.F., and Sherr, E.B. (eds). Lewis publishers, New York, USA.

Klenk, I.D., and Grathwohl, P. (2002) Transverse vertical dispersion in groundwater and the capillary fringe. *J Contam Hydrol* 58: 111-128.

Lehman, R.M., and O'Connell, S.P. (2002) Comparison of extracellular enzyme activities and community composition of attached and free-living bacteria in porous medium columns. *Appl Environ Microbiol* 68: 1569-1575.

Maier, U., Rügner, H., and Grathwohl, P. (2007) Gradients controlling natural attenuation of ammonium. *Appl Geochem* 22: 2606-2617.

Mailloux, B.J., and Fuller, M.E. (2003) Determination of *in situ* bacterial growth rates in aquifers and aquifer sediments. *Appl Environ Microbiol* 69: 3798-3808.

Meckenstock, R.U., Morasch, B., Griebler, C., and Richnow, H.H. (2004) Stable isotope fractionation analysis as a tool to monitor biodegradation in contaminated acquifers. *J Contam Hydrol* 75: 215-255.

Parkes, R.J., Webster, G., Cragg, B.A., Weightman, A.J., Newberry, C.J., Ferdelman, T.G. et al. (2005) Deep sub-seafloor prokaryotes stimulated at interfaces over geological time. *Nature* 436: 390-394.

Prommer, H., Tuxen, N., and Bjerg, P.L. (2006) Fringe-controlled natural attenuation of phenoxy acids in a landfill plume: integration of field-scale processes by reactive transport modeling. *Environ Sci Technol* 40: 4732-4738.

Prosser, J.I., Bohannan, B.J., Curtis, T.P., Ellis, R.J., Firestone, M.K., Freckleton, R.P. et al. (2007) The role of ecological theory in microbial ecology. *Nat Rev Microbiol* 5: 384-392.

Rahman, M.A., Jose, S.C., Nowak, W., and Cirpka, O.A. (2005) Experiments on vertical transverse mixing in a large-scale heterogeneous model aquifer. *J Contam Hydrol* 80: 130-148.

Röling, W.F.M. (2007) Do microbial numbers count? Quantifying the regulation of biogeochemical fluxes by population size and cellular activity. *FEMS Microbiol Ecol* 62: 202-210.

Stookey, L.L. (1970) Ferrozine - a new spectrophotometric reagent for iron. *Anal Chem* 42: 779-781.

Thornton, S.F., Quigley, S., Spence, M.J., Banwart, S.A., Bottrell, S., and Lerner, D.N. (2001) Processes controlling the distribution and natural attenuation of dissolved phenolic compounds in a deep sandstone aquifer. *J Contam Hydrol* 53: 233-267.

Torsvik, V., Ovreas, L., and Thingstad, T.F. (2002) Prokaryotic diversity - magnitude, dynamics, and controlling factors. *Science* 296: 1064-1066.

van der Wielen, P.W., Bolhuis, H., Borin, S., Daffonchio, D., Corselli, C., Giuliano, L. et al. (2005) The enigma of prokaryotic life in deep hypersaline anoxic basins. *Science* 307: 121-123.

Werth, C.J., Cirpka, O.A., and Grathwohl, P. (2006) Enhanced mixing and reaction through flow focusing in heterogeneous porous media. *Water Res Research* 42: 1-10.

Winderl, C., Schaefer, S., and Lueders, T. (2007) Detection of anaerobic toluene and hydrocarbon degraders in contaminated aquifers using benzylsuccinate synthase (bssA) genes as a functional marker. *Environ Microbiol* 9: 1035-1046.

Winderl, C., Anneser, B., Griebler, C., Meckenstock, R.U., and Lueders, T. (2008) Depth-resolved quantification of anaerobic toluene degraders and aquifer microbial community patterns in distinct redox zones of a tar oil contaminant plume. *Appl Environ Microbiol* 74: 792-801.

Zwank, L., Berg, M., Schmidt, T.C., and Haderlein, S.B. (2003) Compound-specific carbon isotope analysis of volatile organic compounds in the low-microgram per liter range. *Anal Chem* 75: 5575-5583.

6. Summary and outlook

For decades, biodegradation processes in contaminated aquifers have been described to proceed successively in a distinct order, according to the energy yielded by the respective terminal electron accepting process (Wiedemeier et al., 1999; Lovley, 2001). Information of subsurface environments has been gathered mostly by means of sampling methods neglecting the real-time scale of mixing and bioactive hot spots, which are in the range of centimeters to decimeters rather than meters. Today, the conceptual idea of an ideally stratified contaminant plume has been displaced by the "plume fringe concept", which suggests biodegradation in porous aquifers to be mainly concentrated at the small transition zones between contaminated and uncontaminated groundwater. The fringes of contaminant plumes therefore form zones of high bioactivity, which are represented by steep gradients of electron donors, electron acceptors, and metabolites. As a driving factor for this phenomenon mixing of reactants, *i.e.* transversal and longitudinal dispersion, was clearly identified. Numerical modelling and bench-scale experiments have been performed to validate this hypothesis (e.g.Cirpka et al., 2006; Ham et al., 2007; Olsson and Grathwohl, 2007; Bauer et al., 2008) and to elucidate further potential factors besides mixing that control biodegradation. Although intensive research noticeably improved our knowledge and experience in this field, data describing biogeochemical interactions and their limitations *in situ* at a spatially and temporally appropriate scale are scarce.

This thesis aimed at investigating natural attenuation processes in a hydrocarbon contaminated porous aquifer and evaluating factors that may be responsible for limited biodegradation at this site with regard to the relevance of spatial and temporal scales. Particular attention was paid on the fringes and the core of the contaminant plume in order to test the transferability of the plume fringe concept to *in situ* conditions. Accordingly, a major objective was to screen for biogeochemical gradients at the transition between contaminated and uncontaminated zones in the aquifer, which are considered to indicate enhanced bioactivities.

Conventional monitoring wells, which generally are equipped with low-resolution filter screens, are biased by a multitude of disadvantages. The application of high pumping rates during sampling always bears the risk of hydraulic shortcuts and mixing of water of different depths. This leads to the destruction of gradients, which may have formed in groundwater during abiotic or biotic processes. The detection of such small-scale gradients may furthermore fail owing to the utilization of large filter screens or due to inadequate spatial resolution of multi-level or fully filtered monitoring wells.

To tackle these constraints, we constructed a special multi-level well that enabled us to withdraw groundwater at vertical intervals of 2.5, 10 and 33 cm, respectively. In June 2005, the well was installed at the former gasworks site in Düsseldorf-Flingern in the horizontal centerline of a petroleum hydrocarbon plume about 20 m downgradient of a tar oil source. Prior to the first field sampling campaign, technical procedures were optimized and analytical protocols tailored to meet the requirements for obtaining biogeochemical gradients in the appropriate scale of centimetres to decimeters.

The first groundwater sampling survey in September 2005 was followed by five further sampling campaigns at temporal intervals of 3-5 months. Additionally, closely spaced sediment liners were obtained from the study site in the course of three borehole drillings. A plethora of data yielded by analysis of both sediment and groundwater samples allowed a good correlation of individual gradients and permitted to track the interactions and interdependencies of biotic and abiotic processes. Thus, deductions from groundwater analysis could be validated, confirming, amongst other things, the dominance of sulfate and iron reduction at our site. Unlike groundwater analysis alone, investigation of the sediments moreover allowed to account for geochemical cycling and precipitation processes, such as re-

oxidation of reduced sulfur or iron species or deposition of iron sulfide minerals. The comparative approach described in this study therefore minimizes the risk of misinterpretation or underestimation of individual redox processes.

Closely spaced sampling of sediments furthermore unveiled variabilities between the investigated sediment cores, for example with respect to the distribution of contaminants. Even in putatively homogeneous sediments distinct zones can be revealed that harbour an increased load of contaminants or enhanced bioactivities. The risk of missing such "hot spots" by inappropriate sampling methods becomes obvious if looking at our gradients.

In 2D experimental setups and numerical simulations it was recently shown that sediment heterogeneities in porous aquifers may substantially increase mixing due to flow focussing and subsequent spreading of the plume (Werth et al., 2006; Bauer et al., submitted). Implementation of high-conductivity lenses in the flow field may therefore exhibit a positive effect on biodegradation rates. To evaluate the effects of sediment heterogeneities on the transport and fate of contaminants and on the biodegradation potential of the inherent microbial community, emphasis is laid on the need for further investigations on comparative high-resolution groundwater and sediment analysis.

The necessity for application of high-resolution monitoring techniques became furthermore obvious from the analysis of our gradients with respect to the localization and characterization of prevailing redox processes. Again, a multiple parameter approach comprising hydrological, geochemical and microbiological analyses proved to be crucial for obtaining reliable statements on the issue of "Who is degrading what, where, and under which conditions?". Steep gradients of electron donors, electron acceptors and metabolic end products in accordance with hydrochemical data (pH, E_h, specific conductivity) indicated sulfate and iron reduction to be the dominant redox processes at our study site. Qualitative evidence of toluene biodegradation coupled to sulfate reduction was obtained by compound-specific stable isotope analysis (CSIA). The accuracy of CSIA even at very low analytical concentrations and the unequivocal assignment of the results to individual microbiological redox processes render this method a promising approach to estimate rates and percentages of biodegradation reactions, which will be tackled in future investigations of the study site. As yet, first qualitative and semi-quantitative hints on the rates at which processes in groundwater environments occur were obtained by measurements on microbial activity and productivity. By far the highest activities and cell numbers were found at the upper plume fringe close to the water table. There, production of up to 10.5 ng carbon and enzymatic turnover of more than 30 nmol phosphate per liter and hour were measured. With increasing degree of contamination, however, microbial activities declined drastically. Thus, only 15 cm below, maximum carbon production rates dropped by a factor of 50; likewise, four times lower phosphatase activities were measured at this zone. A change to more agreeable conditions for microorganisms was indicated by a decent but verifiable increase in cell abundance and bioactivities at the lower plume fringe.

Above all, the high-resolution profiles were applied to evaluate the fringe concept and to assess possible factors influencing biodegradation processes. Steep gradients of individual geochemical parameters at the fringe of the BTEX plume pinpointed pronounced bioactivities to the interface between contaminated and pristine groundwater, which was at a comparable resolution so far only shown in tank experiments. Our data thus confirmed the validity of the plume fringe concept also under *in situ* conditions and emphasized the importance of transverse dispersion as a major factor controlling biodegradation.

Under purely mixing-controlled conditions, however, we would expect a rapid depletion of the reactants at those zones where electron donors and electron acceptors meet. Even though steep biogeochemical gradients indicated increased bioactivities and contaminant removal at these transition zones, neither contaminants nor electron acceptors (*i.e.* sulfate) were completely lacking at any time. Overlapping gradients of sulfate and contaminants

contradicted an instantaneous degradation and, instead, hinted at additional constraints limiting natural attenuation. A number of further factors are candidates that influence the biodegradation potential at our study site, including the toxicity of contaminants and metabolic (by-) products (e.g. sulfide), low cell abundance or unfavourable environmental conditions (e.g. pH, temperature, salinity). Possibly, metabolic turnover is restricted by threshold concentrations of reactants, *i.e.* the amount of electron donors or electron acceptors may be too low to initiate metabolic turnover. Last but not least, considerable constraints on the biodegradation potential may also come along with biokinetic limitations.

During the sampling period from September 2005 until May 2007, we observed exciting dynamics in the spatial and temporal distribution of the contaminants and the respective redox processes, which occurred at least partly independent from hydraulic fluctuations. By now, such dynamics, which may be expected for other subsurface environments as well, have been widely disregarded in natural attenuation assessment studies and numerical simulations, despite their presumably high relevance on actual biodegradation activities and capacities.

Apart from the biogeochemical dynamics occurring under relatively stable hydraulic conditions, we also recorded transient hydraulic conditions that lead to a significant decrease of the water table within a few weeks and a concomitant shift in the position of the BTEX plume. Simultaneously, we observed changes in the distribution of associated biotic and abiotic gradients, which were evaluated with respect to the adaptation potential of the inherent microbial communities. Increased mixing and chromatographic effects resulting from hydraulic changes are likely to exhibit positive effects on the inherent microbial community and to advance biodegradation processes (Schirmer et al., 2001; Prommer et al., 2002; Bauer et al., submitted). The influence of transient fluctuations on the diversity, abundance and activity of the microbial community, however, still has to be evaluated and will be subject of future investigations at the Flingern study site.

The high discretization of the biogeochemical gradients at our study site and temporally close sampling intervals provide data that constitute valuable input variables for modelling studies. High-resolution groundwater sampling therefore indirectly contributes to an improved accuracy and reliability of predictions on natural attenuation potential and plume development. Work is already under way, which heads to establish a reactive transport model to study and quantify biogeochemical and isotopic processes at the Flingern site in an integrated way. For that, isotope fractionation of electron donors and electron acceptors is directly linked to microbiological reactions using the reactive multicomponent transport model PHT3D (Prommer et al., 2003).

The results presented in this thesis markedly contributed to our knowledge on principle processes involved in the natural attenuation of organic contaminants and enlarged our understanding of the complexity of biotic and abiotic reactions taking place in the subsurface. The findings derived from the former gasworks site in Düsseldorf-Flingern, which can be regarded as a model field site, are ideal to be transferred to similar cases in porous aquifers and thus contribute to a sound evaluation and reasonable application of natural attenuation strategies.

Chapter 4 of this thesis has been published in a renowned scientific journal (Anneser et al. 2008, Appl. Geochem. 23: 1715-1730), chapter 2 has been accepted for publication in an IAH-SP series book titled "Advances in subsurface pollution of porous media: indicators, processes and modelling." (Anneser et al. 2008, Taylor & Francis / Balkema). Further chapters will be submitted in the near future to make the outcome of this work available to the scientific community and persons dealing with organically contaminated sites.

References

Anneser, B., Richters, L., and Griebler, C. (2008a) Application of high-resolution groundwater sampling in a tar oil–contaminated sandy aquifer. Studies on small-scale abiotic gradients. In *Adavances in subsurface pollution of porous media: indicators, processes and modelling*. Candela, L., Vadillo, I., and Elorza, F.J. (eds): Taylor & Francis / Balkema.

Anneser, B., Einsiedl, F., Meckenstock, R.U., Richters, L., Wisotzky, F., and Griebler, C. (2008b) High-resolution monitoring of biogeochemical gradients in a tar oil-contaminated aquifer. *Appl Geochem* 23: 1715-1730.

Bauer, R.D., Maloszewski, P., Zhang, Y., Meckenstock, R.U., and Griebler, C. (2008) Mixing-controlled biodegradation in a toluene plume - Results from two-dimensional laboratory experiments. *J Contam Hydrol* 96: 150-168.

Bauer, R.D., Rolle, M., Eberhardt, C., Grathwohl, P., Bauer, S., Kolditz, O. et al. (submitted) Enhanced biodegradation by hydraulic heterogeneities in petroleum hydrocarbon plumes. *J Contam Hydrol*.

Cirpka, O.A., Olsson, A., Ju, Q., Rahman, M.A., and Grathwohl, P. (2006) Determination of transverse dispersion coefficients from reactive plume lengths. *Ground Water* 44: 212-221.

Ham, P.A., Prommer, H., Olsson, A.H., Schotting, R.J., and Grathwohl, P. (2007) Predictive modelling of dispersion controlled reactive plumes at the laboratory-scale. *J Contam Hydrol* 93: 304-315.

Lovley, D.R. (2001) Anaerobes to the rescue. *Science* 293: 1444-1446.

Olsson, A., and Grathwohl, P. (2007) Transverse dispersion of non-reactive tracers in porous media: a new nonlinear relationship to predict dispersion coefficients. *J Contam Hydrol* 92: 149-161.

Prommer, H., Barry, D.A., and Davis, G.B. (2002) Modelling of physical and reactive processes during biodegradation of a hydrocarbon plume under transient groundwater flow conditions. *J Contam Hydrol* 59: 113-131.

Prommer, H., Barry, D.A., and Zheng, C. (2003) MODFLOW/MT3DMS-based reactive multicomponent transport modeling. *Ground Water* 41: 247-257.

Schirmer, M., Durrant, G.C., Molson, J.W., and Frind, E.O. (2001) Influence of transient flow on contaminant biodegradation. *Ground Water* 39: 276-282.

Werth, C.J., Cirpka, O.A., and Grathwohl, P. (2006) Enhanced mixing and reaction through flow focusing in heterogeneous porous media. *Water Res Research* 42: 1-10.

Wiedemeier, T.H., Rifai, H.S., Newell, C.J., and Wilson, J.T. (1999) *Natural Attenuation of Fuels and Chlorinated Solvents in the Subsurface*: John Wiley & Sons, New York.

Appendix

Table A.1 Mass loss of toluene over time during passage of different tube materials as shown in **Fig. 2.2 A**

Time [h]	Fluran HCA		Tygon		Tygon	
	Toluene loss [%]	S.D.	Toluene loss [%]	S.D.	Toluene loss [%]	S.D.
0.25	53.92	0.51	26.53	3.87	48.29	17.45
1.75	13.91	1.48	23.02	6.09	39.09	2.50
5	12.64	4.92	25.65	14.56	49.69	3.51

Table A.2 Mass loss of BTEX compounds over time during passage of Fluran HCA tubes as shown in **Fig. 2.2 B**

Time [h]	Benzene loss [%]	S.D.	Toluene loss [%]	S.D.	Ethylbenzene loss [%]	S.D.
0.50	26.00		41.00		37.00	30
14.50	6.25	7.76	11.00	5.83	12.60	9.45

II

Table A.3 Concentrations of aromatic hydrocarbons and hydrochemistry in groundwater samples from the HR-MLW as shown in **Fig. 2.3**; S.D. = standard deviation

Depth [m]	Total BTEX [mg l^{-1}]	S.D.	Total PAH [mg l^{-1}]	Naph-thalene [mg l^{-1}]	Acenaph-thene [mg l^{-1}]	Fluorene [mg l^{-1}]	DOC [mg l^{-1}]	pH	Redox potential [mV]	Specific conductivity [μS cm^{-1}]
6.41	52.05		19.18	18.98	0.19	0.01	24.44	7.30	-9	980
6.51	59.16		18.14	17.95	0.16	0.02	19.34	7.52	-34	974
6.61	50.11						17.58	7.57	-54	997
6.70	76.44		18.74	18.49	0.21	0.04		7.67	-70	984
6.75	31.71	1.04	17.83	17.34	0.32	0.16	14.93	7.74	-100	986
6.81	16.42	1.15					11.55	7.76	-174	1017
6.91	3.26	0.17	1.99	1.40	0.40	0.19	9.96	7.67	-154	1046
7.01	0.82	0.01					8.33	7.70	-18	1058
7.11	0.22	0.00	2.65	1.33	0.79	0.53	10.00	7.61	-86	1057
7.31	0.04	0.00	1.63	0.20	0.80	0.63	8.81	7.56	-100	1064
7.41	0.04	0.02	1.38	0.10	0.83	0.46	8.17	7.57	-32	1045
7.51	0.05	0.01	1.13	0.05	0.73	0.35	8.41	7.56	-31	1057
7.61	0.04	0.01	1.20	0.01	0.76	0.43	8.43	7.56	14	1060
7.75	0.04	0.01	1.36	0.00	0.74	0.63	7.55	7.58	19	1079
8.05	0.07	0.01	1.55	0.00	0.67	0.88	6.60	7.52	-16	1144
8.35	0.04	0.00	1.02	0.00	0.60	0.42	6.44	7.46	4	1136
8.65	0.03		1.27	0.00	0.70	0.57	6.23	7.46	-42	1122
8.75	0.01		1.27	0.00	0.64	0.63	5.87	7.42	-45	1099
9.05			1.50	0.00	0.69	0.82	6.22	7.39	-21	1078
9.35			0.50	0.00	0.32	0.18	6.10	7.39	-31	1082
9.65			0.04	0.00	0.00	0.04	6.15	7.47	59	1093
9.87			0.00	0.00	0.00	0.00		7.47	-59	1098
10.20			0.75	0.00	0.42	0.33	5.46	7.42	-65	1098
10.86			0.00	0.00	0.00	0.00	5.64	7.37	-46	1116
11.19			0.00	0.00	0.00	0.00	4.94	7.26	-43	1104
11.52			0.00	0.00	0.00	0.00	4.81	7.26	-50	1120
11.85							5.02	7.28	-55	1111
12.18			0.00	0.00	0.00	0.00	4.97	7.31	-42	1089
12.51			0.00	0.00	0.00	0.00	4.46	7.29	-50	1084

Table A.4 Concentrations of aromatic hydrocarbons and hydrochemistry in groundwater samples from the C-MLW as shown in **Fig. 2.3**; S.D. = standard deviation

Depth [m]	Total BTEX mg l^{-1}	Total PAH [mg l^{-1}]	Naphthalene [mg l^{-1}]	DOC [mg l^{-1}]	pH	Redox potential [mV]	Specific conductivity [μS cm^{-1}]
6.5	28.99	6.02	4.60	47	7.32	196	1085
7	5.37	2.23	0.49	22.1	7.35	191	1008
8	0.08	0.58	0.03	5.5	7.33	194	1169
9	0.03	1.47	0.04	5.5	7.33	236	1163
10	0.04	1.86	0.05	6.4	7.29	251	1172

Table A.5 Biogeochemical parameters determined from groundwater samples of the HR-MLW as shown in **Fig. 2.4**; S.D. = standard deviation

Depth [m]	Toluene [mg l^{-1}]	S.D.	Nitrate [mg l^{-1}]	Sulfate [mg l^{-1}]	Sulfide [mg l^{-1}]	S.D	Fe(II) [mg l^{-1}]	S.D.
6.41	26.61		0.14	0.51			3.58	0.24
6.51	41.31		0.19	6.41	0.00	0.00	2.33	0.28
6.61	35.35		0.18	86.22	0.66	0.08	1.71	1.37
6.70	57.11				0.36	0.08	1.10	0.21
6.75	19.96	0.94	0.20	119.53	2.89	0.30	2.05	0.19
6.81	8.16	0.58	0.21		6.62	0.00	2.47	1.02
6.91	0.31	0.00	0.22		6.05	0.80	2.16	0.39
7.01	0.05	0.00	0.24		2.35	0.21	1.61	0.13
7.11	0.04	0.00	0.28		3.58	0.08	1.72	0.21
7.31	0.02	0.00	0.38		4.65	1.26	1.50	0.16
7.41	0.02	0.00	0.38		2.06	0.63	1.47	0.10
7.51	0.02	0.00	0.32		0.42	0.00	0.68	0.31
7.61	0.02	0.00	0.28		0.51	0.13	0.65	0.02
7.75	0.01	0.00	0.17		0.33	0.21	0.88	0.61
8.05	0.01	0.00	0.13		1.31	0.34	2.38	0.78
8.35			0.16		0.39	0.04	0.61	0.14
8.65			0.16		1.46	0.63	1.06	0.48
8.75			0.14		0.60	0.10	0.96	0.50
9.05			0.17		0.39	0.46	0.53	0.01
9.35			0.24		0.95	0.17	0.61	0.13
9.65			0.22		0.36	0.08	1.37	1.06
9.87					1.58	0.55	0.90	0.03

Table A.6 Biogeochemical parameters determined from groundwater samples of the C-MLW as shown in **Fig. 2.4**

Depth [m]	Toluene [mg l^{-1}]	Nitrate [mg l^{-1}]	Sulfate [mg l^{-1}]	Sulfide [mg l^{-1}]
6.5	20.20	0.2	58.3	5.58
7	3.61	0.2	161	0.64
8	0.01	0.2	220	1.4
9	0.01	0.2	250	0.348
10	0.01	0.2	244	0.027

Table A.7   Toluene concentrations as measured at different depths in groundwater samples of the HR-MLW or, respectively, as calculated at intervals of 20, 50 or 100 cm (see **Fig. 2.5)**

	Toluene [mg l^{-1}]			
			calculated	
Depth [m]	measured	20 cm	50 cm	100 cm
6.41	26.61			
6.51	41.31	32.89	34.80	24.08
6.61	35.35			
6.70	57.11			
6.75	19.96			
6.81	8.16	23.25		
6.83	6.50			
6.88	1.00			
6.91	0.31			
6.93	0.10			
6.96	0.05			
6.98	0.05			
7.01	0.05	0.06	2.75	
7.03	0.02			
7.11	0.04			
7.31	0.02	0.03		
7.41	0.02			
7.51	0.02	0.02	0.02	0.02
7.61	0.02			
7.75	0.01	0.02		
8.05	0.01	0.01		
8.35	0.00	0.00		
8.65	0.00	0.00	0.00	
8.75	0.00	0.00		0.00

Table A.8 Concentrations of aromatic hydrocarbons in groundwater samples of the HR-MLW as shown in **Fig. 3.2A**; S.D. = standard deviation

Depth [m]	BTEX [mg l⁻¹]	S.D.	Naphthalene [mg l⁻¹]	S.D.	EPA-PAH [mg l⁻¹]	S.D.
6.39						
6.41	4.15	0.25				
6.44	14.80	0.77	0.44	0.27	0.52	0.29
6.46	27.84	1.46				
6.49	37.94	0.86	11.04	0.77	11.22	0.78
6.51	40.06	5.77				
6.54	45.89	0.28				
6.56	47.13	0.97	3.87	1.82	4.10	1.81
6.59	52.30	0.13				
6.61	55.51	2.31				
6.64	56.58	1.50	14.82	1.69	15.09	1.70
6.67	56.01	0.22				
6.70	57.93	0.65	12.92	2.50	13.18	2.51
6.75	56.99	1.08	16.19	1.68	16.54	1.73
6.81	53.31	0.36	13.53	0.46	13.94	0.44
6.91	46.81	0.63				
7.01			10.14	0.68	10.99	0.69
7.11	12.45	0.15				
7.21	5.83	0.01	3.74	0.25	5.26	0.32
7.31	2.36	0.13				
7.41	1.15	0.05	0.07	0.00	1.13	0.01
7.51	0.25	0.09				
7.61	0.08	0.01				
8.05	0.03	0.00	0.00	0.00	0.75	0.67

Table A.9 Concentrations of aromatic hydrocarbons in sediment samples of Liner 1 as shown in **Fig. 3.2B**; S.D. = standard deviation

Depth [m]	Naphthalene [mg l⁻¹]	S.D.	Acenaphthene [mg l⁻¹]	S.D.	Fluorene [mg l⁻¹]	S.D.	EPA-PAH [mg l⁻¹]	S.D.
6	0.00	0.00	0.00	0.00	0.00	0.00	0.00	0.00
6.4	0.00	0.00	0.00	0.00	0.00	0.00	0.00	0.00
6.65	33.49	19.33	0.71	1.01	1.79	0.08	35.99	20.42
6.9	8.75	1.30	1.26	0.18	10.57	7.52	20.57	9.00
7.1	13.79	10.76	5.87	4.16	6.40	0.63	26.06	14.28
7.6	5.57	0.27	3.85	0.38	3.41	4.82	12.83	5.46
8.1	14.69		2.44		5.01		22.14	
8.4	4.93		1.00		25.71		31.64	
8.8	33.47		2.46		6.21		42.15	
9.2	5.35		0.63		9.87		15.86	
9.7	3.79		0.35		2.56		6.70	
10.2	0.00		0.00		0.92		0.92	
11	0.00		0.00		1.36		1.36	
12	0.00		0.00		0.49		0.49	
13.3	0.00		0.00				0.00	

Table A.10 Concentrations of aromatic hydrocarbons in sediment samples of Liner 2 as shown in **Fig. 3.2C**; S.D. = standard deviation

Depth [m]	Naphthalene [mg l^{-1}]	S.D.	Acenaphthene [mg l^{-1}]	S.D.	Fluorene [mg l^{-1}]	S.D.	EPA-PAH [mg l^{-1}]	S.D.
5.9	0.00	0.00	0.00	0.00	0.00	0.00	0.00	0.00
6.5	0.00		0.00		0.00		0.00	
6.65	16.38	3.39	0.72	0.06	0.32	0.00	17.43	3.45
6.9	15.34	2.61	1.55	0.04	2.53	0.16	19.43	2.81
7.1	8.61	9.04	1.01	0.53	2.38	0.72	12.00	10.29
7.6	6.24	0.12	0.80	0.01	4.50	0.01	11.54	0.14
7.8	9.51	1.03	1.05	0.08	5.61	0.79	16.17	1.90
8.1	11.77	0.12	1.24	0.00	7.01	0.24	20.02	0.36
8.4	10.31	1.51	1.05	0.01	9.77	0.91	21.13	2.40
8.8	37.07	2.67	1.33	0.14	32.23	1.12	70.62	3.92
9.2	0.00	0.00	0.00	0.00	1.38	0.04	1.38	0.04
9.7	0.00	0.00	0.00	0.00	0.18	0.07	0.18	0.07
10.2	8.28	7.87	1.16	0.94	10.86	10.08	20.30	18.90
10.95	0.00		0.00		1.35		1.35	

Table A.11   Hydrological parameters determined from groundwater samples of the HR-MLW as shown in **Fig. 3.3**

Depth [m]	pH	Redox potential [mV]	Specific conductivity [μS cm^{-1}]
6.39	7.07	-20	1096
6.41		-100	1030
6.44			
6.46	7.13	-100	1053
6.49			
6.51			
6.54			
6.56	7.27	-150	1052
6.59			
6.61			
6.64			
6.67	7.40	-190	1081
6.70			
6.75	7.43	-195	1094
6.81	7.46	-235	1138
6.91			
7.01			
7.11	7.42	-230	
7.21			
7.31			
7.41	7.39	-197	1215
7.51			
7.61			
8.05	7.43	-229	1166

Table A.12 Biogeochemical parameters determined from groundwater samples of the HR-MLW as shown in **Fig. 3.4**; S.D. = standard deviation

Depth [m]	BTEX [mg l⁻¹]	S.D.	Sulfate [mg l⁻¹]	S.D.	Sulfide [mg l⁻¹]	S.D.	Fe (II) [mg l⁻¹]	S.D.	Phosphate [mg l⁻¹]	S.D.
6.39			69.16	0.04	0.18	0.00	1.62	0.01		
6.41	4.15	0.25	18.76	0.08	0.24	0.00	2.81	0.04	0.07	
6.44	14.80	0.77	2.35	0.01	0.48	0.00	1.60	0.06	0.58	0.03
6.46	27.84	1.46	1.82	0.02	0.27	0.04	1.62	0.01	0.54	0.02
6.49	37.94	0.86	2.23	0.04	0.51	0.04	1.00	0.00	1.35	0.00
6.51	40.06	5.77	3.35	0.04	0.60	0.08	1.56	0.04	0.81	0.05
6.54	45.89	0.28	5.39	0.03	0.66	0.25	2.04	0.02	0.96	0.08
6.56	47.13	0.97	10.74	0.05	1.58	0.04	0.96	0.02	2.05	0.18
6.59	52.30	0.13	9.94	0.03	2.06	0.13	1.02	0.05	1.16	0.06
6.61	55.51	2.31	11.15		2.15	0.08	0.20	0.02	1.04	
6.64	56.58	1.50	11.90	0.03	2.26	0.00	0.89	0.49	0.94	0.06
6.67	56.01	0.22	12.18	0.08	1.34	0.04	0.28	0.00	1.19	0.17
6.70	57.93	0.65	12.53	0.04	1.70	0.04	0.08	0.00	1.04	0.27
6.75	56.99	1.08	14.34	0.18	1.13	0.08	0.21	0.12	1.07	0.38
6.81	53.31	0.36	21.94	0.00	1.46	0.04	0.46	0.29	1.18	
6.91	46.81	0.63	34.41	0.09	4.35	0.08	0.27	0.03	0.60	0.04
7.01					0.48	0.00	0.22	0.23		
7.11	12.45	0.15	71.34	0.18	9.54	0.59	0.25	0.01	0.44	0.05
7.21	5.83	0.01	93.16	0.17	6.79	0.51	0.22	0.02	1.09	
7.31	2.36	0.13	121.54	0.00	2.71	0.21	0.61	0.19	0.15	
7.41	1.15	0.05	120.81	0.24	1.67	0.08	0.26	0.00	0.95	0.12
7.51	0.25	0.09	121.47	0.07	1.01	0.00	0.26	0.01	1.15	0.76
7.61	0.08	0.01	121.37	0.67	0.80	0.04	0.15	0.00	0.54	0.04
8.05	0.03	0.00	116.12	2.40	1.82	0.04	0.20	0.03	0.57	0.06

Table A.13   Ready extractable iron (0.5M HCl) and crystalline iron (5M HCl) content determined in sediment samples of Liner 1 as shown in Fig**. 3.5**; S.D. = standard deviation

Depth [m]	0.5 M HCl				5 M HCl			
	Fe(II) [g kg^{-1} wwt]	S.D.	Fe(III) [g kg^{-1} wwt]	S.D.	Fe(II) [g kg^{-1} wwt]	S.D.	Fe(III) [g kg^{-1} wwt]	S.D.
6.0	0.03	0.01	0.60	0.16	0.07	0.01	2.89	0.02
6.4	0.17	0.04	0.49	0.07	0.14	0.06	5.52	2.02
6.65	0.45	0.06	0.09	0.13	0.07	0.01	2.04	0.13
6.9	0.46	0.31	0.29	0.42	0.02	0.02	1.57	0.26
7.1	0.36	0.04	0.15	0.05	0.02	0.01	1.79	0.22
7.6	0.47	0.02	0.15	0.07	0.06	0.00	1.81	0.28
7.8	1.22	0.03	0.71	0.34	0.05	0.04	2.29	0.16
8.1	1.20	0.02	0.22	0.09	0.05	0.02	1.59	0.02
8.4	3.20	0.18	0.03	0.04	0.10	0.02	2.80	0.10
8.8	2.24	0.77	0.43	0.61	0.09	0.04	3.07	1.88
9.2	1.33	0.26	0.15	0.22	0.10	0.05	3.55	2.18
9.7	2.14	0.01	0.03	0.01	0.08	0.00	3.33	0.82
10.2	2.93	0.12	3.33	0.11	0.11	0.02	3.06	0.33
11.0	1.38	0.16	0.02	0.02	0.12	0.03	4.09	1.77
12.0	1.08	0.03	0.15	0.12	0.08	0.01	2.50	0.17
13.3	1.03	0.06	0.28	0.15	0.14	0.01	3.12	0.73

Table A.14   Ready extractable iron (0.5M HCl) and crystalline iron (5M HCl) content determined in sediment samples of Liner 2 as shown in **Fig. 3.5**; S.D. = standard deviation

Depth [m]	0.5 M HCl				5 M HCl			
	Fe(II) [g kg^{-1} wwt]	S.D.	Fe(II) [g kg^{-1} wwt]	S.D.	Fe(II) [g kg^{-1} wwt]	S.D.	Fe(II) [g kg^{-1} wwt]	S.D.
5.9	0.16	0.03	0.31	0.09	0.17	0.02	3.41	0.12
6.5	0.58	0.05	0.83	0.11	0.25	0.05	5.48	0.29
6.65	0.75	0.26	0.67	0.94	0.10	0.03	2.30	0.10
6.9	0.54	0.08	0.17	0.02	0.05	0.00	2.32	0.01
7.1	0.62	0.32	0.27	0.38	0.08	0.06	2.48	0.94
7.6	2.48	1.68	1.40	1.54	0.16	0.02	2.61	0.24
7.8	1.95	0.97	0.41	0.58	0.11	0.00	1.71	0.01
8.1	3.18	0.17	0.09	0.12	0.14	0.01	2.23	0.22
8.4	2.50	1.12	1.17	0.87	0.15	0.02	2.42	0.12
8.8	1.58	0.40	0.26	0.34	0.19	0.04	3.32	0.06
9.2	1.32	0.02	2.37	0.43	0.08	0.03	3.02	1.10
9.7	2.15	0.26	0.14	0.20	0.10	0.03	2.77	0.54
10.2	1.47	0.42	0.24	0.33	0.07	0.02	1.58	0.21
10.95	2.39	1.60	0.85	1.20	0.19	0.16	2.87	1.40

Table A.15   Total reduced inorganic sulfur (TRIS) and total organic matter (TOM) extracted from sediment samples of Liner 1 resp. Liner 2 as shown in **Fig. 3.6**; S.D. = standard deviation

	Liner 1				Liner 2	
Depth [m]	TRIS [g kg^{-1} wwt]	S.D.	TOM [% dwt]	S.D.	Depth [m]	TOM [% dwt]
6	0.03	0.00			5.9	3.44
6.4	0.03	0.00			6.5	5.22
6.65	0.04	0.02			6.65	4.39
6.9	0.05	0.00	0.21	0.02	6.9	0.36
7.1	0.21	0.05	0.29	0.04	7.1	37.86
7.6	0.06	0.01	0.18	0.05	7.6	9.31
7.8	0.08	0.01	0.36	0.03	7.8	0.54
8.1	0.07	0.00	0.30	0.03	8.1	9.77
8.4	0.08	0.09	0.52	0.00	8.4	4.88
8.8	0.03	0.01	0.36	0.00	8.8	1.88
9.2	0.12	0.02	0.35	0.03	9.2	36.47
9.7	0.09	0.01	0.39	0.05	9.7	19.45
10.2	0.02	0.00	0.56	0.10	10.2	13.51
11	0.04	0.01	0.34	0.06	10.95	48.80
12	0.49	0.11	0.29	0.02		
13.3	0.03	0.01	0.21	0.04		

Table A.16 Microbiological data determined in groundwater and sediments as shown in **Fig. 3.7**; S.D. = standard deviation

Groundwater					Liner 1							Liner 2				
Depth [m]	MUF-Glc [nmol l^{-1} h^{-1}]	S.D.	MUF-P [nmol l^{-1} h^{-1}]	S.D.	Depth [m]	MUF-Glc [μmol kg^{-1} h^{-1}]	S.D.	MUF-P [μmol kg^{-1} h^{-1}]	S.D.	Cell number [×10^7 kg^{-1} wwt]	S.D.	Depth [m]	MUF-Glc [μmol kg^{-1} h^{-1}]	S.D.	MUF-P [μmol kg^{-1} h^{-1}]	S.D.
6.39	2.68	0.05	31.84	1.99	6.0	20.41	5.99	1119.44	66.79			5.9	76.64	9.68	1704.78	
6.41	3.67	0.20	17.01		6.4	388.97		1162.05	105.30	1450	240	6.5	590.70	68.63	1906.00	
6.44					6.65	388.97		282.65	75.70	270	7	6.65	55.91	0.63	401.42	33.42
6.46	4.81	0.07	23.00	0.89	6.9	9.34	1.73	79.91	7.08			6.9	15.71		175.08	12.65
6.49					7.1	10.69	1.67	61.64	2.09	230	13	7.1	22.04	8.93	218.15	10.65
6.51	4.63	0.12	12.19	0.17	7.6	15.16	6.71	66.92	2.53	216	18	7.6	7.76	0.40	246.98	39.49
6.54					7.8	10.67	0.48	69.78	5.94	280	37	7.8	8.33	0.26	143.27	17.35
6.56	4.22	0.03	8.81	0.31	8.1	8.77	1.17	51.08	5.24	112	13	8.1	6.94	0.39	181.67	19.24
6.59					8.4	4.93	0.22	63.16	16.27	180	19	8.4	5.86	0.10	182.11	17.53
6.61	4.36	0.16	9.01	0.09	8.8	5.12	0.57	38.40	3.15	164	5	8.8	6.12	0.84	189.08	43.66
6.64					9.2	5.09	0.03	41.65	1.59			9.2	4.32	0.14	150.80	3.79
6.67	4.24	0.02	10.14	0.12	9.7	4.98	0.01	55.03	3.80			9.7	8.02	0.52	127.22	18.16
6.70	4.27	0.01	4.60	6.41	10.2	0.98	0.04	57.87	2.76	179	8	10.2	6.59	2.57	193.31	24.67
6.75	4.21	0.04	8.48	0.05	11	0.55	0.10	76.93	7.08			10.95	7.62	2.59	478.79	74.56
6.81	4.06	0.00	8.01	0.12	12	0.74	0.03	32.41	45.83							
6.91	5.01	0.09	6.77	0.09	13.3	2.69	2.80	96.61	4.08							
7.01			7.03													
7.11	5.74	0.34	6.81	0.56												
7.21	5.67	0.06	6.19	0.09												
7.31	3.66	0.03	7.42	0.99												
7.41	3.12	0.18	6.43													

Table A.17   Concentrations of aromatic hydrocarbons (in mg l^{-1}) determined in groundwater samples of the HR-MLW as shown in **Fig. 4.3**

Depth [m]	Benzene	S.D.	Toluene	S.D.	Ethyl-benzene	S.D.	m-/p-Xylene	S.D.	o-Xylene	S.D.	BTEX	S.D.	Naph-thalene	S.D.	Acenaph-thene	S.D.	Fluorene	S.D.
6.31	0.03	0.00	4.20	0.45	2.33	2.65	1.24	0.04	1.02	0.13	6.96	0.65	4.58		0.05			
6.39	0.09	0.00	20.08	0.11	10.09	14.12	4.11	0.05	2.33	0.15	28.19	0.44	13.61		0.24			
6.41	0.10	0.01	30.07	0.81	15.44	20.69	4.77	0.19	2.85	0.05	39.38	0.94	13.16		0.23			
6.44	0.08	0.01	33.58	0.40	16.99	23.46	4.70	0.17	2.50	0.31	42.13	0.16						
6.46	0.07	0.00	35.47	0.02	17.74	25.07	4.57	0.05	2.41	0.09	43.49	0.17	13.19		0.24			
6.54	0.06	0.00	37.59	0.83	19.21	26.00	4.82	0.11	2.56	0.16	45.96	1.13	15.42	5.33	0.18	0.02	0.02	
6.56	0.06	0.00	38.46	1.17	19.81	26.37	5.34	0.19	2.55	0.02	47.36	1.37	15.44	3.70	0.19		0.03	
6.59	0.05	0.00	37.10	2.83	19.97	24.23	5.54	0.50	2.76	0.68	46.47	4.27	15.93	4.20	0.12	0.17	0.04	
6.61	0.04	0.00	34.14	1.33	17.74	23.20	5.90	0.01	2.94	0.24	44.11	1.66	15.52	5.01	0.22	0.01	0.03	0.01
6.64	0.03	0.00	26.58	2.08	14.33	17.32	5.55	0.48	2.87	0.48	36.11	3.23	15.69	4.25	0.24	0.04	0.04	0.01
6.67	0.02	0.00	21.39	0.30	10.84	14.91	5.81	0.12	3.18	0.18	31.60	0.67	16.29	3.67	0.26	0.06	0.05	
6.75	0.01	0.01	5.60	0.39	3.00	3.69	4.57	0.26	2.73	0.06	13.96	0.76	13.99	3.30	0.31	0.05	0.16	0.02
6.81	0.00	0.00	1.84	0.05	0.94	1.26	3.08	0.15	1.89	0.17	7.58	0.42	13.19	2.46	0.39	0.06	0.31	0.02
6.91	0.00	0.00	0.29	0.05	0.17	0.17	1.14	0.00	0.82	0.02	2.54	0.08	7.01	0.15	0.47	0.06	0.44	0.05
7.01	0.00	0.00	0.07	0.01	0.04	0.04	0.43	0.01	0.35	0.00	0.90	0.01	3.32	0.82	0.64	0.14	0.57	0.03
7.08	0.00	0.00	0.04	0.01	0.02	0.02	0.19	0.04	0.15	0.04	0.40	0.07	1.27	0.32	0.74	0.11	0.62	0.06
7.11	0.00	0.00	0.03	0.01	0.02	0.02	0.09	0.00	0.07	0.00	0.20	0.00	0.73	0.18	0.81	0.12	0.69	0.04
7.21	0.00	0.00	0.02	0.01	0.01	0.01	0.03	0.00	0.02	0.00	0.07	0.00	0.17	0.03	0.85	0.11	0.67	0.10
7.31	0.00	0.00	0.02	0.00	0.01	0.01	0.01	0.00	0.00	0.00	0.03	0.00	0.06		0.90	0.16	0.58	0.03
7.41	0.00	0.00	0.03	0.02	0.02	0.00	0.01	0.00	0.00	0.00	0.04	0.02			0.75	0.14	0.43	0.03
7.51	0.00	0.00	0.02	0.01	0.02	0.01	0.01	0.00	0.00	0.01	0.04	0.01			0.80	0.10	0.35	0.04
7.61	0.00	0.01	0.02	0.01	0.01	0.01	0.01	0.00	0.00	0.00	0.03	0.00			0.82	0.09	0.41	0.06
7.75	0.00	0.00	0.01	0.01							0.01	0.01			0.86	0.19	0.48	0.01
8.35	0.02	0.00	0.01	0.01											0.50	0.06	0.29	0.04
8.65	0.02	0.00	0.00	0.01											0.68	0.00	0.38	0.04
8.75	0.01	0.00	0.01	0.01											0.79	0.00	0.56	0.01
9.05															0.59	0.00	0.52	0.02
9.35															0.47	0.01	0.47	0.03
9.65															0.50	0.00	0.64	0.00
9.87															0.66	0.02	0.50	0.01

Table A.18   Isotope ratios of dissolved sulfate and groundwater as shown in **Fig. 3.8**; S.D. = standard deviation

Depth [m]	Sulfate				Groundwater	
	$\delta^{34}S$	S.D.	$\delta^{18}O$	S.D.	δ^2H	$\delta^{18}O$
6.39	5.47	0.04	2.10	0.18	-55.1	-7.63
6.41						
6.44					-55.0	-7.62
6.46						
6.49					-55.0	-7.59
6.51						
6.54						
6.56					-55.2	-7.62
6.59						
6.61						
6.64					-54.8	-7.62
6.67						
6.70					-55.0	-7.65
6.75					-55.6	-7.70
6.81	42.37	0.17	15.21	0.04	-55.9	-7.73
6.91						
7.01					-56.3	-7.79
7.11	25.01	0.20	12.63	0.13		
7.21					-56.7	-7.79
7.31						
7.41					-56.3	-7.81
7.51						
7.61						
8.05	15.88	0.02	11.07	0.11	-56.3	-7.77
9.05	12.48	0.02	10.67	0.05		

Table A.19   Ratios of Fe(II) and sulfide in groundwater and sediments as shown in **Fig. 3.9**

Groundwater			Sediment		
Depth [m]	S/Fe	Fe/S	Depth [m]	Fe/S	S/Fe
6.39	0.11	9.06	6	1.04	0.96
6.41	0.08	11.77	6.4	5.32	0.19
6.44	0.30	3.36	6.65	11.50	0.09
6.46	0.17	6.03	6.9	9.86	0.10
6.49	0.51	1.98	7.1	1.69	0.59
6.51	0.38	2.62	7.6	8.24	0.12
6.54	0.32	3.11	7.8	14.69	0.07
6.56	1.64	0.61	8.1	17.80	0.06
6.59	2.01	0.50	8.4	39.86	0.03
6.61	10.67	0.09	8.8	65.11	0.02
6.64	2.55	0.39	9.2	11.40	0.09
6.67	4.78	0.21	9.7	24.55	0.04
6.70	22.53	0.04	10.2	139.95	0.01
6.75	5.47	0.18	11	37.90	0.03
6.81	3.19	0.31	12	2.20	0.45
6.91	16.19	0.06	13.3	36.71	0.03
7.01	2.13	0.47			
7.11	38.24	0.03			
7.21	31.10	0.03			
7.31	4.48	0.22			
7.41	6.35	0.16			
7.51	3.97	0.25			
7.61	5.48	0.18			
8.05	8.87	0.11			

Table A.20 Concentrations of aromatic hydrocarbons (in mg l^{-1}) determined in groundwater samples of the C-MLW as shown in **Fig. 4.3**

Depth [m]	Toluene	BTEX	Ethyl-benzene	m-/p-Xylene	Naph-thalene	Acenaph-thene
6.5	4.50	11.24	0.44	5.00	0.54	0.51
7	0.11	0.29	0.02	0.11	0.33	0.31
8	0.02	0.08	0.00	0.03	0.05	0.41
9	0.02	0.08	0.01	0.03	0.02	0.31
10	0.03	0.07	0.00	0.03	0.03	0.31

Table A.21 Physical and hydrochemical parameters determined in groundwater samples of the HR-MLW as shown in **Fig. 4.4**; S.D. = standard deviation

Depth [m]	Redox potential [mV]	pH	Specific conductivity [µS cm⁻¹]	Nitrate [mg l⁻¹]	S.D.	DOC [mg l⁻¹]	DIC [mg l⁻¹]	TDC [mg l⁻¹]
6.31	30	7.13	1080	0.19	0.00	13.04	49.19	62.23
6.39	-4	7.35	1037	0.01	0.00	29.14	120.69	149.63
6.41	-55	7.49	1033	0.02	0.00	26.94	95.49	122.63
6.44	-182	7.58	1037	0.08	0.02	23.44	114.69	138.63
6.46	-239	7.62	1053	0.14	0.00	36.24	120.69	156.63
6.54	-244	7.70	1067	0.13	0.02	25.24	114.69	139.63
6.56	-272	7.74	1076	0.14	0.00	35.94	118.69	154.63
6.59	-282	7.72	1082	0.12	0.01	31.44	114.69	154.63
6.61	-290	7.73	1088	0.12	0.00	17.14	108.69	125.63
6.64	-299	7.74	1101	0.64	0.01	34.74	114.69	149.63
6.67	-333	7.74	1118	0.65	0.01	27.34	111.69	139.63
6.75	-300	7.74	1147	0.79	0.01	19.64	103.69	123.63
6.81	-299	7.73	1167	1.78	0.06	12.45	95.66	108.01
6.91	-281	7.63	1176	1.95	0.02	8.35	92.76	101.01
7.01	-230	7.60	1171	0.39	0.00	5.84	67.46	73.31
7.08	-278	7.51	1171	1.05	0.03	5.18	93.56	99.01
7.11	-238	7.48	1158	0.29	0.01	4.44	93.66	98.01
7.21	-258	7.41	1154	0.54	0.00	3.99	92.56	97.01
7.31	-222	7.42	1154	0.85	0.01	4.11	86.96	91.21
7.41	-216	7.42	1151	0.76	0.01	4.21	90.06	94.21
7.51	-191	7.42	1156	0.91	0.02	4	84.33	88.39
7.61	-199	7.42	1166	0.29	0.01	3.46	83.73	87.09
7.75	-202	7.47	1182	0.10	0.00	3.51	83.53	86.99
8.35	-165	7.37	1168	0.93	0.03	3.6	80.43	83.99
8.65	-198	7.40	1137	0.27	0.03	3.03	86.33	89.29
8.75	-191	7.42	1152	0.14	0.05	2.88	88.63	91.49
9.05	-165	7.37	1156	1.74	0.05	3.45	85.93	89.39
9.35	-156	7.47	1163	0.61	0.00	2.91	84.13	86.99
9.65	-148	7.65	1178	0.55	0.01	2.98	78.83	81.79
9.87	-131	7.52	1164	0.11	0.01	3.13	81.43	84.59

Table A.22 Physical and hydrochemical parameters determined in groundwater samples of the C-MLW as shown in **Fig. 4.4**

Depth [m]	Redox potential [mV]	pH	Specific conductivity [µS cm⁻¹]	Nitrate [mg l⁻¹]	DOC [mg l⁻¹]
6.5	4	7.61	1171	0.52	18.1
7	32	7.37	1189	0.31	16.4
8	110	7.31	1196	0.55	6.1
9	139	7.35	1192	0.11	6
10	155	7.25	1196	0.11	6.4

Table A.23 Biogeochemical parameters (in mg l^{-1}) determined in groundwater samples of the HR-MLW used in **Fig. 4.5** and **Fig. 4.9**; S.D. = standard deviation

Depth [m]	BTEX	S.D.	Sulfate	S.D.	Sulfide	S.D.	Fe (II)	S.D.
6.31	6.96	0.65	41.43	0.11	0.00	0.00	0.48	0.08
6.39	28.19	0.44	3.62	0.02	0.00	0.00	0.31	0.11
6.41	39.38	0.94	1.39	0.01	0.03	0.04	1.70	0.17
6.44	42.13	0.16	1.72	0.08	0.48	0.00	0.08	0.00
6.46	43.49	0.17	3.85	0.09	1.58	0.13	0.14	0.03
6.54	45.96	1.13	8.04	0.12	0.12	0.08	0.17	0.08
6.56	47.36	1.37	14.72	0.13	4.41	0.84	0.25	0.03
6.59	46.47	4.27	19.13	0.05	6.59	0.63	0.35	0.05
6.61	44.11	1.66	26.55	0.02	6.88	0.04	0.14	0.03
6.64	36.11	3.23	36.21	0.01	8.14	0.38	0.17	0.08
6.67	31.60	0.67	48.40	0.34	7.90	0.21	0.44	0.14
6.75	13.96	0.76	101.79	1.37	7.45	0.42	1.31	0.13
6.81	7.58	0.42	146.05		5.93	0.30	0.31	0.03
6.91	2.54	0.08			2.44	0.08	0.31	0.03
7.01	0.90	0.01	169.96		0.12	0.00	0.46	0.05
7.08	0.40	0.07	166.67	1.28	1.40	0.13	0.43	0.00
7.11	0.20	0.00	167.01	1.23	0.03	0.04	0.85	0.085
7.21	0.07	0.00	167.11	0.16	1.31	0.34	0.29	0.08
7.31	0.03	0.00	180.16	1.46	0.39	0.04	0.25	0.03
7.41	0.04	0.02	185.18	1.59	0.12	0.08	0.39	0.05
7.51	0.04	0.01	190.81	2.37	0.09	0.04	0.21	0.03
7.61	0.03	0.00	207.08	1.20	0.24	0.17	0.00	0.00
7.75	0.01	0.01	220.89	2.73	0.42	0.17	0.08	0.00
8.35			206.61	7.94	0.00	0.00	0.00	0.00
8.65			162.90	3.71	0.09	0.13	0.00	0.00
8.75			182.78	4.03	0.00	0.00	0.00	0.00
9.05			201.96	4.52	0.00	0.00	0.00	0.00
9.35			198.08	4.67	0.00	0.00	0.03	0.00
9.65			178.48	4.47	0.00	0.00	0.04	0.00
9.87			201.70	0.64	0.00	0.00	0.29	0.08

Table A.24 Biogeochemical parameters determined in groundwater samples of the C-MLW as shown in **Fig. 4.5**

Depth [m]	BTEX [mg l^{-1}]	Sulfate [mg l^{-1}]	Sulfide [mg l^{-1}]
6.5	11.24	108	3.88
7	0.29	168	2.24
8	0.08	197	0.96
9	0.08	192	0.133
10	0.07	217	0.024

Table A.25 Concentrations of ready available iron (0.5M HCl) and crystalline iron (5M HCl) as well as pyrite sulfur content (all concentrations in mg l^{-1}) extracted from sediment samples as shown in **Fig. 4.6**; S.D. = standard deviation

	0.5 M HCl				5 M HCl				
Depth [m]	Fe(II)	S.D.	Fe(II)	S.D.	Fe(II)	S.D.	Fe(II)	S.D.	Pyrite-S
0.15	0.01	0.01			0.29	0.25	3.40	2.23	
0.9	0.20	0.02			0.80	0.01	2.91	0.11	
1.7	0.15	0.01			0.06	0.04	3.14	1.38	
2.2	0.07	0.02			0.08	0.00	4.22	0.70	
2.5	0.16	0.02			0.27	0.05	5.48	0.57	
3.2	0.17	0.02			0.11	0.05	4.50	1.15	
3.9	0.19	0.00			0.09	0.02	5.33	0.17	
4.65	0.30	0.04	0.73	0.12	0.15	0.08	7.83	3.56	0
5.6	0.15	0.00	0.67	0.17	0.05	0.00	3.24	0.26	0
6.3	0.45	0.20	0.38	0.11	0.13	0.05	6.56	1.61	0
6.6	1.12	0.47	0.03		0.01	0.00	2.17	0.67	0.2
6.8	0.58	0.04	0.00		0.02	0.01	1.72	0.01	0.2
7.2	0.90	0.10	0.00		0.01	0.01	2.70	0.26	0.2
7.35	2.03	1.02	0.10		0.01	0.01	2.99	1.12	0.3
7.6	3.30	0.63	0.00		0.05	0.00	2.99	0.27	0
8.1	3.87	0.56	0.00		0.07	0.00	2.60	1.01	0
8.4	3.18	1.41	0.00		0.04	0.02	3.20	0.98	0
8.7	3.51	0.26	0.00		0.08	0.01	3.24	0.34	0.2
9.1	2.76	0.07	0.00		0.11	0.04	4.17	0.88	0.2
9.5	2.55	0.73	0.08		0.09	0.03	3.48	0.37	0.3
9.8	2.24	0.25	0.00		0.07	0.00	2.09	0.09	0.2
10.2	1.64	0.09	0.08	0.00	0.06	0.00	1.85	0.04	0.2
10.6	1.20	0.10	0.00		0.07	0.00	2.00	0.03	0.2
11.2	2.12	0.28	0.00		0.10	0.01	2.20	0.45	0.2
11.7	1.96	0.37	0.00		0.29	0.23	3.66	0.23	0
12.3	1.28	0.05	0.00		0.12	0.01	2.66	0.43	
12.7	1.32	0.07	0.07		0.16	0.02	4.76	0.71	

Table A.26   Concentrations and stable isotope ratios of $^{34}S/^{32}S$ and $^{18}O/^{16}O$ of groundwater sulfate used in **Fig. 4.7A** and **Fig. 4.8**; S.D. = standard deviation

| Depth [m] | Sulfate [mg l^{-1}] | S.D. | Sulfate isotopes | | | | |
			$\delta^{34}S$ [‰]	S.D.	$\delta^{18}O$ [‰]	S.D.
6.31	41.43	0.11	14.93	0.16	4.69	0.57
6.39	3.62	0.02				
6.41	1.39	0.01				
6.44	1.72	0.08				
6.46	3.85	0.09				
6.54	8.04	0.12			18.44	0.62
6.56	14.72	0.13				
6.59	19.13	0.05				
6.61	26.55	0.02	43.40	0.13	15.40	0.02
6.64	36.21	0.01				
6.67	48.40	0.34				
6.75	101.79	1.37	25.23	0.05	13.78	0.32
6.81	146.05		20.79	0.02	12.43	0.33
6.91						
7.01	169.96		20.61	0.09	13.38	0.56
7.08	166.67	1.28				
7.11	167.01	1.23	20.27	0.10	13.63	0.57
7.21	167.11	0.16	19.79	0.07	13.28	0.23
7.31	180.16	1.46				
7.41	185.18	1.59	15.53	0.12	12.01	0.00
7.51	190.81	2.37	14.28	0.04	11.27	0.07
7.61	207.08	1.20				
7.75	220.89	2.73				
8.35	206.61	7.94	10.79	0.02	10.72	0.25
8.65	162.90	3.71				
8.75	182.78	4.03				
9.05	201.96	4.52	9.80	0.01	10.58	0.13
9.35	198.08	4.67				
9.65	178.48	4.47				
9.87	201.70	0.64	10.64	0.03	11.49	0.25

Table A.27   Concentrations of BTEX and cell numbers determined in groundwater samples of the HR-MLW as shown in **Fig. 4.7B**; S.D. = standard deviation

Depth [m]	BTEX [mg l^{-1}]	S.D.	Cell number [per ml $\times 10^5$]
6.31	6.96	0.65	26.71
6.39	28.19	0.44	8.02
6.41	39.38	0.94	2.28
6.44	42.13	0.16	3.02
6.46	43.49	0.17	5.32
6.54	45.96	1.13	8.73
6.56	47.36	1.37	5.05
6.59	46.47	4.27	3.88
6.61	44.11	1.66	5.34
6.64	36.11	3.23	0.97
6.67	31.60	0.67	3.56
6.75	13.96	0.76	4.20
6.81	7.58	0.42	10.90
6.91	2.54	0.08	14.72
7.01	0.90	0.01	11.42
7.08	0.40	0.07	9.84
7.11	0.20	0.00	13.04
7.21	0.07	0.00	14.57
7.31	0.03	0.00	6.64
7.41	0.04	0.02	11.39
7.51	0.04	0.01	7.22
7.61	0.03	0.00	6.75
7.75	0.01	0.01	6.77
8.35			7.34
8.65			11.73
8.75			16.82
9.05			15.24
9.35			16.58
9.65			7.18

Table A.28 Physical-chemical parameters determined in groundwater samples of the HR-MLW as shown in **Fig. 5.1**; S.D. = standard deviation

Depth [m]	pH	Redox [mV]	BTEX [mg l^{-1}]	Naphthalene [mg l^{-1}]	Acenaphthene [mg l^{-1}]	Fluorene [mg l^{-1}]	Sulfate [mg l^{-1}]	Sulfide [mg l^{-1}]	Fe (II) [mg l^{-1}]
6.56	6.91	291	1.00	1.53	0.00	0.00	425.38	0	0.33
6.59	7.02	-45	4.45	6.55	0.11	0.00	184.26	2.09	0.23
6.61	7.07	-81	14.74	15.13	0.22	0.01	49.80	4.53	0.25
6.64	7.14	-66	30.06	18.16	0.23	0.02	45.24	2.71	0.31
6.67	7.22	-66	44.69	19.67	0.24	0.03	51.12	3.73	0.14
6.70	7.32	-63	56.60	20.57	0.24	0.04	57.32	2.41	0.19
6.75	7.35	-42	65.99	20.15	0.23	0.08	51.30	1.49	0.15
6.78	7.5	-24	62.82	19.34	0.23	0.11	51.77	0.72	0.15
6.81	7.56	-34	64.51	19.79	0.26	0.15	54.74	0.48	0.15
6.83	7.56	-33	66.18	19.82	0.27	0.20	57.22	0.69	0.08
6.88	7.62	-29	67.04	19.52	0.28	0.21	59.72	0.36	0.29
6.91	7.63	-25	58.12	18.33	0.29	0.21	64.68	0.69	0.19
6.93	7.66	-37	61.73	17.70	0.32	0.23	71.76	0.75	0.31
7.01	7.64	-57	42.40	16.38	0.40	0.32	80.73	0.36	0.23
7.11	7.58	-87	15.79	12.80	0.63	0.54	90.83	1.61	0.19
7.21	7.52	-70	4.78	5.03	0.83		121.39	1.79	0.21
7.28	7.47	-43	2.76	2.50	1.00	0.78	127.90	0.95	0.41
7.31	7.44	-42	1.73	1.94	1.09	0.80	125.16	1.10	0.25
7.33	7.49	-34	1.15	1.61	1.07	0.66	120.28	0.98	0.33
7.41	7.47	-33	0.82	1.19	1.06	0.47	118.45	0.63	0.37
7.46	7.45	-8	0.96	0.78	0.97	0.46	120.17	0.48	0.31
7.51	7.49	-4	0.74	0.56	1.04	0.45	128.36	0.45	0.46
7.56	7.45	39	0.23	0.35	0.99	0.43	129.08	-0.03	0.27
7.61	7.5	2		0.22	1.06	0.48	130.48	0.45	0.27
7.75	7.5	25		0.03	0.56	0.30	154.21	0.06	0.35
8.05	7.46	-25		0.00	0.65	0.34	166.07	0.92	0.12
8.35	7.42	23		0.00	0.65	0.27	184.57	0.09	0.19
8.65	7.42	10		0.00	0.69	0.36	143.67	0.27	0.14
8.75	7.44	20		0.00	0.81	0.50	108.38	0.12	0.29

Table A.29   Vertical distribution of BTEX, sulfate and sulfide (all given in mg l^{-1}) in groundwater sampled from the HR-MLW at different dates as shown in **Fig. 5.2**

\	September 2005			\	February 2006			\	May 2006		
Depth [m]	BTEX	Sulfate	Sulfide	Depth [m]	BTEX	Sulfate	Sulfide	Depth [m]	BTEX	Sulfate	Sulfide
6.41	52.05	0.51		6.39		69.16	0.18	6.39	21.48	5.70	0.00
6.51	59.16	6.41	0.00	6.41	4.15	18.76	0.24	6.41	35.33	4.24	0.36
6.61	50.11	86.22	0.66	6.44	14.80	2.35	0.48	6.44	50.75	8.80	1.49
6.70	76.44		0.36	6.46	27.84	1.82	0.27	6.46	58.08	19.77	1.19
6.75	31.71	119.53	2.89	6.49	37.94	2.23	0.51	6.51	58.71	18.64	1.91
6.81	16.42		6.62	6.51	40.06	3.35	0.60	6.54	66.12	15.26	1.97
6.91	3.26		6.05	6.54	45.89	5.39	0.66	6.56	69.38	33.08	4.41
7.01	0.82		2.35	6.56	47.13	10.74	1.58	6.59	68.69	35.49	4.59
7.11	0.22		3.58	6.59	52.30	9.94	2.06	6.61	68.33	38.33	6.02
7.31	0.04		4.65	6.61	55.51	11.15	2.15	6.64	68.56	41.23	5.54
7.41	0.04		2.06	6.64	56.58	11.90	2.26	6.67	63.77	44.27	5.78
7.51	0.05		0.42	6.67	56.01	12.18	1.34	6.70	63.04	48.75	7.15
7.61	0.04		0.51	6.70	57.93	12.53	1.70	6.75	58.07	53.59	6.11
7.75	0.04		0.33	6.75	56.99	14.34	1.13	6.81	50.80	54.61	7.09
8.05	0.07		1.31	6.81	53.31	21.94	1.46	6.91	42.17	60.99	7.66
8.35	0.04		0.39	6.91	46.81	34.41	4.35	7.01	23.55		9.36
8.65	0.03		1.46	7.01			0.48	7.11	10.88	109.13	13.44
8.75	0.01		0.60	7.11	12.45	71.34	9.54	7.21	3.45	174.75	5.22
				7.21	5.83	93.16	6.79	7.31	1.06	192.47	2.92
				7.31	2.36	121.54	2.71	7.41	0.53	190.25	2.06
				7.41	1.15	120.81	1.67	7.51	0.33	191.90	0.95
				7.51	0.25	121.47	1.01	7.61	0.13	194.15	0.92
				7.61	0.08	121.37	0.80	7.75	0.02	187.80	1.16
				8.05	0.03	116.12	1.82	8.05		181.14	3.16
								8.35		177.19	0.12
								8.65			0.86
								8.75			0.83

Continuation of **Table A.29**

August 2006				February 2007				May 2007			
Depth [m]	BTEX	Sulfate	Sulfide	Depth [m]	BTEX	Sulfate	Sulfide	Depth [m]	BTEX	Sulfate	Sulfide
6.31	6.96	41.43	0.00	6.56	1.00	425.38	0.00	6.51	1.27	151.04	0.00
6.39	28.19	3.62	0.00	6.59	4.45	184.26	2.09	6.54	8.38	38.17	0.06
6.41	39.38	1.39	0.03	6.61	14.74	49.80	4.53	6.59	22.44	7.74	2.89
6.44	42.13	1.72	0.48	6.64	30.06	45.24	2.71	6.61	45.80	2.28	3.25
6.46	43.49	3.85	1.58	6.67	44.69	51.12	3.73	6.64	67.22	10.42	2.18
6.54	45.96	8.04	0.12	6.70	56.60	57.32	2.41	6.67	95.91	26.39	2.62
6.56	47.36	14.72	4.41	6.75	65.99	51.30	1.49	6.70	58.14	27.56	1.52
6.59	46.47	19.13	6.59	6.78	62.82	51.77	0.72	6.75	55.61	34.36	1.82
6.61	44.11	26.55	6.88	6.81	64.51	54.74	0.48	6.78	48.29	37.47	2.50
6.64	36.11	36.21	8.14	6.83	66.18	57.22	0.69	6.81	43.62	37.30	3.61
6.67	31.60	48.40	7.90	6.88	67.04	59.72	0.36	6.83	53.50	36.52	4.02
6.75	13.96	101.79	7.45	6.91	58.12	64.68	0.69	6.86	50.91	35.05	2.62
6.81	7.58	146.05	5.93	6.93	61.73	71.76	0.75	6.88	30.89	35.36	3.75
6.91	2.54		2.44	7.01	42.40	80.73	0.36	6.91	24.97	37.16	2.29
7.01	0.90	169.96	0.12	7.11	15.79	90.83	1.61	6.93	31.75	42.27	3.13
7.08	0.40	166.67	1.40	7.21	4.78	121.39	1.79	7.01	10.97	51.21	0.18
7.11	0.20	167.01	0.03	7.28	2.76	127.90	0.95	7.11	5.01	78.06	1.40
7.21	0.07	167.11	1.31	7.31	1.73	125.16	1.10	7.21	1.23	139.31	2.50
7.31	0.03	180.16	0.39	7.33	1.15	120.28	0.98	7.31	0.35	149.89	1.55
7.41	0.04	185.18	0.12	7.41	0.82	118.45	0.63	7.41	0.01	139.38	1.01
7.51	0.04	190.81	0.09	7.46	0.96	120.17	0.48	7.51	0.00	166.19	0.45
7.61	0.03	207.08	0.24	7.51	0.74	128.36	0.45	7.61	0.01	168.86	0.54
7.75	0.01	220.89	0.42	7.56	0.23	129.08	0.00	7.75	0.00	160.99	0.00
8.35		206.61	0.00	7.61		130.48	0.45	8.05	0.02	125.01	0.86
8.65		162.90	0.09	7.75		154.21	0.06	8.35	0.02	145.65	0.21
8.75		182.78	0.00	8.05		166.07	0.92	8.65	0.02	154.78	0.33
				8.35		184.57	0.09	8.75	0.01	159.20	0.09
				8.65		143.67	0.27				
				8.75		108.38	0.12				

Table A.30   Concentrations of sulphate and toluene and respective stable isotope ratios determined in groundwater samples in February 2006 and February 2007 as shown in **Fig. 5.3**

	February 2006						February 2007					
Depth [m]	Toluene [mg l^{-1}]	δ^{13}C [‰]	S.D.	Sulfate [mg l^{-1}]	δ^{34}S [‰]	S.D.	Depth [m]	Toluene [mg l^{-1}]	δ^{13}C [‰]	S.D.	Sulfate [mg l^{-1}]	δ^{34}S [‰]	S.D.
6.39	0.00	-23.4	0.13	69.16	5.5	0.0	6.56	0.15	-20.3	0.10	425.38	6.6	0.02
6.41	2.83	-24.0	0.03				6.59	1.65	-21.5	0.14	184.26	8.4	0.01
6.44	10.72	-24.1	0.16				6.61	6.96	-23.1	0.42	49.80	23.1	0.07
6.46	21.09	-24.1	0.36				6.64	17.26	-23.6	0.06	45.24	29.9	0.07
6.49	29.45	-24.3	0.02		12.5	0.0	6.67	26.72	-24.0	0.03	51.12	32.7	0.13
6.51	31.60	-24.3	0.07				6.70	36.05	-24.1	0.11	57.32	34.3	0.01
6.54	36.91	-24.4	0.10				6.75	40.74	-24.3	0.15	51.30	46.0	0.08
6.56	38.08	-24.4	0.02				6.78	37.97	-24.3	0.12	51.77	45.7	
6.59	42.12	-24.4	0.07				6.81	38.02	-24.3	0.06	54.74	45.1	
6.61	44.75	-24.5	0.09				6.83	37.96	-24.3	0.06	57.22	44.7	0.15
6.64	45.38	-24.5	0.06				6.88	37.35	-24.3	0.13	59.72	42.2	0.03
6.67	44.66	-24.4	0.05				6.91	31.11	-24.3	0.02	64.68	39.3	0.02
6.70	45.34	-24.5	0.02				6.93	30.74	-24.3	0.21	71.76	37.1	0.14
6.75	43.53	-24.4	0.05				7.01	17.94	-24.2	0.10	80.73	34.27	0.05
6.81	39.80	-24.5	0.14	21.94	42.4	0.2	7.11	2.59	-22.2	0.00	90.83	33.2	0.19
6.91	31.97	-24.5	0.03				7.21	0.65	-21.3	0.15	121.39	24.8	0.60
7.01		-23.9	0.06				7.28	0.29	-21.7	0.01	127.90	23.4	0.11
7.11	4.08	-21.8	0.07	71.34	25.0	0.2	7.31	0.10	-22.0	0.47	125.16	23.7	0.05
7.21	1.32	-21.9	0.27				7.33	0.05	-21.4		120.28	24.9	0.04
7.31	0.35	-21.3	0.11				7.41	0.05	-21.3		118.45	25.5	0.02
7.41	0.21	-22.3	0.02				7.46	0.06	-21.0	0.50	120.17	25.0	0.01
7.51	0.15	-22.2	0.04				7.51	0.06	-21.2	0.07	128.36	23.9	0.00
7.61	0.08	-22.5	0.06				7.56	0.05	-21.8		129.08	23.4	0.23
8.05	0.00	-22.6	0.09	116.12	15.9	0.0	7.61	0.04			130.48	22.7	0.01
							7.75				154.21	19.2	0.09
							8.05				166.07	21.7	0.01
							8.35				184.57	15.8	0.05
							8.65				143.67	21.0	0.11
							8.75				108.38	28.3	0.03

Table A.31 Vertical distribution of total BTEX and of microbiological parameters in groundwater sampled from the HR-MLW at different dates as shown in **Fig. 5.4**

August 2006			February 2007				May 2007			
Depth [m]	BTEX [mg l^{-1}]	Cells [×10^8 l^{-1}]	Depth [m]	BTEX [mg l^{-1}]	Cells [×10^8 l^{-1}]	Productivity [nmol C l^{-1} h^{-1}]	Depth [m]	BTEX [mg l^{-1}]	Cell number [×10^8 l^{-1}]	Productivity [nmol C l^{-1} h^{-1}]
6.31	6.96	27	6.56	1.00	6	0.27	6.51	1.27	41	0.27
6.39	28.19	8	6.59	4.45	13	1.73	6.54	8.38	26	2.20
6.41	39.38	2	6.61	14.74	86	0.10	6.59	22.44	60	10.49
6.44	42.13	3	6.64	30.06	58		6.61	45.80	45	4.85
6.46	43.49	5	6.67	44.69	55	0.00	6.64	67.22	29	
6.54	45.96	9	6.70	56.60	8		6.67	95.91	23	0.95
6.56	47.36	5	6.75	65.99	22	0.06	6.70	58.14	22	
6.59	46.47	4	6.78	62.82	14		6.75	55.61	14	0.23
6.61	44.11	5	6.81	64.51	5		6.78	48.29	12	
6.64	36.11	1	6.83	66.18	4		6.81	43.62	9	
6.67	31.60	4	6.88	67.04	4		6.83	53.50	9	
6.75	13.96	4	6.91	58.12	7	0.00	6.86	50.91	9	
6.81	7.58	11	6.93	61.73	13		6.88	30.89	8	
6.91	2.54	15	7.01	42.40	4	0.00	6.91	24.97	8	0.02
7.01	0.90	11	7.11	15.79	7		6.93	31.75	8	
7.08	0.40	10	7.21	4.78	8	0.07	7.01	10.97	8	0.22
7.11	0.20	13	7.28	2.76	3		7.11	5.01	8	
7.21	0.07	15	7.31	1.73	15		7.21	1.23	16	0.25
7.31	0.03	7	7.33	1.15	16		7.31	0.35	9	
7.41	0.04	11	7.41	0.82	9	0.00	7.41	0.01	8	0.03
7.51	0.04	7	7.46	0.96	14		7.51	0.00	9	
7.61	0.03	7	7.51	0.74	10		7.61	0.01	8	
7.75	0.01	7	7.56	0.23	26		7.75	0.00	8	0.05
8.35		7	7.61		14		8.05	0.02	21	
8.65		12	7.75		10	0.00	8.35	0.02	15	
8.75		17	8.05		12		8.65	0.02	13	
			8.35		13		8.75	0.01	9	
			8.65		19					
			8.75		16					

Curriculum vitae

Bettina Anneser

* 24 October 1978 in Trostberg

Education

1998 – 2004	Studies in Biology at the Technical University in Munich major subject: microbiology minor subjects: Biochemical engineering, Limnology
2003 – 2004	Diploma thesis at the Department of Microbial Ecology (Prof. Dr. M. Wagner) / Faculty of Life Sciences, University of Vienna, Austria

Dissertation

2004 –2008	PhD thesis at the Center for Applied Geoscience, Eberhard Karls University of Tübingen; the work was performed at the Institute of Groundwater Ecology, Helmholtz Zentrum München (supervisors: Prof. Dr. R. Meckenstock and Dr. C. Griebler)
02 – 04/2008	Research stay at the Commonwealth Scientific and Industrial Research Organisation (CSIRO) in Perth, Western Australia
since 07/2008	Postdoc at the Institute of Groundwater Ecology, Helmholtz Zentrum München

Publications

Anneser B., Einsiedl F., Meckenstock R. U., Richters L., Wisotzky F., Griebler C. (2008) High-resolution monitoring of biogeochemical gradients in a tar oil-contaminated aquifer. Appl. Geochem. 23: 1715-1730.

Anneser B., Meckenstock R. U., Richters L., Griebler C. (2008) Application of high-resolution groundwater sampling in a tar oil-contaminated sandy aquifer. Studies on small-scale abiotic gradients. In: Adavances in subsurface pollution of porous media: indicators, processes and modelling. Candela, L., Vadillo, I., and Elorza, F.J. (eds), Taylor & Francis / Balkema, Leiden, NL; *in press.*

Anneser B., Einsiedl F., Meckenstock R. U., Richters L., Griebler C. (2008) Small-scale biogeochemical gradients in a tar oil-contaminated aquifer - match and dismatch of groundwater vs. sediment information. *In preparation.*

Anneser B., Einsiedl F., Meckenstock R. U., Richters L., Griebler C. (2008) The hidden dynamics of biogeochemical processes in an organically contaminated porous aquifer. *In preparation.*

Anneser B., Prommer H., Rolle M., Einsiedl F., Griebler C. (2008) Biogeochemical and isotopic gradients in a BTEX/PAH contaminant plume: model-based interpretation of a high-resolution field data set. *In preparation.*

Anneser B., Richters L., Griebler C. (2007) Small-scale distribution of biodegradation processes in a contaminated aquifer revealed by high-resolution sampling of sediments and groundwater. XXXV IAH congress „Groundwater and Ecosystems", 17-21 September 2007, Lisbon, Portugal.

Anneser B., Richters L., Griebler C. (2007) Identification and localization of redox processes in an aromatic hydrocarbon plume via high-resolution sampling of biotic and abiotic gradients. International Conference on WAter POllution in natural POrous media at different scales WAPO[2]. Assessment of fate, impact and indicators. COST action 629, 11-13 April 2007, Barcelona, Spain.

Winderl C., Anneser B., Griebler C., Meckenstock R. U., Lueders T. (2008) Depth-resolved quantification of anaerobic toluene degraders and aquifer microbial community patterns in distinct redox zones of a tar-oil contaminant plume. Applied and Environmental Microbiology 74: 792-801.

Stupp H. D., Gass M., Bakenhus A., Anneser B., Richters L., Griebler C. (2008) Ausbreitung von BTEX im Grundwasser – neue Aspekte zur zukünftigen Beurteilung von Natural Attenuation. Altlasten Spektrum 1/2008: 16-23, Erich Schmidt Verlag, Berlin.

Bauer R., Anneser B. & Griebler C. (2007) Das Schadstofffahnenrand-Konzept – Ökologie und Biochemie des biologischen Abbaus in organisch kontaminierten Grundwasserökosystemen. *Deutsche Gesellschaft für Limnologie (DGL) – Tagungsbericht 2006 (Dresden)*, Werder, pp 1-9.

Selected contributions to national and international scientific meetings

Anneser B., Prommer H., Einsiedl F., Richters L., Griebler C. (2008) Small-scale distribution of biodegradation processes in a contaminated aquifer revealed by high-resolution groundwater sampling. 16 April 2008, CSIRO Land & Water, Perth, Australia (oral presentation)

Anneser B., Einsiedl F., Richters L., Meckenstock R. U., Griebler C. (2008) High-resolution groundwater sampling in a tar oil-contaminated porous aquifer – insights into small-scale biodegradation processes. Research seminar Applied Geology, 18 January 2008, Center for Applied Geosciences, University of Tübingen (oral presentation)

Anneser B., Richters L., Einsiedl F., Meckenstock R. U., Griebler C. (2007) Small-scale distribution of biodegradation processes in a tar oil-contaminated aquifer revealed by high-resolution groundwater sampling. IAH-Congress, 17-21 September 2007, Lisbon, Portugal (oral presentation)

Anneser B., Richters L., Einsiedl F., Meckenstock R. U., Griebler C. (2007) High-resolution investigations in a tar oil-contaminated aquifer. Final conference WAPO^2 of COST action 629, 11-13 April 2007, Barcelona, Spain (oral & poster presentation)

Anneser B., Meckenstock R. U., Griebler C. (2007) High-resolution analysis of physical-chemical gradients in a tar oil-contaminated aquifer. VAAM Annual Conference, 01-04 April 2007, Osnabrück, Germany (poster presentation)

Anneser B., Meckenstock R. U., Griebler C. (2007) High-resolution measurements of physical-chemical and microbiological gradients in a petroleum hydrocarbon plume. Symposium "In-situ-Sanierung", 20-21 November 2006, Dechema, Frankfurt, Germany (poster presentation)

Anneser B. & Griebler C. (2006): Fine-scale depth resolved analysis of the fringe of a petroleum hydrocarbon plume – I: Physico-chemical and microbiological gradients. VAAM annual conference, 19-22 March 2006, Jena, Germany (oral presentation)

Anneser B. & Griebler C.: High-resolution measurements of physical-chemical and microbiological gradients at the fringe of a petroleum hydrocarbon plume in a contaminated aquifer. COST action 629, 24 September – 1 October 2005, Malaga, Spain (poster presentation)

Acknowledgements

The multi-level story began with a simple drawing of the well and certain uncertainties on the feasibility concerning the construction and installation of the well and the detection of small-scale biogeochemical gradients.
Meanwhile, the well provides several working groups with samples and data and thus created a broad cooperation network within and outside the IGÖ.
The success of this project and, consequently, of my PhD thesis was only possible with the help of a number of people. To some of them I'm particularly indebted:

First and foremost I want to thank my supervisor Dr. Christian Griebler; he was the "creator" of the multi-level well and an unexhaustible source of ideas and concepts, which provided the basis for this fruitful project. I'm glad to have landed up in this field of research and in his working group.
I also want to appreciate my mentor Prof. Dr. Rainer Meckenstock for the opportunity to perform this work at his institute and for advice and support at any time.
Especially I want to appreciate Lars Richters from the Stadtwerke Düsseldorf for his continuous support. Thanks for patiently answering all my annoying queries on the Flingern site and for the reliable supply with technical equipment and coffee!
Many thanks to Dr. Martin Elsner, Dr. Holger Penning, Armin Meyer, Dr. Thomas Kuhn and Nadezda Kadlec for instructing me at the GC-C-IRMS, which I occupied for many weeks, and for their indispensable help during that time.
I also thank Dr. Willibald Stichler and Dr. Florian Einsiedl for their valuable contributions to the isotope data collection of the Flingern site.
Thanks to Dr. Tillmann Lueders, Christian Winderl (alias CJ) and Giovanni Pilloni for fruitful cooperation and discussions and for providing information on the molecular scale.
I count myself very lucky that I met Henning Prommer and Massimo Rolle, who introduced me into the world of modelling, surfing and no worries and made me spend ten wonderful weeks Down Under. I'm also indebted to members of the research group "Reactions in porous media", especially to Prof. Dr. Peter Grathwohl, for realizing the trip to Australia and for inspiring discussions and motivating suggestions.
I'm very grateful to Michael Stöckl, Harald Lowag and Günter Teichmann, who were always on the spot to tackle technical problems and troubles with computers. For help with most other little aches and pains and bureaucratic harassments I want to thank our good soul Brigitta Friesleben.
For helping hands, smouldering heads, cooling beers and great ideas I want to thank all my collegues at the IGÖ, particularly the "old" PhD staff, consisting of Robert, Kathrin, Tine, Muna, Eva, Claudia, Heike, Mark and CJ. Thank you for being such good collegues and for making me feel comfortable at work – even in the dark, sunshineless northern office, which was clearly brightened up by Kathrin, Claudia, Robert, Nidal, CJ and Giovanni.

My special thanks go to Burkhard for faithfully enjoying, suffering and standing by me during the last years. I want to thank him, my family and my friends for helping me out of occasional downs and for providing innumerable highlights.
Last but not least I want to thank my dad. He was the one who sparked my interest for sciences and continuously nourished my ambitions, thus finally bringing me to that point I reached now.

XXX